

**Retrieval of Tropospheric Trace Gas Nitrogen Dioxide (NO<sub>2</sub>)  
by exploiting 1st South Asia's NASA Pandora Spectrometer**



By

**Talha Saeed**

**(Registration No: 00000363791)**

Institute of Environmental Sciences & Engineering (IESE)

School of Civil & Environmental Engineering

National University of Sciences & Technology (NUST)

Islamabad, Pakistan

(2024)

# **Retrieval of Tropospheric Trace Gas Nitrogen Dioxide (NO<sub>2</sub>) by exploiting 1st South Asia's NASA Pandora Spectrometer**



By

**Talha Saeed**

(Registration No: 00000363791)

A thesis submitted to the National University of Sciences and Technology, Islamabad,

in partial fulfillment of the requirements for the degree of

Master of Science in  
Environmental Sciences

**Supervisor: Dr. Muhammad Fahim Khokhar**

**Co Supervisor: Dr. Salman Tariq**

Institute of Environmental Sciences & Engineering (IESE)

School of Civil & Environmental Engineering (SCEE)

National University of Sciences & Technology (NUST)

Islamabad, Pakistan

(2024)

## CERTIFICATE OF APPROVAL

This is to certify that the research work presented in this thesis, entitled

“Retrieval of Tropospheric Trace Gas Nitrogen Dioxide (NO<sub>2</sub>) by exploiting 1st South Asia’s NASA Pandora Spectrometer”

submitted by

Mr. Talha Saeed

for partial fulfillment of the requirements for the degree of Master of Science in Environmental Sciences from Institute of Environmental Sciences & Engineering (IESE), School of Civil & Environmental Sciences (SCEE), National University of Sciences and Technology, Islamabad.

Supervisor: \_\_\_\_\_

Dr. Muhammad Fahim Khokhar  
Tenured Professor  
Environmental Sciences

Dr. Muhammad Fahim Khokhar

Tenured Professor

SCEE (IESE), NUST

Co-Supervisor: \_\_\_\_\_

Dr. Salman Tariq

Assistant Professor

Department of Space Science, University  
of the Punjab

GEC Member: \_\_\_\_\_

Dr. Hassan Anwer  
Assistant Professor  
SCEE (IESE), NUST

GEC Member: \_\_\_\_\_

Dr. Muhammad Arshad  
Professor  
SCEE (IESE), NUST

Dr. Muhammad Arshad  
Tenured Professor  
IESE (SCEE) NUST Islamabad

Dr. Hassan Anwer  
Assistant Professor  
IESE (SCEE) NUST Islamabad

## CERTIFICATE OF THESIS ACCEPTANCE

Certified that final copy of MS Thesis written by Mr. Talha Saeed (Registration No. 363791), of Institute of Environmental Sciences & Engineering (IESE) has been vetted by undersigned, found complete in all respects as per NUST Statutes/ Regulations/ Masters Policy, is free of plagiarism, errors, and mistakes and is accepted as partial fulfillment for award of Master of Science in Environmental Sciences. It is further certified that necessary amendments as pointed out by GEC members of the scholar have also been incorporated in the said thesis.

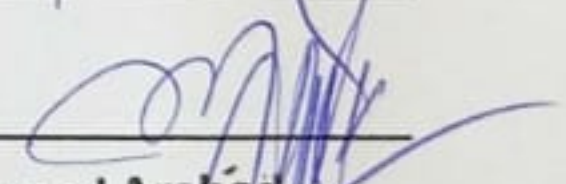
Signature:   
Dr. Muhammad Fahim Khokhar  
Tenured Professor  
Environmental Sciences  
SCEE (IESE) NUST Islamabad

Name of Supervisor Dr. Muhammad Fahim Khokhar

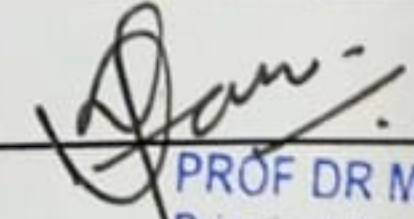
Date: 09/07/24

Head of Department:   
Dr. Muhammad Fahim Khokhar  
Tenured Professor  
Environmental Sciences  
SCEE (IESE) NUST Islamabad

Date: 09/07/24

Associate Dean :   
Dr. Muhammad Arshad  
Tenured Professor  
ESE (SCEE) NUST Islamabad

Date: 09-07-2024

Principal & Dean (SCEE):   
PROF DR MUHAMMAD IRFAN  
Principal & Dean  
SCEE, NUST

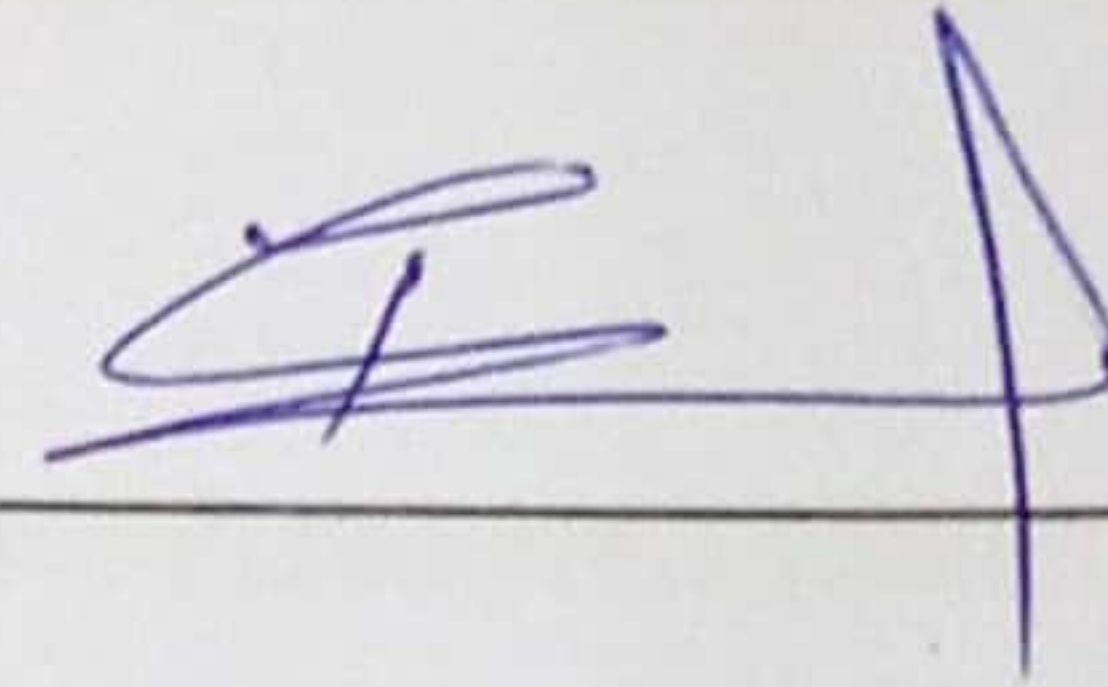
Date: 10 JUL 2024

## CERTIFICATE OF AUTHOR'S DECLARATION

I Talha Saeed hereby state that my MS thesis titled "Retrieval of Tropospheric Trace Gas Nitrogen Dioxide NO<sub>2</sub> by exploiting 1st South Asia's NASA Pandora Spectrometer" is my own work and has not been submitted previously by me for taking any degree from National University of Sciences and Technology, Islamabad or anywhere else in the country/ world.

At any time if my statement is found to be incorrect even after I graduate, the university has the right to withdraw my MS degree.

Student Signature: \_\_\_\_\_



Name of Student: Talha Saeed


Date: 09/07/2024

## CERTIFICATE OF PLAGIARISM UNDERTAKING

I solemnly declare that research work presented in the thesis titled “**Retrieval of Tropospheric Trace Gas Nitrogen Dioxide (NO<sub>2</sub>) by exploiting 1st South Asia’s NASA Pandora Spectrometer**” is solely my research work with no significant contribution from any other person. Small contribution/ help wherever taken has been duly acknowledged and that complete thesis has been written by me.


I understand the zero-tolerance policy of the HEC and National University of Sciences and Technology (NUST), Islamabad towards plagiarism. Therefore, I as an author of the above titled thesis declare that no portion of my thesis has been plagiarized and any material used as reference is properly referred/cited.

I undertake that if I am found guilty of any formal plagiarism in the above titled thesis even after award of MS degree, the University reserves the rights to withdraw/revoke my MS degree and that HEC and NUST, Islamabad has the right to publish my name on the HEC/University website on which names of students are placed who submitted plagiarized thesis.

Student Signature: 

Name: Talha Saeed

Date: 09/07/24

Supervisor Signature: 

Name: Dr. Muhammad Fahim Khokhar

Date: 09/07/24

## DEDICATION

*I dedicate this thesis to my family and my  
mentor Dr. Muhammad Fahim  
Khokhar for their belief in me, continuous  
support, and motivation.*

## ACKNOWLEDGMENTS

First and foremost, I'd like to express my heartfelt gratitude to Allah Almighty, whose immeasurable graces and beneficence enabled me to successfully complete my thesis. His compassionate assistance enabled me to find the patience and understanding I required to complete this challenging assignment.

My supervisor, Dr. Muhammad Fahim Khokhar, offered energetic and inspirational leadership throughout my research, for which I am really thankful. His encouragement, wise advice, effective teaching tactics, and abundance of creative ideas have been beneficial to my academic success. I would especially want to thank Dr. Hassan Anwer and Dr. Muhammad Arshad from the Graduate Examination Committee (GEC) for their important guidance and unwavering support. I also want to thank Dr. Salman Tariq, my co-supervisor, for his assistance and advice, which were extremely beneficial to me during my research.

I'd like to thank my coworkers at C-CARGO in particular: Mr. Shehzeb Anjum; Mr. Kamran Khan; Mr. Mahad Khaliq; Mr. Muhammad Talha Zahid; Mr. Suhaib Malik; Mr. Hassan Nawaz; Mr. Naveed Ahmad; Mr. Kashif Imran; Mr. Emad ud Din; Ms. Abeer Salman; Ms. Madiha Javed; and Ms. Rabia Majeed. Their desire to help and share knowledge when needed has been a source of inspiration and strength.

I'm grateful to my family and friends for their monetary and emotional support, which has helped to build my perseverance and willpower. Their continuous support and encouragement transformed my doubts into moments of persistence and ambition. Muhammad Adam, Tariq Ali, and Muhammad Talha Zahid deserve special gratitude for their unwavering encouragement and confidence during this journey.

Last but not least, I want to offer my heartfelt gratitude to my parents. My ambitions and accomplishments are based on the foundation laid by their unending sacrifices and life lessons. I'll be eternally grateful to them for their unwavering love and support, which have served as my guiding light.



# TABLE OF CONTENTS

<b>ACKNOWLEDGMENTS</b>	<b>VIII</b>
<b>TABLE OF CONTENTS</b>	<b>IX</b>
<b>LIST OF TABLES</b>	<b>XII</b>
<b>LIST OF FIGURES</b>	<b>XIII</b>
<b>LIST OF SYMBOLS, ABBREVIATIONS AND ACRONYMS</b>	<b>XV</b>
<b>ABSTRACT</b>	<b>XVI</b>
<b>CHAPTER 1: INTRODUCTION</b>	<b>1</b>
<b>1.1 Background History of Environment</b>	<b>1</b>
<b>1.2 Quantification Techniques of Atmospheric Trace Gases</b>	<b>2</b>
<b>1.3 Categorization of Spectroscopic Techniques</b>	<b>3</b>
<b>1.4 Factors for Classification of Spectroscopic Instruments</b>	<b>4</b>
<b>1.5 Differential Optical Absorption Spectroscopy</b>	<b>5</b>
<b>1.6 Active &amp; Passive DOAS Instruments</b>	<b>5</b>
<b>1.7 Categorization of Passive DOAS Instrumentation</b>	<b>6</b>
1.7.1 Long-Path DOAS (LP-DOAS)	6
1.7.2 Profiling Refelctors LP-DOAS	6
1.7.3 Tomographic DOAS	7
1.7.4 Folded-Path DOAS	7
1.7.5 Direct Sunlight DOAS	8
1.7.6 Balloon-based direct sunlight DOAS	8
1.7.7 Satellite-Occultation based DOAS	9
1.7.8 Zenith Scattered Light (ZSL-DOAS)	9
1.7.9 Multi-Axis DOAS (MAX-DOAS)	10
1.7.10 Airborne Multi-Axis DOAS (AMAX-DOAS)	10
1.7.11 Imaging DOAS	11
1.7.12 Satellite-borne DOAS	11
1.7.13 Inverse DOAS (Determination of the Photon Path Length L in Clouds)	12
<b>1.8 DOAS Experimental Setup</b>	<b>12</b>
<b>1.9 Ground vs Satellite DOAS</b>	<b>14</b>
<b>1.10 Current Study Instrumentation</b>	<b>15</b>
1.10.1 Ground-Based DOAS (Pandora Spectrometer)	15
1.10.2 Ground-Based Monitor (Horriba NOx Analyzer)	15
1.10.3 Satellite Borne DOAS (OMI & TropOMI)	16
<b>1.11 Significance of the Study</b>	<b>18</b>
<b>1.12 Study Objectives</b>	<b>18</b>
<b>CHAPTER 2: LITERATURE REVIEW</b>	<b>20</b>
<b>2.1 Earth's Source of Light</b>	<b>20</b>

<b>2.2 Energy Flow Mechanism of Climate System</b>	<b>21</b>
<b>2.3 Interaction of Solar Radiation with Atmosphere</b>	<b>21</b>
<b>2.4 Earth's Atmospheric Layers &amp; Composition</b>	<b>22</b>
<b>2.5 Planetary Boundary Layer</b>	<b>23</b>
<b>2.6 Atmospheric Chemistry &amp; Transport of NO<sub>x</sub></b>	<b>25</b>
<b>2.7 Historical Background of Spectroscopic Measurements</b>	<b>30</b>
<b>2.8 Research Studies on NO<sub>2</sub> Monitoring</b>	<b>32</b>
<b>2.9 NASA Pandora Spectrometer</b>	<b>35</b>
<b>2.10 Research Gaps &amp; Limitations</b>	<b>36</b>
<b>SUMMARY OF RESEARCH WORK</b>	<b>37</b>
<b>CHAPTER 3: METHODOLOGY</b>	<b>38</b>
<b>3.1 Research Instrumentation and Study Area</b>	<b>38</b>
<b>3.2 Installation of South Asia's 1st NASA Pandora Spectrometer</b>	<b>40</b>
3.2.1 Pandora Spectrometer	41
3.2.2 Pandora Sun Tracker	42
3.2.3 Pandora Main Control Box Unit	43
<b>3.3 Fiber &amp; Tracker Cable Layout</b>	<b>44</b>
<b>3.4 Software Installation &amp; System Settings</b>	<b>45</b>
3.4.1 Location File Creation	46
3.4.2 Checking Connections	46
3.4.3 Home Position Setting of Sun Tracker	47
3.4.4 Azimuth Home Position	49
3.4.5 Zenith Home Position	49
3.4.6 Initial Azimuth & Zenith Angle Correction	50
3.4.7 Sky Scan Azimuth Configuration	52
<b>3.5 NASA Pandora Spectrometer Common Routines</b>	<b>52</b>
3.5.1 Alignment Visualization	53
3.5.2 Maintenance Check	55
<b>3.6 Data Products of NASA Pandora Spectrometer</b>	<b>55</b>
3.6.1 Formaldehyde (fuh5):	55
3.6.2 Nitrogen Dioxide (nvh3):	55
3.6.3 Ozone (ous1):	55
3.6.4 Sulphur Dioxide (sus1)	55
<b>3.7 OMI &amp; TROPOMI</b>	<b>56</b>
<b>CHAPTER 4: RESULTS &amp; DISCUSSION</b>	<b>57</b>
<b>4.1 NO<sub>2</sub> Ground Based Measurements</b>	<b>57</b>
4.1.2 NASA Pandora Spectrometer Tropospheric NO <sub>2</sub> Column Densities	57
<b>4.2 NO<sub>2</sub> Satellite Based Measurements</b>	<b>61</b>
4.2.1 AURA Ozone Monitoring Instrument (OMI)	62
4.2.2 Sentinel 5P TROPospheric Ozone Monitoring Instrument (TROPOMI)	64
<b>4.3 Ground based Instrument Intra Monitoring Validation</b>	<b>66</b>
4.3.1 NASA Pandora vs HORRIBA NO <sub>2</sub> Surface Concentration	66
<b>4.4 Ground vs Satellite Based NO<sub>2</sub> Measurements Validation</b>	<b>67</b>
4.4.1 NASA Pandora vs OMI Satellite Based Validation	68

4.4.2 NASA Pandora vs TROPOMI NO <sub>2</sub> Measurements Validation	69
<b>4.5 Meteorological Effects on NO<sub>2</sub> Measurements</b>	<b>70</b>
4.5.1 Impact of Solar Radiance on NASA Pandora NO <sub>2</sub> Measurement	70
4.5.2 Temperature effects on NASA Pandora Spectrometer NO <sub>2</sub> Measurements	71
4.5.3 Wind Speed effects on NASA Pandora Spectrometer NO <sub>2</sub> Measurements	71
4.5.4 Impact of Relative Humidity on NASA Pandora Spectrometer NO <sub>2</sub> Measurements	72
<b>4.6 Pandora Data Validation with GEMS Satellite</b>	<b>75</b>
<b>CHAPTER 5: CONCLUSION &amp; RECOMMENDATIONS</b>	<b>77</b>
<b>REFERENCES</b>	<b>81</b>
<b>PLAGIARISM REPORT</b>	<b>91</b>

## LIST OF TABLES

	<b>Page No.</b>
Table 1: Active and Passive DOAS Precision & Accuracy Comparison .....	5
Table 2: NASA Pandora Spectrometer Routine Abbreviations .....	52

## LIST OF FIGURES

	Page No.
Figure 1: Optical Measurement techniques for trace gases .....	4
Figure 2: Schematic Diagram of LP-DOAS, Vertical LP-DOAS, Tomographic DOAS and Folded Path DOAS.....	8
Figure 3: Schematic Diagram of Direct Sunlight DOAS, Ballon Born DOAS, Satellite DOAS and Zenith Scattered DOAS.....	10
Figure 4: Schematic Diagram of Multi-Axis DOAS and Airborne Multi-Axis DOAS ...	11
Figure 5: Schematic Diagram of Imaging, Satellite Nadir, Satellite Scattered and Inverse DOAS.....	12
Figure 6: DOAS Experimental Setup Schematic Flowchart.....	14
Figure 7: Atmospheric Chemistry cycle of NO <sub>x</sub> .....	29
Figure 8: Stratospheric & Tropospheric Reactions of NO <sub>x</sub> .....	30
Figure 9: NASA Pandora Spectrometer & Horriba Analyzer installed in Air Noise Lab of IESE, NUST.....	39
Figure 10: Working Principle of Satellite Based Observations .....	40
Figure 11: NASA Pandora Head Sensor Components .....	42
Figure 12: NASA Pandora Tracker Components .....	43
Figure 13: NASA Pandora Main Control Unit Components .....	44
Figure 14: NASA Pandora Spectrometer Fiber Cable Layout.....	45
Figure 15: NASA Pandora Spectrometer LufBlick M Software Display.....	46
Figure 16: NASA Pandora Tracker Home Position.....	48
Figure 17: NASA Pandora Zenith Home Position Settings.....	50
Figure 18: NASA Pandora Spectrometer Slight Alignment.....	51
Figure 19: Good Alignment of NASA Spectrometer .....	54
Figure 20: Bad Alignment of NASA Pandora Spectrometer.....	54
Figure 21: Timeseries analysis of Pandora Tropospheric NO <sub>2</sub> columns .....	58
Figure 22: Diurnal Cycle of Pandora Tropospheric NO <sub>2</sub> .....	59
Figure 23: Weekly Cycle of Pandora Tropospheric NO <sub>2</sub> .....	60
Figure 24: Monthly Cycle of Pandora Tropospheric NO <sub>2</sub> .....	61
Figure 25: Seasonal Cycle of Pandora Tropospheric NO <sub>2</sub> .....	61
Figure 26: Timeseries of OMI Tropospheric NO <sub>2</sub> .....	62
Figure 27: Weekly Cycle of OMI Tropospheric NO <sub>2</sub> .....	63
Figure 28: Monthly Cycle of OMI Tropospheric NO <sub>2</sub> .....	63
Figure 29: Seasonal Cycle of OMI Tropospheric NO <sub>2</sub> .....	64
Figure 30: Timeseries Analysis of TROPOMI Tropospheric NO <sub>2</sub> .....	65
Figure 31: Weekly Cycle of Pandora Tropospheric NO <sub>2</sub> .....	66
Figure 32: Monthly Cycle of Pandora Tropospheric NO <sub>2</sub> .....	66
Figure 33: Seasonal Cycle of Pandora Tropospheric NO <sub>2</sub> .....	66
Figure 34: Timeseries Analysis of Pandora compared to Horriba Surface Concentration (ppb).....	67

Figure 35: Validation of Daily Tropospheric NO <sub>2</sub> Pandora and Horriba Surface Concentration.....	67
Figure 36: Timeseries Analysis of Pandora with OMI Tropospheric NO <sub>2</sub> .....	68
Figure 37: Validation of Pandora Daily Tropospheric NO <sub>2</sub> with OMI .....	68
Figure 38: Validation of Pandora Monthly Tropospheric NO <sub>2</sub> with OMI.....	69
Figure 39: Timeseries Analysis of Daily Pandora Tropospheric NO <sub>2</sub> with TROPOMI...	69
Figure 40: Validation of Pandora Daily Tropospheric NO <sub>2</sub> with TROPOMI .....	70
Figure 41: Validation of Pandora Monthly Tropospheric NO <sub>2</sub> with TROPOMI .....	70
Figure 42: Comparison of Pandora Tropospheric NO <sub>2</sub> with Solar Radiation (W/m <sup>2</sup> ).....	71
Figure 43: Comparison of Pandora Tropospheric NO <sub>2</sub> with Temperature (C).....	71
Figure 44: Comparison of Pandora Tropospheric NO <sub>2</sub> with Wind Speed (m/s) .....	72
Figure 45: Comparison of Pandora Tropospheric NO <sub>2</sub> with Relative Humidity (%).....	72
Figure 46: Correlation Matrix of Pandora, OMI, TROPOMI, GEMS, Relative Humidity, Temperature, Solar Radiation and Wind Speed.....	74
Figure 47: Pandora & GEMS Monthly Tropospheric NO <sub>2</sub> Map for the month of May 2024 and April 2024. ....	75
Figure 48: Timeseries Analysis of Pandora Tropospheric NO <sub>2</sub> with GEMS Satellite \....	75
Figure 49: Validation of Daily Pandora Tropospheric NO <sub>2</sub> with GEMS Satellite .....	76

## LIST OF SYMBOLS, ABBREVIATIONS AND ACRONYMS

<b>µg/m<sup>3</sup></b>	Microgram per Cubic meter
<b>HNO<sub>3</sub></b>	Nitric Acid
<b>MAX-DOAS</b>	Multi-axis Differential Optical Absorption Spectroscopy
<b>NO<sub>2</sub></b>	Nitrogen Dioxide
<b>NO<sub>2</sub> VCD</b>	Nitrogen Dioxide Vertical Column Density
<b>NO<sub>2</sub><sup>-</sup></b>	Nitrites
<b>NO<sub>3</sub><sup>-</sup></b>	Nitrates
<b>NO<sub>x</sub></b>	Oxides of Nitrogen
<b>O<sub>3</sub></b>	Ozone
<b>OMI</b>	Ozone Monitoring Instrument
<b>PAN</b>	Peroxy Acetyl Nitrile
<b>UTC</b>	Coordinated Universal Time
<b>UV</b>	Ultra-Violet
<b>VOCs</b>	Volatile Organic Compounds
<b>ppb</b>	Parts per Billion
<b>RMS</b>	Root Mean Square
<b>OMI</b>	Ozone Monitoring Instrument
<b>WHO</b>	World Health Organization

## ABSTRACT

The primary anthropogenic sources of nitrogen oxide emissions are fossil fuel combustion, industrial pollution, and intentional burning. Nitrogen dioxide (NO<sub>2</sub>) is an atmospheric trace gas necessary for the synthesis of tropospheric ozone, a short-lived climatic pollutant. Short-lived climatic pollutants not only disrupt the natural ecosystem but also have long term drastic atmospheric impacts i.e., global warming. In Pakistan, there is an absence of continuous ground-based monitoring equipment for assessing atmospheric trace gas profiles. In Pakistan, South Asia's first NASA Pandora Spectrometer is recently deployed at NUST, Islamabad to continuously monitor the atmospheric profile of these trace gases. This study focused on the data retrievals of two ground-based monitors (the Pandora Spectrometer and the Horriba NO<sub>x</sub> Analyzer) and three satellite-based instruments (OMI, TROPOMI & GEMS). The study is first of its kind in the South Asian region where Pandora NO<sub>2</sub> Tropospheric column retrieved from Pandora Spectrometer & validated with in-situ measurements. Analysis of diurnal, weekly, monthly, seasonal cycles of Tropospheric NO<sub>2</sub> columns showed the peak values during office opening or closing hours. Weekdays have high values of tropospheric NO<sub>2</sub> compared to weekends, and similarly high values during winter & post monsoon season. Furthermore, OMI & TROPOMI satellite only covers the region once a day, but incorporation of GEMS data enhanced the validity of ground based NO<sub>2</sub> tropospheric columns which cover the region 6-8 hours a day. Pandora tropospheric NO<sub>2</sub> column densities exhibited a correlation of 71 and 77 percent with OMI and TROPOMI, respectively, while Pandora Surface NO<sub>2</sub> concentrations were 81% correlated with Horriba NO<sub>2</sub> surface concentrations. Data validation of Pandora spectrometer with GEMS showed the highest correlation of 87% with Pandora NO<sub>2</sub> tropospheric columns. In addition, meteorological parameters were also analyzed to validate the trends of NO<sub>2</sub> observations.

**Keywords:** Tropospheric nitrogen dioxide, Seasonal, In-situ, GEMS



## **CHAPTER 1: INTRODUCTION**

This chapter explains the brief history of major environmental disasters and pollution events which triggered environmental monitoring and protection measures. It also emphasizes the various atmospheric analytical techniques available, addressing spectroscopic measurements and differential optical absorption measurements. Depending upon the source of light, passive differential optical spectroscopic techniques are discussed and outlines the ground-based and satellite-based monitoring tools for measuring atmospheric trace gases especially NO<sub>2</sub>.

### **1.1 Background History of Environment**

The Earth is encased by various layers of atmosphere, the lowest of which is the troposphere, where living beings interact. For so long, the nature of Earth has been unaffected by any form of pollution; only natural activity such as volcanic eruptions contaminate the atmosphere, but natural cycles balance the destructive emissions of natural activities. Humans disrupted the Earth's ecosystem by using its natural resources for their so-called development purposes. The Industrial Revolution altered the global ecosystem as humans became more concerned with the necessities of life (Ugletti et al 2015). The rat race began when humans started using combustion engines to save time and make a living. Under these conditions, the most essential component for humans to breathe, live, and connect with is air. Humans are unable to determine the condition of the breathable air unless they see the results with their own naked eyes or something catastrophic occurs that opens their eyes. The same is true for air pollution, as seen in 1952 when London haze claimed many lives and Los Angeles residents began to experience breathing issues and eye irritation (Polvika et al 2018). As contaminants can travel long distances and change the makeup of the atmosphere, scientists will be able to analyze and explore it. DDT (dichloro-diphenyl-trichloroethane), a persistent organic pollutant, created

major environmental and health problems in 1960, resulting in the quiet spring because this insecticide is so persistent that it may become part of fatty tissues and travel vast distances in the upper atmosphere (Seagren et al 2005). DDT is currently classified as a probable carcinogen by the International Agency for Cancer Research (IARC). Farman et al. discovered an ozone hole in Antarctica in 1985, demonstrating the long-term atmospheric transport of pollutants and the effects of industrialization, which were mostly caused by the surface use of chlorofluorocarbons. Following these scenarios, the scientific community expressed concerns about the primary causes of air pollution, prompting an increase in interest in evaluating and quantifying pollutants, as well as signing multilateral environmental agreements (MEA) to limit pollutants and recover the ozone layer by 2050 (Steinbrecht et al 2018). According to Flemming (1998), fluctuations in atmospheric composition are the primary cause of climate change. Weather patterns shifted, as demonstrated by a 1.2-degree Celsius global temperature drop over five years following Krakatau volcanic activity in 1883 (Schaller et al. 2009). Rounce et al. (2023) argue that rising global temperatures have hastened glacier melting.

## **1.2 Quantification Techniques of Atmospheric Trace Gases**

U. Platt (1999) enlisted various analytical techniques for monitoring atmospheric trace gases which include gas chromatography, optical spectroscopy, mass spectrometry, chemiluminescence, chemical amplification technique, photoacoustic detection, electrochemical techniques, matrix isolation techniques, Derivatization techniques, colorimetric analysis, and high-performance liquid chromatography techniques.

As of right now, no single measurement strategy can completely satisfy all requirements. Thus, the species to be assessed, whether many species need to be determined simultaneously, and the necessary accuracy, temporal resolution, and geographic resolution all play a role in selecting a particular approach within a given

application. The installation of light sources or retroreflectors, power needs, and the viability of integrating the device on transportable platforms are examples of logistical challenges.

### **1.3 Categorization of Spectroscopic Techniques**

Spectroscopic techniques are broadly divided into two categories:

1. Those that rely on the sample absorbing radiation from an external source.
2. Those that evaluate radiation emitted by the sample itself.

The selected wavelength range determines how the radiation interacts with the internal states of the sample molecules, allowing for further classification. Depending on the wavelength ranges, the spectroscopic technique can be categorized into three subcategories:

1. Microwave Absorption Spectroscopy (Rotational)
2. Infra-red Absorption Spectroscopy (Vibrational)
3. Ultra-violet & Visible Absorption Spectroscopy (Electronic)

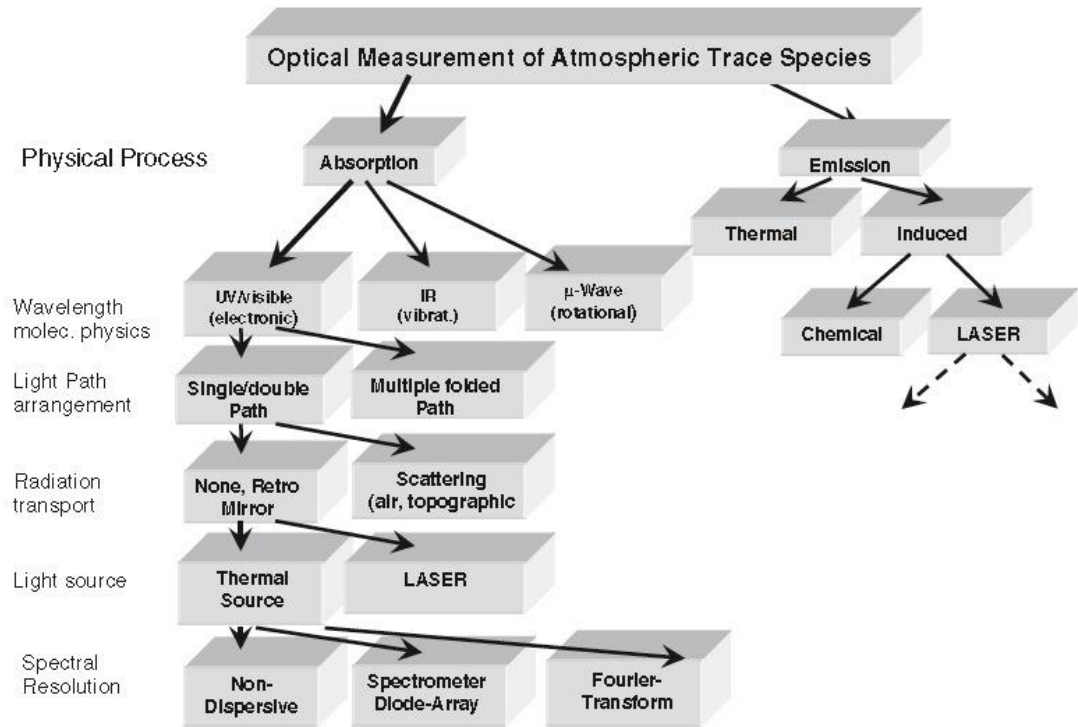


**Figure 1: Optical Measurement techniques for trace gases**

#### 1.4 Factors for Classification of Spectroscopic Instruments

Atmospheric trace gas monitoring techniques available are Differential Optical Absorption Spectroscopy (DOAS), Cavity Ring-Down Spectroscopy (CRDS), Differential Absorption LIDAR (DIAL), Tunable Diode Laser Spectroscopy (TDLS), Laser-Induced Fluorescence (LIF), Mask Correlation Spectroscopy, and Photoacoustic Spectroscopy (PAS). Depending on the environment whether it is open or closed, these methods including LIDARM DIAL, LIF, and DOAS are significant for identifying light channels. The operational wavelength range, underlying physical principles (such as absorption or emission spectroscopy), light route configuration (open or enclosed, often with folding designs), and light source type are the characteristics that define spectroscopic instruments.

## **1.5 Differential Optical Absorption Spectroscopy**

When light from a broad-spectrum source, characterized by an initial intensity denoted as  $I_0(\lambda)$ , is directed through a volume containing absorbing entities, such as the Earth's atmosphere, its intensity is diminished as it traverses this medium. The decrease in intensity is a result of specific trace gases within the atmosphere absorbing wavelengths of light. The scattering of air molecules and aerosol particles, as well as the absorption effects of other trace gases, can also reduce the intensity of light. The transmissivity of the system—which is influenced by optical components like mirrors, gratings, and retro-reflectors—also plays a role in the decrease in light intensity. Turbulence in the atmosphere can cause the light beam to broaden, leading to additional intensity loss. The main principle is dependent on Lamber-Beer Law.

## **1.6 Active & Passive DOAS Instruments**

Regarding light sources, active and passive DOAS are not the same. While active DOAS makes use of artificial light, passive DOAS depends on natural light sources like the sun, moon, and stars.

### **Table 1: Active and Passive DOAS Precision & Accuracy Comparison**

Type of instrument	Precision	Accuracy
Active DOAS	<ul style="list-style-type: none"> <li>Noise</li> <li>Unexplained spectral structures</li> <li>Insignificant: path length</li> </ul>	<ul style="list-style-type: none"> <li>Noise</li> <li>Unexplained spectral structures</li> <li>Insignificant: path length</li> <li>Accuracy of absorption cross-section</li> </ul>
Passive direct light DOAS	<ul style="list-style-type: none"> <li>Noise</li> <li>Removal of Fraunhofer bands</li> <li>Temperature-dependent absorption cross-section</li> <li>Unexplained spectral structures</li> </ul>	<ul style="list-style-type: none"> <li>Noise</li> <li>Removal of Fraunhofer bands</li> <li>Temperature-dependent absorption cross-section</li> <li>Unexplained spectral structures</li> <li>Accuracy of absorption cross-section</li> </ul>
Passive scattered light DOAS	<ul style="list-style-type: none"> <li>Noise</li> <li>Removal of Fraunhofer bands</li> <li>Temperature-dependent absorption cross-section</li> <li>Unexplained spectral structures</li> <li>Path length/radiative transfer</li> </ul>	<ul style="list-style-type: none"> <li>Noise</li> <li>Removal of Fraunhofer bands</li> <li>Temperature-dependent absorption cross-section</li> <li>Unexplained spectral structures</li> <li>Path length/radiative transfer</li> <li>Accuracy of absorption cross-section</li> </ul>

## 1.7 Categorization of Passive DOAS Instrumentation

Passive DOAS can be further categorized into direct and scattered light DOAS. Following are the different types of DOAS:

### 1.7.1 Long-Path DOAS (LP-DOAS)

What distinguishes this system is its essential design: light from  $I_0$ , the initial source, must travel a significant distance through the atmosphere before reaching the detector. The long optical path increases the interaction volume of light and air elements, which improves trace gas detection sensitivity. This makes LP-DOAS ideal for monitoring low-concentration atmospheric gases across large spatial areas.

### 1.7.2 Profiling Reflectors LP-DOAS

In this setup, the light emitted by a combined lamp and detector unit is directed vertically upward, reflecting off several retro-reflectors at varied elevations. This configuration

enables the profiling of atmospheric trace gas concentrations at various heights, providing atmospheric vertical profile data required for understanding atmospheric layers and dynamics. The reflectors virtually double the light path, which improves the sensitivity and resolution of vertical concentration profiles.

### *1.7.3 Tomographic DOAS*

Tomographic DOAS generates several overlapping paths through the atmosphere using an advanced system of light sources and retroreflectors. This setup enables the examination of trace gas spatial concentration patterns in a way analogous to medical tomography. It provides a precise three-dimensional depiction of the distribution of atmospheric gases, which is critical for both local toxin detection and understanding spatially diversified atmospheric phenomena.

### *1.7.4 Folded-Path DOAS*

Using mirrors or other reflective surfaces, this method compresses the light path into a tiny region, resulting in a long, elegant optical path. Because the multiphases design significantly extends the period of interaction between light and ambient trace gases without necessitating a comprehensive geographical strategy, enhanced detection sensitivity and accuracy are possible. Folded-path DOAS is extremely useful when a long light path with no overlap over long distances is required.

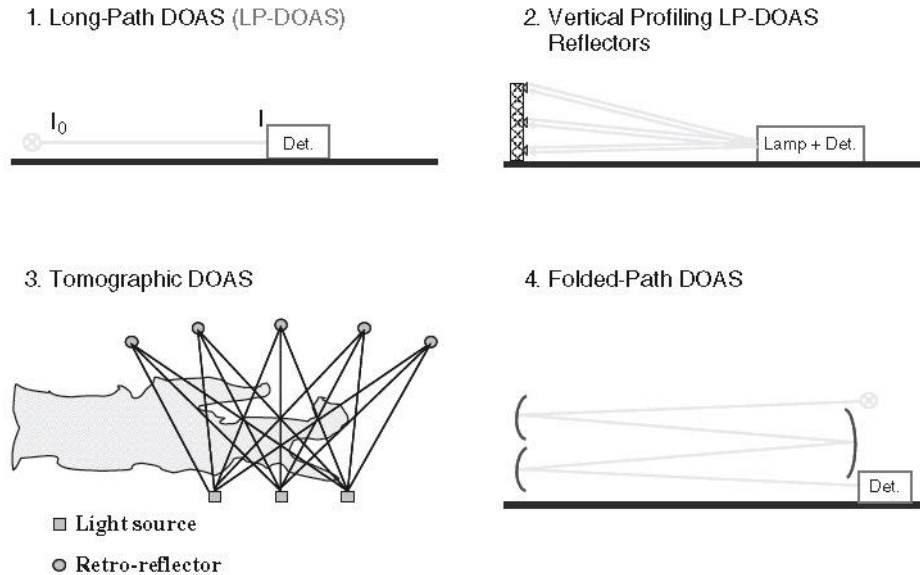


**Figure 2: Schematic Diagram of LP-DOAS, Vertical LP-DOAS, Tomographic DOAS and Folded Path DOAS**

### 1.7.5 Direct Sunlight DOAS

In this configuration, the sun serves as the light source, transmitting light through the atmosphere and into the detector. This method's strength is its ability to correctly account for the bright sunlight, allowing the study of trace gases at extremely low concentrations. The levels of atmospheric components can be determined by measuring sunlight that has passed through the Earth's atmosphere and accounting for each element's unique absorption properties.

### 1.7.6 Balloon-based direct sunlight DOAS

This setup, which employs a balloon to lift the DOAS equipment, enables high-altitude measurements closer to the stratosphere, yielding new insights into the vertical profiles of atmospheric trace gases. One advantage is that measurements can be done in areas with



reduced air dispersion and interference from ground-level sources, potentially increasing the accuracy of trace gas observations.

#### *1.7.7 Satellite-Occultation based DOAS*

This technique, known as occultation, uses a satellite equipped with DOAS technology, such as SCIAMACHY, to follow light from the sun or another star as it approaches the Earth's atmospheric horizon. By monitoring light at various altitudes throughout satellite orbits, it is feasible to track changes in gas flow over time and undertake a comprehensive analysis of the composition of the atmosphere.

#### *1.7.8 Zenith Scattered Light (ZSL-DOAS)*

When ZSL-DOAS is employed, the detector detects light that has diffused to the Earth's surface and guides it upward, or towards the zenith. This design is ideal for investigating the stratosphere and high troposphere. Twilight is an ideal moment to investigate atmospheric chemistry because sunlight remains in the stratosphere for the longest period of time, allowing for precise analysis of stratospheric compounds.

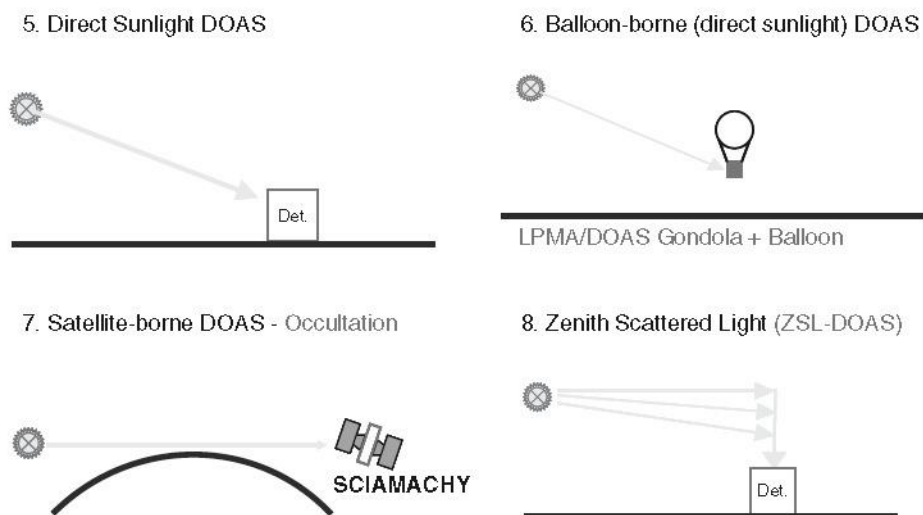


**Figure 3: Schematic Diagram of Direct Sunlight DOAS, Ballon Born DOAS, Satellite DOAS and Zenith Scattered DOAS.**

#### *1.7.9 Multi-Axis DOAS (MAX-DOAS)*

The Multi-Axis DOAS approach employs a fixed detector that records light from a variety of angles and paths, including the horizon, zenith, and several angles in between. This design enables the simultaneous recovery of trace gas concentrations at multiple altitudes, ranging from the stratosphere to ground level. MAX-DOAS provides a vertical profile of atmospheric trace gases by detecting scattered sunlight from various viewing angles. This allows for a more comprehensive understanding of air stratification and the spatial dispersion of contaminants.

#### *1.7.10 Airborne Multi-Axis DOAS (AMAX-DOAS)*

When installed on an airplane, the MAX-DOAS in flight provides broad and flexible coverage over a wide variety of altitudes and geographic locations. While in flight, the aircraft's instrumentation collects scattered sunlight from various angles, allowing for data

collection across a three-dimensional region of the sky. Two applications where AMAX-DOAS is quite beneficial are mapping the distribution of trace gases across large areas and determining air composition in remote or otherwise inaccessible locations.

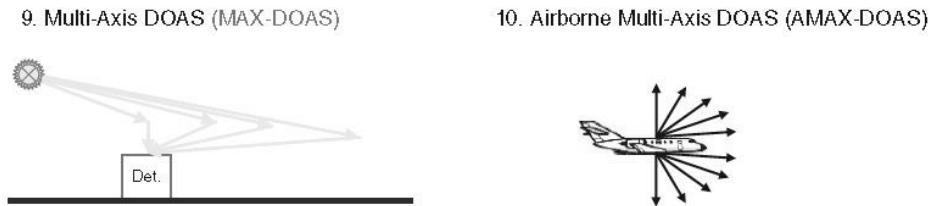


**Figure 4: Schematic Diagram of Multi-Axis DOAS and Airborne Multi-Axis DOAS**

#### *1.7.11 Imaging DOAS*

By exercising image technology to gather spatially resolved spectrum data, image DOAS expands on the capabilities of traditional DOAS. Using a two-dimensional detector array, this apparatus records dispersed light across a wide field of view, resulting in images that simultaneously provide spectral information from multiple regions of the atmosphere. An extensive area mapping of gas distributions using this design is highly beneficial for identifying pollution sources and dispersion patterns.

#### *1.7.12 Satellite-borne DOAS*

Using a satellite platform, this DOAS arrangement directs the detection system directly downward (nadir) to the Earth's surface. The satellite collects backscattered light from the atmosphere, allowing for a large-scale and continuous assessment of atmospheric trace gases. The nadir observational geometry enables continuous monitoring of the atmospheric column underneath the satellite's path, which contributes to global mapping of air quality and environmental changes. Another method of scattered light measurements is where the satellite's DOAS system detects light scattered at the limb of the Earth's atmosphere, or the

edge as seen from the satellite. This method enables the profiling of atmospheric layers and the identification of trace gases at various altitudes, particularly in the stratosphere and high troposphere. Limb measurements are essential for comprehending the vertical structure of the atmosphere and the kinetics of atmospheric processes.

*1.7.13 Inverse DOAS (Determination of the Photon Path Length  $L$  in Clouds)*

Optical depths and scattering qualities can be found by estimating photon path length in clouds using 'inverse DOAS'. By measuring the light scattered by clouds, researchers can get insight into how clouds impact light propagation and, consequently, atmospheric trace gas absorption and scattering processes.

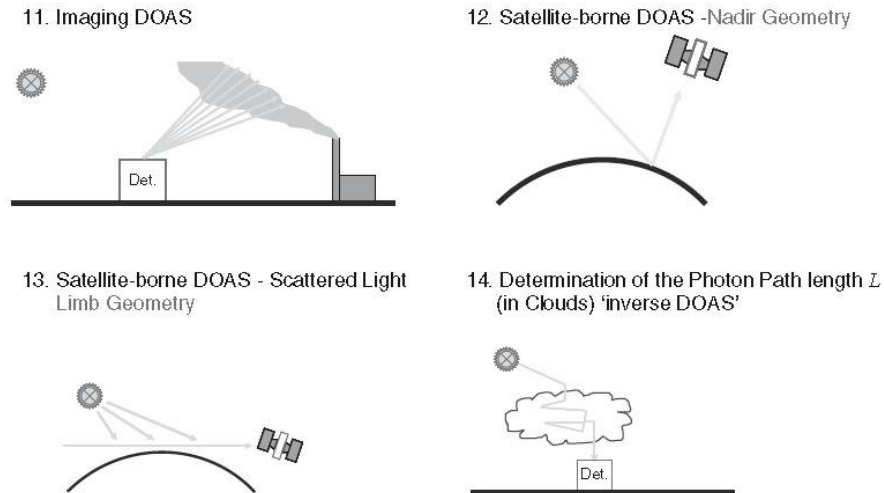


**Figure 5: Schematic Diagram of Imaging, Satellite Nadir, Satellite Scattered and Inverse DOAS.**

**1.8 DOAS Experimental Setup**

At the core of the setup is a light source that emits radiation, which traverses the atmospheric path of length  $L$  and is subjected to absorption by various trace gases within

the atmosphere. The transmitted light is then collected by a detector. A spectrograph is utilized to disperse the light into its constituent wavelengths, which are then recorded by a two-dimensional detector array and sent to a personal computer (PC) for further analysis.

The data processing involves several steps depicted on the right side of the figure:

a. The raw spectrum  $I(\lambda, L)$  is first presented, showing the intensity of light across a range of wavelengths (in this case, approximately 300 to 320 nm), where the absorption features due to atmospheric constituents are visible as dips in the spectrum.

b. The raw spectrum is then convolved with an instrument function  $H$ , resulting in the convolved spectrum  $I'(\lambda, L)$ . This step simulates the effect of the instrument's resolution on the measured spectrum, which can smooth out the finer details due to the instrument's finite resolving power.

c. The processed spectrum is further discretized into binary units (pixels) corresponding to the detector array, resulting in  $I'(i)$ , where  $i$  represents the pixel number. This discretization is necessary for digital data analysis and facilitates the next steps in the processing chain.

Finally, the logarithm of the discrete spectrum  $J(i)$  is taken, which is a common step in DOAS analysis to linearize the Beer-Lambert law and simplify the retrieval of gas concentrations from the measured absorbance features.

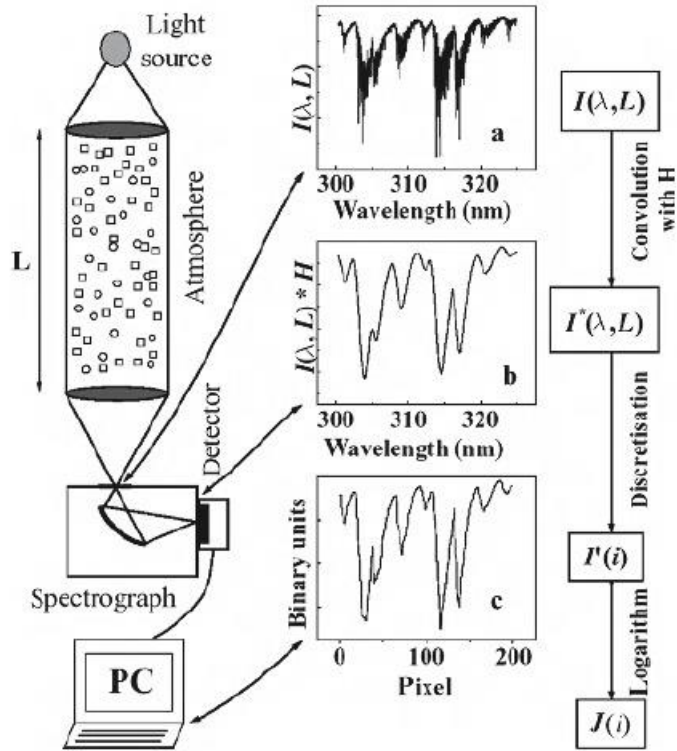


**Figure 6: DOAS Experimental Setup Schematic Flowchart**

### 1.9 Ground vs Satellite DOAS

For the ground-based system, different light paths demonstrate the various angles at which air observations can be taken. These routes show sunlight being scattered by the atmosphere and reaching ground-based detectors at various angles, allowing for the investigation of atmospheric composition over multiple layers. This method can involve measurements of the sun directly, off-axis, and at the zenith, all of which yield valuable information for vertical trace gas profiling in the atmosphere. The satellite-borne DOAS system has to gather sunlight that has been backscattered by Earth's atmosphere in order to operate. Because of the satellite's wide coverage, atmospheric trace chemicals may be monitored globally. These measurements are crucial for long-term atmospheric monitoring

and help us understand global climate and environmental change. Both methods are based on the same underlying principle: measure the absorption of sunlight by air gases at various wavelengths to determine concentrations.

## **1.10 Current Study Instrumentation**

### *1.10.1 Ground-Based DOAS (Pandora Spectrometer)*

The NASA Pandora spectrometer is utilised in atmospheric chemistry research to quantify the amounts of trace gases, including ozone (O<sub>3</sub>), nitrogen dioxide (NO<sub>2</sub>), and formaldehyde (CH<sub>2</sub>O), in the atmosphere. It functions by detecting the different UV-visible absorption signals that these gases cause in sunlight. Pandora use Differential Optical Absorption Spectroscopy (DOAS) to compare the actual sun spectra with a theoretical reference. Any deviations in the spectra are attributed to the absorption interactions between trace gases in the observed air column. Pandora utilises its spectrum detection skills to precisely identify the quantities of trace gases present during the transmission of solar light to Earth's surface. These trace gas levels are extremely small and challenging to observe. By employing this advanced detection technique, it is possible to monitor the atmosphere in near-real-time with a temporal precision of 80 seconds for detecting the levels of trace gases.

### *1.10.2 Ground-Based Monitor (Horriba NO<sub>x</sub> Analyzer)*

The Horriba NO<sub>x</sub> Analyzer enables the instantaneous quantification of nitrogen oxides (NO<sub>x</sub>), comprising nitrogen dioxide (NO<sub>2</sub>), nitric oxide (NO), and their amalgamation. It employs the well-known technique of cross-flow modulated semi-decompression chemiluminescence, a dependable and precise method for detecting nitrogen oxides. This approach is based on the chemiluminescent interaction of NO and ozone, which generates a luminescence signal that is proportional to NO concentration.

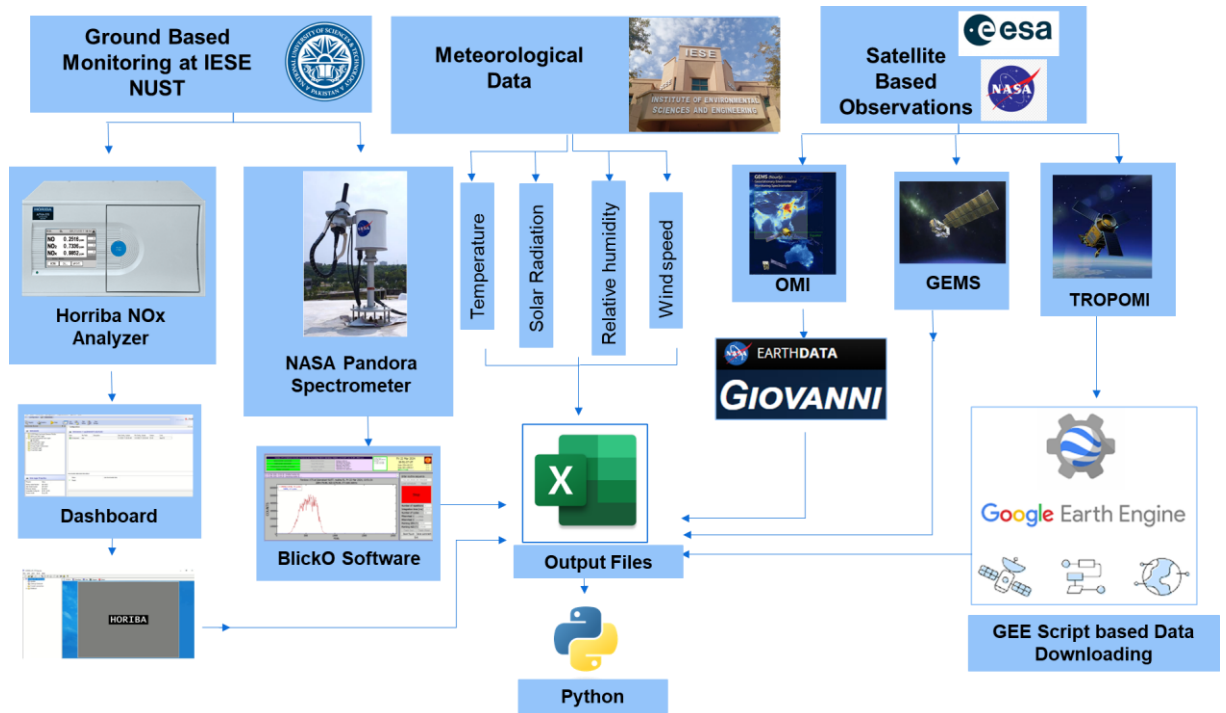
The conversion of NO<sub>2</sub> to NO enables an indirect assessment of NO<sub>2</sub>, allowing for detailed monitoring of NO<sub>x</sub> levels. The Horriba NO<sub>x</sub> Analyzer is distinguished by its internal, self-sufficient dry-method sampling technology, which improves sensitivity and accuracy. The Horriba NO<sub>x</sub> Analyzer advantages greatly from this dry-method technology, which eliminates the need for wet chemical treatments and allows for reduced maintenance and continuous monitoring. It also ensures that the sample gas will remain unchanged during analysis, a crucial component of accurate air quality monitoring.

### *1.10.3 Satellite Borne DOAS (OMI & TropOMI)*

An approach to remote sensing known as Differential Optical Absorption Spectroscopy (DOAS) that is carried out by satellites allows for the determination of atmospheric trace gas concentrations from orbit. This novel method makes use of spectrometers carried by spacecraft to detect the Earth's surface and atmospheric scattering and reflection of sunlight. Satellite-based DOAS is a great tool for worldwide air quality, greenhouse gas, and other atmospheric constituent monitoring because it assesses spectral absorption properties that signal different atmospheric gases. One of the key benefits of satellite-borne DOAS is its capacity to cover large geographic areas and generate a comprehensive and consistent dataset for regional and global atmospheric assessments. In contrast to spatially limited ground-based measurements, satellite observations can fill in data gaps in data-poor locations such remote land areas and the ocean. This thorough coverage is essential for following long-distance pollutant transmission and comprehending global atmospheric processes.

1. OMI (Ozone Monitoring Instrument)
2. TropOMI (TROPOspheric Monitoring Instrument)
3. Geostationary Environmental Monitoring Spectrometer (GEMS)





The study uses a NASA Pandora Spectrometer and a Horiba NO<sub>2</sub> Analyzer for ground-based monitoring, with NO<sub>2</sub> measurements taken monthly. These measurements are supplemented with weather station data to cover any gaps in the temporal and spatial variability of NO<sub>2</sub> levels that may have been caused by the weather. This way of thinking is established by evaluating previously published literature to ensure that a novel approach is developed following current scientific understanding and methodology. The study influences satellite-based monitoring by analyzing data from two main satellite instruments: the Ozone Monitoring Instrument (OMI) and the TROPOspheric Monitoring Instrument (TROPOMI). These sensors are extensive global satellite datasets from which additional tropospheric NO<sub>2</sub> profiles geospatially relevant to Islamabad will be extracted. The next step in this phase is to conduct statistical studies on the acquired data. This evaluation comprises both trend analysis, which determines changes in NO<sub>2</sub> levels over

time, and correlation analysis, which describes the relationships between NO<sub>2</sub> concentration and environmental factors.

### **1.11 Significance of the Study**

Environmental science is bound to have a major impact on ecology and human health because of the abundance of trace gases in the air. There is a strong correlation between the changing composition of the atmosphere and the negative health effects it has on human populations, as shown by the escalating air pollution levels around the world. These trace gases affect atmospheric chemistry and climatic dynamics to a large extent, regardless of their concentration in the atmosphere. The rapid alteration of atmospheric conditions brought about by the emission of substances such as sulphur dioxide (SO<sub>2</sub>), nitrogen dioxide (NO<sub>2</sub>), ozone (O<sub>3</sub>), and formaldehyde (HCHO) can have devastating effects on the environment. The US Environmental Protection Agency (EPA) has classified nitrogen dioxide (NO<sub>2</sub>) as a criterion air pollutant. The majority of nitrogen dioxide (NO<sub>2</sub>) emissions come from combustion activities and cars. It is this gas that serves as a building block for tropospheric ozone. As a temporary greenhouse gas that increases the trapping of infrared radiation, tropospheric ozone is a major contributor to both urban smog and climate change. Since NO<sub>2</sub> has such a profound effect on human health and helps produce huge tropospheric ozone through photochemical processes, an important driver of climate change and global warming, studying this gas is of the utmost importance.

### **1.12 Study Objectives**

- To install and set up the NASA Pandora Spectrometer.
- To quantify atmospheric trace gas Nitrogen dioxide.
- To validate satellite-based NO<sub>2</sub> with Pandora and other ground-based instruments



## CHAPTER 2: LITERATURE REVIEW

All of the atmospheric components are described in detail in this chapter. The light source and its interactions with Earth's atmospheric profile are described in the text. Radiative equilibrium and the dynamics of the climate are also covered in detail. This article delves into the nitrogen oxide atmospheric chemistry and the significance of planetary boundary layers. This article provides a thorough analysis of how spectroscopic observations of trace gases in the atmosphere have evolved over time. To do this, it examines previous research with a critical eye and explains how these gases were better monitored over time. In this section, we look at the shortcomings and restrictions of past and present studies.

### 2.1 Earth's Source of Light

The Sun serves as the primary source of electromagnetic (EM) radiation, vital for remote sensing endeavors on Earth. While the average Earth-Sun distance is approximately 149.6 million kilometers, allowing sunlight to reach us in just over eight minutes, the Sun's EM emission is subject to fluctuations. Solar activities such as sunspots and solar flares, governed by the Sun's magnetic field, can cause variability in solar radiation, potentially affecting the precision of remote sensing data. These inconsistencies, along with the fusion processes within the Sun and the varying Earth-Sun distance over time, must be meticulously accounted for in remote sensing to ensure data accuracy.

For assessing the climate and inhabitability of any planet, there is a principle known as radiative equilibrium. Radiative equilibrium is referred to as the equilibrium between the incoming emitted longwave solar radiation and the absorbed short-wave radiation. The delicate equilibrium between the incoming and outgoing radiation of the planet is determined by Stefan Boltzmann's law and the Earth's albedo. The legislation

unequivocally emphasizes the significance of radiation chemistry on the Earth's surface. Hence, this equilibrium involves temperature estimation of the Earth that provides the enhanced understanding of the Earth's climate and the sources & sinks of the incoming & outgoing heat, which is more concentrated at the equator and diminishes toward the poles, resulting in varied insolation and climate patterns across different latitudes.

## **2.2 Energy Flow Mechanism of Climate System**

The climate system plays a crucial role in regulating the energy dynamics of Earth. In this scenario, the Earth's rate of solar energy absorption and the rate at which it emits thermal radiation into space are finely matched. Both the Earth's surface and atmosphere absorb solar radiation, aided by aerosols and clouds that enhance the reflectivity of the atmosphere. The major source of the greenhouse effect is the balance between energy production and absorption, which leads to an increase in surface temperatures and a drop in air pressure due to the reflection of absorbed energy. Oceans play a crucial role in this energy transfer due to their ability to store and transfer heat through processes such as evaporation and condensation.

The interaction between Earth's surface and the atmosphere is characterized by a nuanced energy exchange, wherein approximately half of the incoming shortwave solar radiation penetrates the surface, and a smaller proportion, about 19%, is absorbed by atmospheric gases. While the Earth's surface emits energy, certain atmospheric windows permit a fraction of this radiation to escape directly into space. However, the bulk of the energy is absorbed and subsequently re-radiated by the atmosphere, enhancing the planet's thermal retention through the greenhouse effect. This atmospheric modulation elevates Earth's mean temperature from a hypothetical 255 K to about 288 K, an increment essential for sustaining the planet's life-supporting climate.

## **2.3 Interaction of Solar Radiation with Atmosphere**

The basic effects of radiation in the atmosphere include absorption, emission, scattering, refraction, reflection, diffraction, and interference. These processes describe how radiation interacts with molecules, particles, and surfaces within the atmosphere, which is essential for understanding phenomena such as the greenhouse effect and the overall climate system. The primary factors that determine atmospheric energy budgets are reflection, scattering, and emission. Clouds, aerosols, and the Earth's surface primarily deflect or disperse around 30% of the solar radiation that penetrates Earth's atmosphere, redirecting it back into space. 30% of the energy is re-emitted by clouds and the Earth's surface, and a portion of this is transported through convection. The phenomenon of light absorption in the atmosphere is extensively explained by mathematical equations and concepts such as Lambert-Beer's law. This law establishes a relationship between the absorption coefficient and the route length, which both contribute to the decrease in light intensity as it passes through the medium.

## **2.4 Earth's Atmospheric Layers & Composition**

The only planet in our solar system having liquid water on its surface is Earth which is home to a wide variety of life forms due to its diverse chemical composition and favorable environment. Earth completes one full round around the Sun every 24 hours. It takes around eight minutes for light from the Sun to reach Earth. Earth System comprises of Atmosphere, Hydrosphere, and Lithosphere. Earth is surrounded by some protective layers of atmosphere having distinguished thermal characteristics, chemical composition, movement, and density, and the layers of most important concern are the Troposphere & Stratosphere. The lowest layer troposphere (7 miles above Earth's surface) contains three-fourths of all air and is composed of a variety of gases in specific amounts (nitrogen about 78% of air, oxygen 21% & argon 0.93%, water vapors & CO<sub>2</sub> in trace amounts). There are several forms of water vapour in the atmosphere and on the surface of the Earth, including liquid, solid, and vapour aerosols. Cloud condensation nuclei (CCNs) are formed when

minute particles in the atmosphere dissolve in water and have the advantageous characteristics of both scattering and absorbing sunlight. The ozone layer, which is found 7–31 miles above the troposphere, acts as a natural screen, absorbing solar UV radiation and protecting the Earth's surface from harm. The Mesosphere (31–53 miles), Thermosphere (53–375 miles), and Exosphere (375–6200 miles) are the layers that sit directly above the Stratosphere.

A number of mechanisms, including adiabatic vertical transport, radiative cooling of water vapour, ozone layer absorption, and thermosphere oxygen absorption, influence the vertical temperature structure of Earth's atmosphere. This structure results in a dynamic atmosphere with strong mixing in the troposphere, stratified and stable conditions in the stratosphere, and very low humidity above the tropopause. Other types of limited interaction between the troposphere and stratosphere include tropical convection, tropopause folds, and subsidence in polar latitudes.

Light throughout the visible and ultraviolet spectrums interacts with different layers of the atmosphere based on their respective wavelengths. Wavelengths ranging from 100 to 240 nanometers are classified as far-ultraviolet and are absorbed by harmful gases in the thermosphere and mesosphere. Ozone gas in the stratosphere mostly absorbs ultraviolet C radiation, which has a wavelength range of 250–290 nanometers. UV-B radiation undergoes a reaction with tropospheric ozone gas within the range of wavelengths from 290 to 320 nm. Specifically, the UV-A spectrum encompasses wavelengths ranging from 320 to 380 nm within the polluted troposphere, where the interaction of oxygen and nitrogen dioxide occurs. The range of 400–750 nm, commonly referred to as visible light, is the region where numerous atmospheric trace gas species are absorbed and engage with the Earth's surface.

## **2.5 Planetary Boundary Layer**

When investigating the mechanisms of air pollution and quality, the Planetary Boundary Layer (PBL) is an indispensable component of Earth's atmosphere. The PBL is the region of the troposphere that experiences direct surface interaction and responds in approximately an hour to surface forcings such as heat, moisture, and momentum. It might fluctuate depending on the weather, topography, and time of day. In mid-latitudes, it usually stretches from the ground up to 0.5 to 2 km during the day.

The three levels of PBL are the surface, mixed, and transition. About 10% of the depth of the Planetary Boundary Layer (PBL) is the Earth's surface, namely the layer that lies nearest to it. Significant frictional forces from the Earth's surface have a major impact on the atmosphere. Mixed Layer is Located above the surface layer, this region experiences turbulent mixing due to thermal convection (warm air rising and cool air descending), making the temperature and concentrations of gases and particles more uniform. Entrainment Zone/Transition Layer is the top part of the PBL that acts as a buffer between the well-mixed air below and the more stable, stratified air of the free troposphere above. With sunrise, the surface heats up, causing the air to warm and rise, leading to the growth of the convective mixing layer. This process dilutes pollutants and can improve air quality. From midday to Afternoon, the PBL reaches its maximum depth due to strong surface heating and vertical mixing, leading to a relatively uniform distribution of air pollutants within the PBL. From Evening to Night, as the surface cools, vertical mixing decreases, leading to a more stable atmosphere with less mixing. This results in a shallower PBL, where pollutants can accumulate, potentially worsening air quality. The depth of the PBL directly affects the concentration of pollutants near the surface. A shallower PBL can lead to higher concentrations of pollutants, impacting human health. During the day, the PBL is deeper with more mixing, which can dilute pollutants. At night, the PBL is shallower and more stable, which can trap pollutants near the surface. The PBL depth varies seasonally, typically being deeper in the summer due to stronger heating and shallower in the winter.

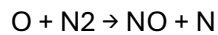


## 2.6 Atmospheric Chemistry & Transport of NO<sub>x</sub>

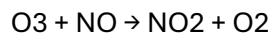
NO<sub>x</sub> atmospheric chemistry is of significant importance as it can impact the formation and destruction of Hydroxyl radicals which are considered to be detergents of the atmosphere due to their oxidizing ability. NO<sub>x</sub> not only pollutes the atmosphere emitted by various natural & anthropogenic sources but also has a significant role as a catalyst in various natural cycles such as tropospheric ozone, formaldehyde and sulfur dioxide. NO<sub>x</sub> role as a catalyst will ultimately disturb the natural equilibrium of the ozone cycle destroying the stratospheric ozone layer that acts as a protecting shield of the earth from severe solar radiation and global warming events. Naturally, NO<sub>x</sub> is formed by lightning strikes on earth, wildfires, soil & vegetation emissions, marine emissions, or volcanic activities. Anthropogenic sources include automobile combustion engines, power plants, extensive agricultural farming, intentional forest fires, and various industrial emissions. Nitrogen species which play an important role in atmospheric chemistry are NO<sub>x</sub>(NO+NO<sub>2</sub>), N<sub>2</sub>O, and NH<sub>3</sub>. N<sub>2</sub>O is a potent greenhouse gas emitted during nitrogen fixation by bacteria in soil and marine environments. NH<sub>3</sub> is predominantly emitted from livestock, and agricultural waste and acts as a neutralizing agent in the atmosphere for nitric and sulfuric acids.

So, before going into in-depth chemistry of NO<sub>x</sub>, there is a need to understand the chemistry of ozone in the atmosphere. Ozone in the troposphere is potentially a short-lived greenhouse gas which is the major component of photochemical smog, injurious to human health, animals, and plants as well. Tropospheric ozone also serves as a precursor to the atmospheric detergent OH. Ozone in the stratosphere forms a protective layer known as the ozone layer which undergoes natural formation and destruction cycle. Oxygen molecules change into oxygen atoms when they are subjected to short-wave ultraviolet radiation. The next step is for these atoms to react with other oxygen molecules, which creates ozone.

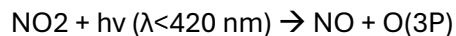
Most nitrogen oxides in the air are produced by nitric acid (HNO<sub>3</sub>). It is a component of acid rain when mixed with sulfuric acid (H<sub>2</sub>SO<sub>4</sub>). Ozone in the air oxidises nitric oxide (NO) lasting more than a few seconds. Throughout the day, nitrogen oxides quickly react with one another. Combustion and other processes that raise air temperatures above 2000 Kelvin produce nitrogen oxides in the atmosphere. Here, the heat energy is sufficient to split O<sub>2</sub> into its component oxygen atoms. Subsequently, these atoms combine with nitrogen molecules to form nitrogen oxides (NO).



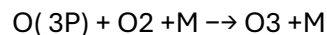
The production of N<sub>2</sub>O is a further consequence. N<sub>2</sub>O does not have any chemical function in the troposphere because it is inert there (residence duration of about 120 years). Atomic oxygen can be released for further reactions when strong ultraviolet (UV) radiation in the stratosphere break down N<sub>2</sub>O at approximately 298 nm. Quick oxidation of NO by ozone yields NO<sub>2</sub>:



The sun's ultraviolet light (UV) below 420 nm can photolyze most of the NO<sub>2</sub> generated, leading to the creation of ozone. This happens rapidly in mid-afternoon sunlight, and the typical residence period for NO<sub>2</sub> is just a few minutes.



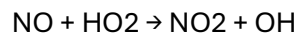
As ozone (O<sub>3</sub>) is formed by quick reaction of O(3P) with oxygen (O<sub>2</sub>):



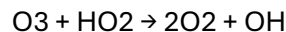
Due to the interaction between energy and rotational momentum during collisions, M, such as nitrogen (N<sub>2</sub>) or oxygen (O<sub>2</sub>), is a crucial counterpart. The need for O(3P) in the processes is eliminated as each NO<sub>2</sub> molecule generates two ozone molecules and one NO molecule. However, the mechanism that produces nitrogen oxide (NO) and ozone (O<sub>3</sub>) will also restore nitrogen dioxide (NO<sub>2</sub>). Ultimately, the Leighton ratio (Leighton, 1961) manifests as a photo-stationary condition of NO<sub>2</sub> and NO.

$$[NO][NO_2] = jNO_2kNO.[O_3]$$

Depending on ozone levels and photolysis frequency, the Leighton ratio in the lower atmosphere can range from 0.5 to 1. The faster rate of NO<sub>2</sub> photolysis causes the ratio to rise with altitude. In the photo-stationary state, ozone does neither form or diminish. When there are enough nitrogen oxides (NO<sub>x</sub>) to interact with hydroxyl radicals (RO<sub>2</sub>), peroxy radicals, and HO<sub>2</sub>, ozone is formed. The following reaction might occur under specific conditions:



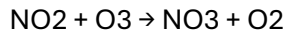
Volatile organic compounds, or VOCs, are frequently found in urban settings and have the ability to oxidise and produce peroxy radicals. During this process, it is anticipated that other chemicals, like HNO<sub>3</sub>, will be produced in trace amounts. Consequently, ozone is produced by the aforementioned mechanism, although NO does not significantly reduce it. This could result in photochemical smog, which is characterised by a high concentration of ozone, oxidised volatile organic compounds, and organic aerosols. However, OH and molecular oxygen can be produced through the reaction of ozone with peroxy radicals. Having said that, this only matters at very low NO<sub>x</sub> concentrations.



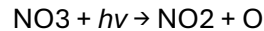
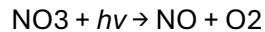
Hence, whether more ozone is created or eliminated by the aforementioned reactions is influenced by the relative abundances of NO<sub>x</sub> and VOC. The interaction with OH produces the majority of NO<sub>2</sub>'s breakdown product, nitric acid (HNO<sub>3</sub>).



As a result, this process serves as a sink for both NO<sub>2</sub> and OH. Thus, NO<sub>2</sub> helps to degrade the quantity of the hydroxyl radical. NO<sub>2</sub> can be oxidized even more to NO<sub>3</sub>:



There are two possible ways of NO<sub>3</sub> interacting with sunlight during daylight which results in breakdown of NO<sub>3</sub> due to photolysis:



NO<sub>3</sub> quickly interacts with NO to form NO<sub>2</sub>:



A significant rise in NO<sub>3</sub> levels is not possible during the day due to photolysis and NO levels. Nevertheless, NO<sub>3</sub> can accumulate in the air throughout the night since photolysis doesn't happen and NO levels are low. Also, NO<sub>3</sub> and NO<sub>2</sub> can combine to form N<sub>2</sub>O<sub>5</sub>:



NO<sub>3</sub>, NO<sub>2</sub>, and N<sub>2</sub>O<sub>5</sub> are in a state of thermodynamic equilibrium, which is extremely temperature-dependent. N<sub>2</sub>O<sub>5</sub> is mostly decomposed by interaction on aerosol surfaces, and it is an essential NO<sub>x</sub> process in local, regional and global context.

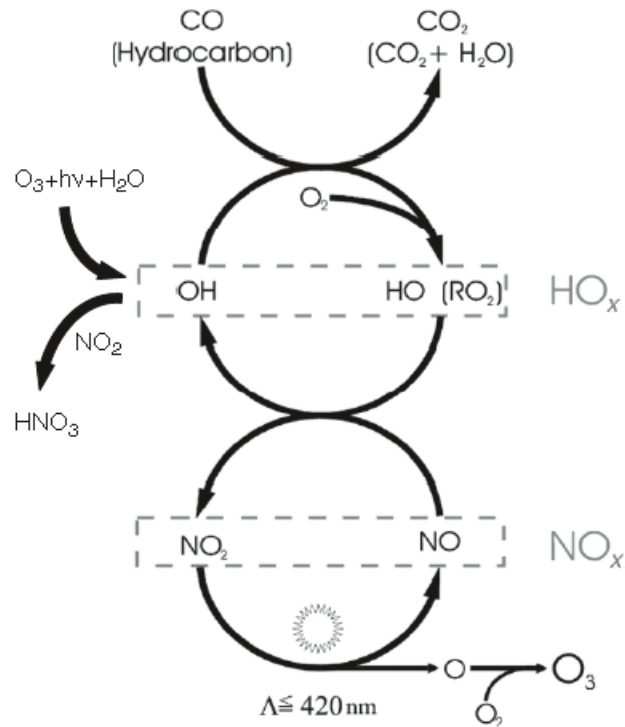
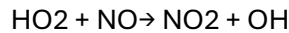


**Figure 7: Atmospheric Chemistry cycle of NO<sub>x</sub>**

NO<sub>2</sub> is formed in the presence of HO<sub>2</sub> radicals, whereas HO<sub>2</sub> radicals are produced in the atmosphere by CO oxidation.



Assuming a low tropospheric NO<sub>x</sub> limit, the rate of O<sub>3</sub> generation is concentration-independent and increases linearly with NO. By increasing NO<sub>x</sub>, the amount of generated O<sub>3</sub> decreases, although it climbs linearly with CO and HO<sub>x</sub> in the high NO<sub>x</sub> limit. A number of environmental chemical compounds react with NO<sub>3</sub>. Isoprene and terpene reactions, interactions with Dimethyl sulphide, and other natural volatile organic compound interactions stand out.

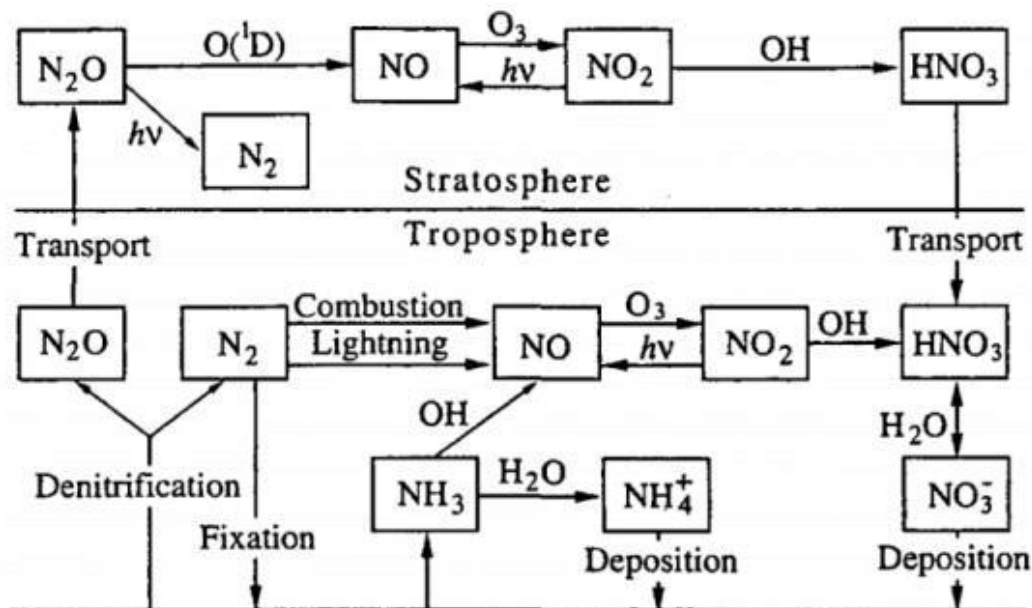


**Figure 8: Stratospheric & Tropospheric Reactions of NO<sub>x</sub>**

## 2.7 Historical Background of Spectroscopic Measurements

Over the last century, spectroscopic analysis of the Earth's atmosphere has given substantial findings, punctuated by watershed moments that have significantly impacted our understanding of atmospheric composition. The trip began in 1879 when Marie Alfred

Cornu concluded a trace species producing UV absorption based on observed intensity decrease at the UV spectrum edge. In 1880, Sir Walter Noel Hartley discovered that ozone absorbs UV radiation below 300 nm, introducing what is now known as the Hartley bands. In the meantime, M. J. Chappuis discovered that ozone absorbs visible light, which is why the Chappuis band was named after it and hypothesized that ozone contributes to the blue colour of the sky. The field was further extended with the discovery of the Huggins bands, named after Sir William Huggins' 1890 finding of new spectral lines in Sirius that were attributed to ozone. The enhanced knowledge was assisted in 1904 by Knut Johan Ångström's discovery of ozone's infrared absorption at wavelengths.

Major progress was achieved throughout the 20th century, as evidenced by Albert Wigand's balloon observations in 1913, which showed that ozone consistently absorbed UV light up to a height of 10 km. According to Lord Rayleigh's 1918 calculations, atmospheric ozone must exist in a layer above 10 km height. Charles Fabry and Henri Buisson's 1920 measurements of the ozone column supported this notion. Gordon Miller Bourne Dobson's use of a specialized ozone spectrometer in 1925 made research easier, and Paul Götz's 1926 observation of the 'Umkehr' effect verified the altitude of the ozone layer at about 25 km. Erich Regener's direct observation of the ozone layer using UV spectroscopy in 1934, as well as Marcel Migeotte's identification of methane and carbon monoxide using near-infrared absorption spectroscopy in 1948, demonstrated the variety of atmospheric species. David R. Bates and Marcel Nicolet discovered the hydroxyl radical's emission bands in the nightglow in 1950, and Dieter Perner and his team detected the first OH radicals using differential optical absorption spectroscopy in 1975, highlighting the complex interplay of atmospheric chemistry. These milestones, which each represent major advancements in the discipline, highlight the history of our understanding of atmospheric spectroscopy and its importance in atmospheric science.

NO<sub>2</sub> absorbs visible light and has a strong absorption band in the visible spectrum, particularly around 400-500 nm. This range is characterized by a broad absorption feature known as the "NO<sub>2</sub> Chappuis band." NO<sub>2</sub> also absorbs ultraviolet (UV) light, with significant absorption bands below 400 nm, which are used in DOAS and other remote sensing techniques for atmospheric NO<sub>2</sub> measurements. The visible absorption spectrum of NO<sub>2</sub> allows for its detection in the lower atmosphere, where it is a significant pollutant contributing to photochemical smog and adverse health effects.

## **2.8 Research Studies on NO<sub>2</sub> Monitoring**

Oppenheimer et al. (2004) measured the amount of NO<sub>2</sub> released into the air when burning sugarcane fields using a tiny UV spectrometer. Similar to this, Oppenheimer et al. (2005) used scattered UV light spectroscopy and came to the conclusion that the main source of NO<sub>2</sub> in Antarctica was the active lava lake of Mt. Erebus. Platt and Stutz (2008) established the foundation for DOAS and promoted advancements in atmospheric chemistry and atmospheric trace gas measurements by investigating the atmospheric chemistry of trace gases and assembling a variety of DOAS equipment. Platt (2008) gave a summary of the technology being used to monitor air pollution today and what is to come in terms of tracking various air contaminants in the future. In 2009, Kern created the SO<sub>2</sub> camera, which was utilised in conjunction with DOAS to study the effects of SO<sub>2</sub> on atmospheric chemistry and volcanic emissions. Kern et al. 2020 measured the different gases released by the 2018 eruption of Kilauea Volcano using ground-based DOAS equipment.

In order to study the seasonal and vertical atmospheric patterns of NO<sub>2</sub>, Wang et al. (2017) used MAX-DOAS and other trace gases. Their findings held true even in cloudy situations. When weather patterns were taken into consideration, the analysis demonstrated how local industrial emissions from 2011 to 2014 might travel great distances in the sky. After obtaining TROPOMI data, Marias et al. 2021 used cloud slicing techniques and GEOS



Chem Modelling to study NO<sub>x</sub> emissions in the upper troposphere. Pinardi et al. 2020 assessed the tropospheric NO<sub>2</sub> column of the MAX-DOAS and direct sun instrumentation networks using the GOME 2A satellite instrument. Judd et al. 2020 compared the tropospheric NO<sub>2</sub> vertical column concentrations in Long Island Sound and New York City obtained from Sentinel 5P TropOMI with data from the NASA Pandora Spectrometer and Airborne DOAS. In a cooperative US-Korean air quality campaign in 2020, Choi et al. investigated NO<sub>2</sub> retrievals from NASA Pandora Spectrometer, Airborn Spectrometer, and Aura OMI, revealing discrepancies in the data. Kreher et al. 2020 compared a number of atmospheric trace compounds, including NO<sub>2</sub>, using MAX-DOAS and a zenith-sky UV visible spectrometer during the CINDI-2 Campaign. Sentinel 5P TropOMI NO<sub>2</sub> vertical column density accuracy and uncertainty assessment were studied by Zhao et al. 2020 in Toronto, Canada. A correlation of up to 63% was found when Ialongo et al. 2020 in Helsinki, Finland, compared the NO<sub>2</sub> total vertical column densities of the Sentinel 5P Tropomi and Pandora Spectrometer. Gryphon et al. 2019 used high-resolution NO<sub>2</sub> data retrievals from TROPOMI to conduct the first-ever study of Canadian oil sands and discovered no bias in the findings. Herman et al 2019 researched the discrepancies among the NO<sub>2</sub> retrievals from OMI and several Pandora Spectrometers. Judd et al 2019 evaluated Tropospheric NO<sub>2</sub> and the impact of spatial resolution of various satellite and airborne spectrometers in populated cities in the US. Tzortziou et al 2015 studied the Washington-Baltimore corridor and the Chesapeake Bay spatiotemporal changes in NO<sub>2</sub> and O<sub>3</sub> vertical columns using Pandora Spectrometer. Reed et al 2015 explored the meteorological effects on O<sub>3</sub> and NO<sub>2</sub> vertical column retrievals from OMI and Pandora Spectrometer in Maryland, US. Roscoe et al 2010 compared the NO<sub>2</sub> columns using MAX-DOAS and zenith sky UV Visible Spectrometer during the CINDI-2 campaign. Wang et al 2010 used three different spectrometers (MF-DOAS, Pandora, FTUVS) for the direct sun measurements at Table Mountain Facility California. Herman et al 2009 discussed the advantages of NO<sub>2</sub> retrievals from Direct Sun DOAS and compared the NO<sub>2</sub> retrievals with

OMI for validation purposes at Thessaloniki, Greece and Maryland, USA. Diemoz et al 2021 used a Brewer Spectrometer which is also a direct sun spectrometer and validated it with the 20 years of recorded data of NO<sub>2</sub> retrievals in Rome, Italy. Verhoelst et al 2021 experimented with ZSL-DOAS, MAXDOAS and Pandora Global Network. Tzortziou et al 2023 tracked the NO<sub>2</sub> pollution over New York City by comparing the total column of NO<sub>2</sub> from Pandora Spectrometer and Tropomi Retrievals which revealed that the surface concentration correlated about 87 per cent with the total NO<sub>2</sub> column of TropOMI retrievals. Di Benardino et al 2023 recently explored the NO<sub>2</sub> and O<sub>3</sub> levels of Rome Italy by exploiting Pandora and in-situ monitoring. Zhao et al 2022 monitored the levels of NO<sub>2</sub> and O<sub>3</sub> in the Greater Toronto Area, Canada by retrieving data from the Pandora spectrometer during the COVID-19 pandemic. Similarly, Tzortziou et al 2022 followed the same procedure in New York City to explore the trends of atmospheric trace gases. Karl et al 2023 proposed that the increase in NO<sub>x</sub> levels will induce the increased toxic downward ozone flux in the atmosphere which will lead to global warming events. Kotsakis et al 2023 used the HYSPLIT model to assess the impact of meteorology over NO<sub>2</sub> and O<sub>3</sub> surface Pandora Retrievals. Early 2022 studied the strategy to validate trace gas retrievals with MAX-DOAS.

Ul-Haq et al 2014 presented the monthly averaged NO<sub>2</sub> tropospheric vertical column using OMI satellite data for four years. Similarly, Ul-Haq et al 2015 explored the OMI decade data to assess the tropospheric column over South Asia. Ul-Haq et al 2018 applied a model for tropospheric NO<sub>2</sub> in South Asia climatic zones and found an 82 per cent correlation. Ul-Haq et al 2017 assessed the tropospheric NO<sub>2</sub> column and various anomalies over different river basins. Tariq et al 2023 reported the greenhouse gas emissions from intentional crop burning using remote sensing satellites.

According to Anjum et al 2021, Pakistan lies in an Indo-Gigantic region where countries are succumbing to air pollution and there is a need for mutually coordinated scientific

research and collaboration to tackle air pollution scenarios. Khokhar et al 2022 reported the recurring smog events in Pakistan and the need for regional cooperation. In Pakistan, a major source of NO<sub>2</sub> is transportation followed by industries and power plants (Anjum et al 2021). Majeed et al 2024 researched the consecutive smog events in the most polluted city in the world Lahore where AQI exceeded the hazardous level. Saeed et al 2023 explored the toxic trace metals among brick kiln workers in Lahore. Murtaza et al 2018 reported the spatiotemporal variations of Tropospheric NO<sub>2</sub> columns extracted from SCIAMACHY, OMI & GOME-2. Khokhar et al 2017 investigated the NO<sub>2</sub> concentration in Islamabad using MAX-DOAS and compared it with satellite-based validation in which the result showed an 81 per cent correlation. Khokhar et al 2016 assess the two scenarios of the utilization of compressed natural gas and without compressed natural gas by retrieving NO<sub>2</sub> data from MAX-DOAS over twin cities of Pakistan. Khokhar et al 2015 analyzed the seasonal & temporal variation over a decade utilizing SCIAMACHY NO<sub>2</sub> data retrieval of Pakistan. Shoaib et al 2020 researched formaldehyde using MAX-DOAS in Pakistan. Khan et al 2018 followed the phenomenon of Car MAX-DOAS to assess the formaldehyde profile of the campaign region. Zeb et al 2019 exploited the various satellite-based data products of atmospheric trace gases for the temporal & seasonal analysis.

## **2.9 NASA Pandora Spectrometer**

Pakistan has acquired the NASA Pandora Spectrometer for South Asia in order to investigate the composition of atmospheric trace gases. The spectrometer is a terrestrial apparatus that may be operated from a distance. It detects the optical characteristics of trace gases in the atmosphere to create a vertical profile of their distribution. In order to ascertain the optical characteristics of the air column, the Pandora spectrometer employs differential optical absorption spectroscopy. The device has the ability to measure a diverse array of trace gases, including formaldehyde (HCHO), ozone (O<sub>3</sub>), sulphur dioxide (SO<sub>2</sub>), and nitrogen dioxide (NO<sub>2</sub>). The atmospheric concentration of these gases exerts a substantial

influence on agricultural productivity, human well-being, and climate dynamics. These gases are derived from both natural and anthropogenic sources, rendering them very consequential. Finally, a significant achievement in the field of regional atmospheric science has occurred with the establishment of the inaugural NASA Pandora Spectrometer of South Asia in Pakistan. Thanks to the instrument's adaptability in quantifying various trace gases and offering a vertical profile of the atmospheric composition, scientists will get a more comprehensive understanding of the sources and ultimate fate of these gases in the atmosphere. The acquisition of data by the device would substantially enhance the development of legislation aimed at mitigating the adverse effects of airborne pollutants on ecosystems and human health.

## **2.10 Research Gaps & Limitations**

After a thorough literature review, it has been found that till 2000, there were few advancements in the assessment of atmospheric trace gas retrievals. Satellite-based data products were available but either those required specialized skills to explore them or it was time-consuming. The publication of Platt & Stutz 2004, from there, opened futuristic opportunities for researchers all over the world to work on the DOAS measurements and how to make them more accurate with time. While the world is busy working on such innovative techniques, developing countries cannot even think about such technological advancements it will usually take five to ten years to address such things due to lack of knowledge and interest. A similar situation occurred in Pakistan till 2010, merely some studies done by researchers utilizing satellite-based data as ground-based measurements were not accessible due to financial constraints. MAX-DOAS and Pandora Spectrometer are the only existing ground-based monitors which are installed at IESE and NUST. MAX-DOAS is the previous version of Pandora. Pandora is named by the innovators because when they were at the initial stages of development of the instruments, they always forgot something put in the box, so they had to open it up again.

The instrument provides the direct sun and multi-axis DOAS system and allows a high-intensity spectrum of the measurement, and there is no need to add a ring effect as the instrument has the option to continuously track the sun, sky and moon as well. The Pandora instrument installed is the first one in South Asia and will be able to provide long-term atmospheric data. The study conducted will be the first one in Pakistan in which the data is validated with In-situ, TROMPOMI, and OMI satellite data.

## **SUMMARY OF RESEARCH WORK**

It is first of its kind of a research study in which first time NASA Pandora Spectrometer is used in order to monitor atmospheric trace gas and ground-based ambient air monitor HORRIBA NO<sub>x</sub> analyzer used to compare two different analytical techniques along with satellite-based data products of NO<sub>2</sub>.

## **CHAPTER 3: METHODOLOGY**

This section explains the methodology opt for conducting research. The installation of first South Asia's NASA Pandora Spectrometer in IESE, NUST and data downloading and processing techniques for tropospheric NO<sub>2</sub>.

### **3.1 Research Instrumentation and Study Area**

South Asia's 1<sup>st</sup> NASA Pandora spectrometer was installed at the Institute of Environmental Sciences (IESE), National University of Science and Technology (NUST), Islamabad, Pakistan (33.65, 72.98). The Air Noise Lab of IESE is equipped with its own autonomous LSI Weather Station, Metone Nephelometer Instruments, Low-cost Air Quality Monitor, Japanese Horriba Analyzers of NO<sub>x</sub>, SO<sub>x</sub>, O<sub>3</sub>, and CO. Addition of NASA Pandora Spectrometer not only integrated the lab-based measurements but also allowed the researchers of Pakistan to study the atmospheric trace gases which allows the detailed analysis of atmospheric chemistry and assessment of climatic effects. Moreover, the NASA Pandora Spectrometer filled the research gap by providing ground-truth data to validate the existing satellite-based measurements.

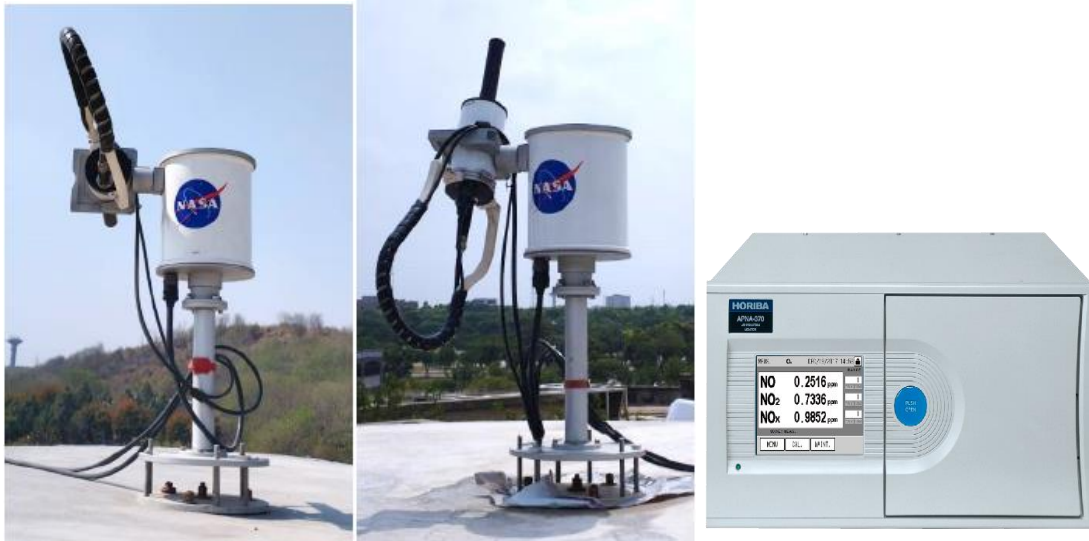


**Figure 9: NASA Pandora Spectrometer & Horriba Analyzer installed in Air Noise Lab of IESE, NUST**

The NASA Pandora Spectrometer site is surrounded by a vegetation mount peak on the west, Kashmir Srinagar Highway in the North, the East side Rawalpindi side skirts area, and the South side is clear for measurements. The study comprises rooftop instruments analysis of IESE where all the Air quality monitoring equipment is installed. For this categorical study, the ground-truth data of the NASA Pandora Spectrometer and Japanese Horriba NO<sub>x</sub> Analyzer were exploited to assess the surface concentration & tropospheric vertical column of NO<sub>2</sub>. For the validation of ground-truth datasets of these two instruments, satellite-based data from NASA Aura Ozone Monitoring Instrument and ESA Sentinel 5P TROPOspheric Monitoring Instrument were retrieved for the same coordinates (33.62, 72.98).

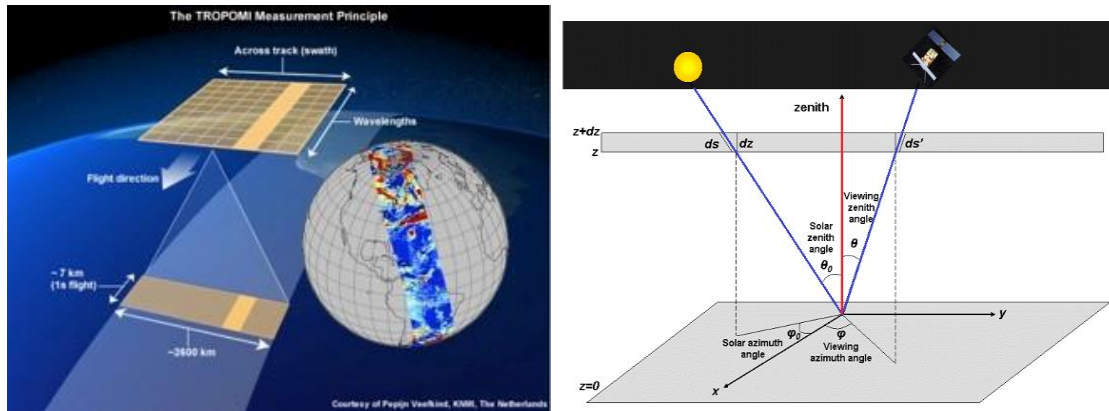


**Figure 10: Working Principle of Satellite Based Observations**

### 3.2 Installation of South Asia's 1st NASA Pandora Spectrometer

South Asia's 1st NASA Pandora Spectrometer is the first of its kind of advanced spectroscopic tool made available on the land of Pakistan due to the efforts of Dr. Muhammad Fahim Khokhar and his research group "Climate Change & Atmospheric Research Group (CCARGO) – Pakistan. NASA Pandora Spectrometer is an advanced version of the Multi Axial Differential Absorption Spectroscopy (MAX-DOAS) which was difficult & sensitive to operate for the assessment of atmospheric trace gas vertical column densities. Due to the efforts of Ulrich Platt, Jochen Stutz and Thomas Wagner in the first decade of the 20th century invented the DOAS mechanism furthermore researchers like Khokhar et.al (2006) along with research fellows worked on MAX-DOAS and it made available to Pakistani researchers in 2014. MAX-DOAS had been exploited for about 7 years for various research campaigns and publications, but it only analyzed the sky-scattered spectral measurements and the calibration, data manipulation and extraction of results were quite time-consuming and laborious. Moreover, the major limiting factors were its only scans in 0-90 degrees from horizontal to vertical and the intensity of spectra more often low due to changing weather patterns. The reference spectra were used for the MAX-DOAS spectral fitting and removing uncertainty from the measurements.



So, in October 2022, the NASA Pandora Spectrometer was officially installed in support of NASA, PGN, Luft-Blick team. The NASA Pandora Spectrometer not only scans sky scattered light but also scans sun & moonlight to check and validate the shift and squeeze mechanism by provisions of scanning from sunrise to sunset. Whenever moonlight is available it also scans the atmospheric profile of various trace gases as there are chances of major industrial & vehicular emissions.

NASA Pandora Spectrometer comprises of following main parts:

- 1. Pandora Spectrometer**
- 2. Pandora Sun Tracker**
- 3. Pandora Main Control Box Unit**

### *3.2.1 Pandora Spectrometer*

There are two types of Pandora Spectrometer, one with only a UV wavelength range of almost 100-400 nm (one collimator) and the other with both a UV and Visible Spectral range of 270-900 nm (two collimators). Spectrometer further can be classified into small parts.

- A. Spectrometer Head
- B. Optical Fiber Guide
- C. Collimator
- D. Optical Fiber Cable for Control Box Spectrometer
- E. Cable Head for Control Box

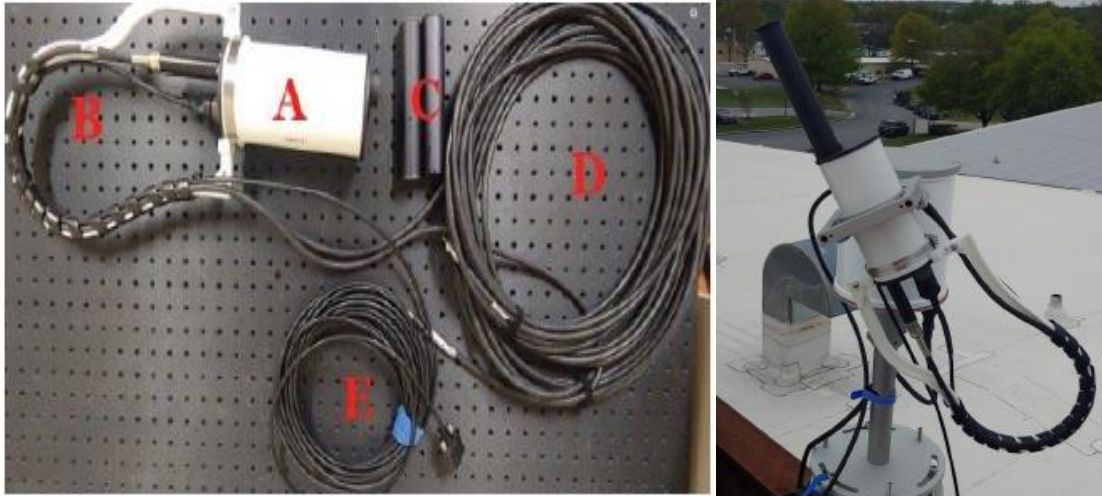


**Figure 11: NASA Pandora Head Sensor Components**

The spectrometer head is fixed, and factory installed with fibre optic cable and restricted to unplug any cable from the head. The collimator needs to be installed on the sensor head after the assembly process of the instrument is completed. USB 2.0 port connection with the mounted PC inside the Control Box is necessary as USB 3.0 is not compatible with the processing of the spectrometer analyzed data from the head. The digital signal will be received by the PC for further analysis and validation.

### *3.2.2 Pandora Sun Tracker*

There are three main components of Pandora Sun Tracker; the first one is the Central Tracker Motor (A), the second one is the Clamp Head for the Sensor Head (B), and the third one is Baseplate (C). Pandora Sun Tracker should be installed at a site where there is no obstruction in the field of view from sunrise to sunset (east to west). There is a need for key terms understanding of the axes of Pandora Sun Tracker as it involves 360-degree movements. Zenith (ZE) is the vertical movement angle concerning the base of the Pandora Sun Tracker while Azimuth (AZ) is the horizontal angle to the base. So considering the

importance of the base plate, there is a need to level the base plate on the ground, proper angle estimation and direction measurements. To fix the sensor head on the sun tracker, there is a need for various sizes of Allen wrench (L-keys) specifically 9/64 for opening the bracket to fix the head inside it.



**Figure 12: NASA Pandora Tracker Components**

### *3.2.3 Pandora Main Control Box Unit*

The main control box comprises a spectrometer box (A) containing UV & Visible Spectrometers (B), a box of relay board (C) and computer ports (D). It is worth mentioning that there is a need to put silica gel bags inside the spectrometer boxes as there are chances of humidity inside the chamber. Moreover, the relay box comprises the ports for the head sensor, sun tracker, power cable and monitor cable header attached. There is a special careful need to apply a procedure for connecting the sensor header fibre cable head inside the spectrometer box (the point on the above side should be on the top position on the cable

header after removing the red-coloured nozzle). The baseplate of the main control box unit should be levelled.



**Figure 13: NASA Pandora Main Control Unit Components**

### **3.3 Fiber & Tracker Cable Layout**

The layout of fibre and tracker cable is really important in maintaining the instrument as it not only obstructs the field of view but also damages the cables which will result in replacing the cable and re-setting the pandora instrument. To check the fibre layout, there are various routines (**RTTRTDRT**) recommended by the developers where 'RT' will do a tracker reset, 'TR' will point to the 4 cardinal points and the zenith in the middle and 'TD' routine will point down as it is set in the instrument operation file.



**Figure 14: NASA Pandora Spectrometer Fiber Cable Layout**

### **3.4 Software Installation & System Settings**

After the manual installation of the Pandora Spectrometer, software installation is done by default by NASA representatives but if by chance the software installation not working or is uninstalled, the software package can be downloaded and installed from the Pandora Global Network website.

(<https://pandonia-global-network.org/home/documents/software/>).

After attaching the mouse, keyboard, and monitor to the system, there are three software developed by LuftBlick named BlickO (Operating), Blick P(Processing of raw Data files) and Blick F (Files pushing to the server). The whole operating software system is based on a Python environment.

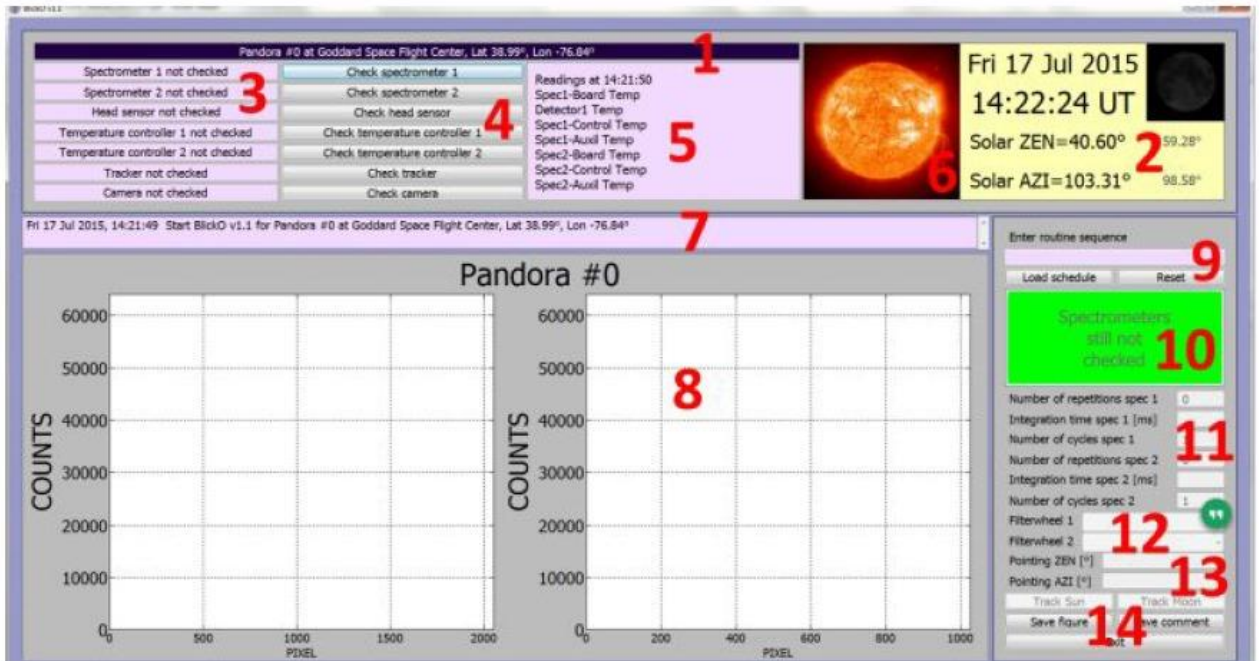


**Figure 15: NASA Pandora Spectrometer LufBlick M Software Display**

### 3.4.1 Location File Creation

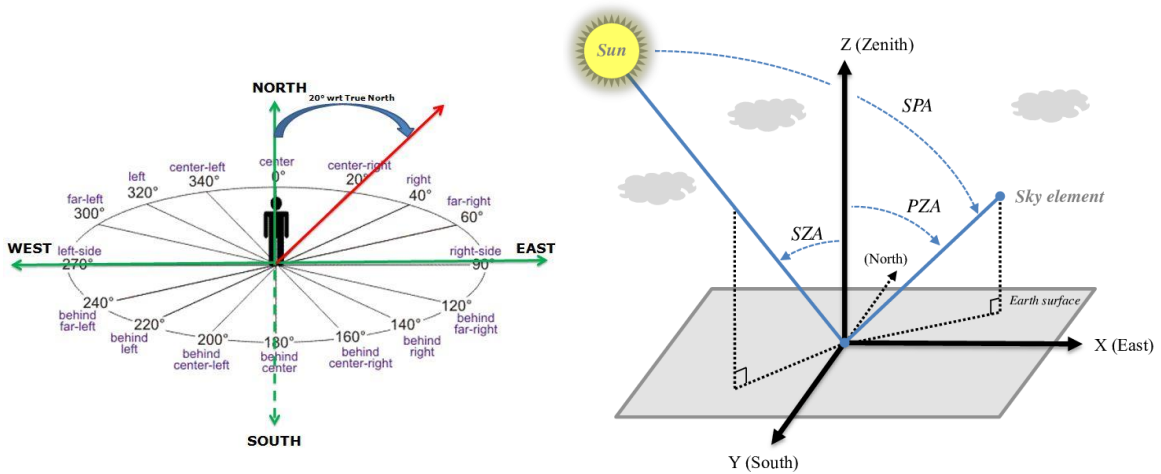
Whenever the NASA Pandora Spectrometer is installed, there is a need to update the location of the instrument which one can do by sending an email to PGN Network Operators(pgn-ops@pandonia-global-network.org) and providing information about the Location Name where the instrument is installed and Location Coordinate including Altitude. If the location file already exists, after starting BlickO, on the right side of the application, there is a bar where above ‘Enter routine sequence’ is mentioned, to check whether the file exists or not, one needs to enter “cl” which will open a dialogue box where all the location of the Pandor Spectrometer Network available and selection of correct location can be done.

### 3.4.2 Checking Connections

After setting up the location of the Pandora Spectrometer, first, there is a need to check and connection of the ports of the sun tracker and sensor head. There are buttons available (1) in BlickO where first connect with the tracker, filter wheels 1 & 2, temperature controller, and at the end spectrometer. When the bar shows a green color means the connections are successfully done.

### 3.4.3 Home Position Setting of Sun Tracker

**Important Key Concepts for Setting Tracker Home Position:** Azimuth is the horizontal angle at which the sun tracker moves in the horizontal direction which is represented by degrees. The pictures depict the various angles of the azimuth motor.



Similarly, the Zenith is the vertical top-to-bottom distance covered by the zenith motor having the sensor head of a spectrometer on it. Earth is not flat but spherical, so the Solar Zenith Angle is of great importance as not it only allows us to have a reference spectrum but also to understand the shift and squeeze mechanism for Fraunhofer lines. Similar concepts of Fraunhofer lines and other key terminologies of the earth's surface. Setting up different pointing zenith angles (PZA) provides the spherical enlarged atmospheric column density

of Earth. That's why calibrating and alignment of the NASA Pandora Spectrometer is important.

The default setting for the home position of the sun tracker is where the top side of the sensor head is on the southward side and the bottom side is on the northward side. The tracker bracket clamp face of the head sensor should be towards the east of the location and opposite to it should be the west side. The concept behind it is to assess the horizon information on different possible angles while the collimator of the sensor should be upwards and the tracker bracket clamps 90 degrees to it.

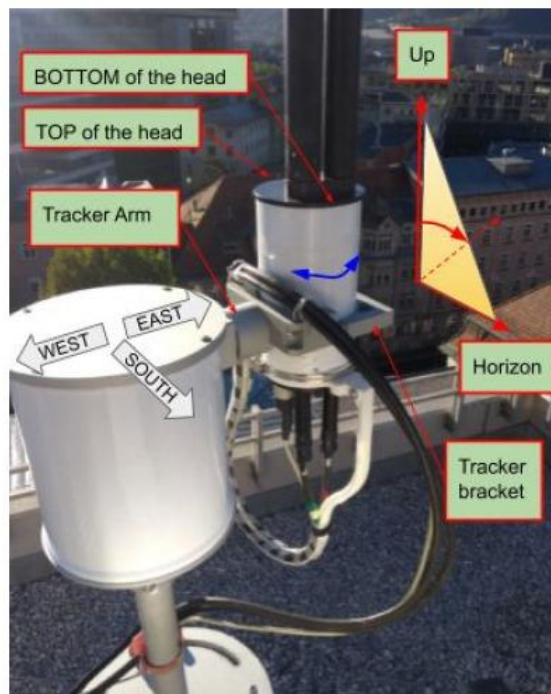


**Figure 16: NASA Pandora Tracker Home Position**

In doing so, there are some minor correction options available after which the angle correction can be done via BlickO software. After opening the software and connecting to



the tracker, write 'hs' in the schedule bar and there will be a Slight Alignment dialogue box open up and there will be the following options available:

#### *3.4.4 Azimuth Home Position*

After typing 'hs' in routine and pressing enter will open up a 'low-level serial communication dialog box' where there will be two options available in selecting the serial connection 'Headsensor/Tracker' or 'Temperature Controller'. Selecting the head sensor and tracker option, move on to the YELLOW bar where type 'TRpXXXX' where XXXX represents the angle measured to 1/100 degrees which means that TRp6000 will move +60 degrees to the previously set home position and TRp-19000 means -190 degrees to previous home position. If the Azimuth motor is aligned with the reference home position mentioned above then type 'Mah' which stands for motor azimuth at home position now.

#### *3.4.5 Zenith Home Position*

Just like the azimuth motor, follow the 'hs' routine and type 'TRtXXXX' which will move the zenith previously set home position in degrees and when it is set according to the mentioned reference home position the type 'MZh' which stands for motor zenith at home position now.

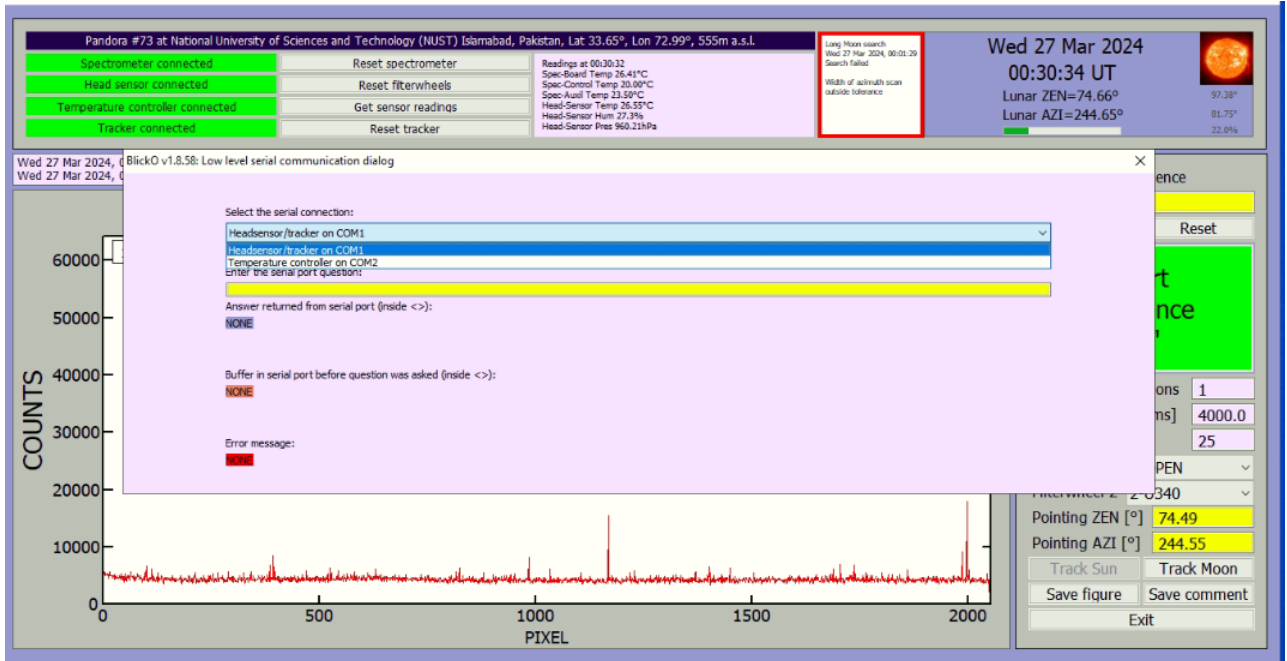


**Figure 17: NASA Pandora Zenith Home Position Settings**

### 3.4.6 Initial Azimuth & Zenith Angle Correction

NASA Pandora Spectrometer after all setups requires a manual search for the sun by initial alignment. Before doing the initial alignment, it is recommended to check the perfect weather conditions when the sun is rising early in the morning on a clear day and make sure the time is in UTC and the location is updated. After this, write 'FI' in routine sequence and the 'Slight Alignment Dialog box' will open up. Tap on the 'Reset' button right beneath the command bar adjust the default parameters of the spectrometer and set the Filterwheel 1 & 2 to open settings along with some integration time changes if want to. Now tap on 'measure continuously & display' to check the spectral signal strength.

In the slight alignment dialogue box, there are two options available, one move in azimuth by 10 degrees counterclockwise, 1 degree counterclockwise, 0.1 degrees counterclockwise, 0.1 degree clockwise, 1 degree clockwise, or 10 degrees clockwise. While the other one

moves in zenith only provides 0.1 degrees up and 0.1 degrees down. Moving first azimuth and then zenith in such a way that the maximum spectral signal counts can be achieved. If the spectral signal got saturated (extended beyond the graph) then there is a need to change the filter wheel 1 to ND1 or ND2, ND3, ND4 from open to reduce the amount of light by inserting a neutral density filter. After the maximum signal is found, save the settings. The saving setting will be new if the instrument is relocated or undergoes some technical maintenance. Otherwise adding the new setting in previous versions can also be done. To check whether the alignment is right or wrong, just simply type FN about 3-5 times which will greenline the white-box on top of the BlickO where Sun Search failed or was successfully written.



Figure 18: NASA Pandora Spectrometer Slight Alignment

After this alignment, there is a need for at least a full clear day on ‘align. sked’ routine for highly precise sun tracking (50 sun searches for different times of the day). Then finally load the schedule ‘uv\_sun\_moon\_sky\_hsm.sked for the NASA Pandora Spectrometer installed at IESE, NUST.

#### *3.4.7 Sky Scan Azimuth Configuration*

More often called ‘Standard Azimuth for Elevation Scans’ for regularly scheduled sky scan measurements done at fixed azimuth angles but different zenith angles. This can be performed by accessing the ‘config’ folder in Drive C\Blick\config\Pandora73\_config.txt usually set (0N-90E degree) where there is no obstruction in the field of view of Pandora Spectrometer.

Starting BlickO and load ‘EO’ routine to check whether the sensor is headed towards the desired azimuth direction with different zenith angles.

### **3.5 NASA Pandora Spectrometer Common Routines**

Following are various BlickO routines which are necessary to know:

#### **Table 2: NASA Pandora Spectrometer Routine Abbreviations**

<b>RT</b>	Do a tracker reset (Same effect as clicking in the connect/reset tracker button)
<b>RF</b>	Do a filterwheels reset.
<b>FN</b>	Finds the Sun, and resets the tracker if the offset angle is too large
<b>FA</b>	Finds the Sun without resetting the tracker.
<b>FD</b>	Finds the Sun with Diffuser filters in.
<b>FU</b>	Finds the Sun with U340 filter in.
<b>FI</b>	Manually align the zenith and azimuth
<b>TD</b>	Moves the tracker to point down to maximum zenith angle, and waits 5 secs.
<b>TR</b>	Moves the head to the four cardinal positions along the horizon and the zenith from 0° to 90°. (Useful to test the fiber/cables layout)
<b>TP</b>	Parks the tracker (By default zenith=90° and azimuth=90°, but is configurable in the instrument config file)
<b>T0</b>	Moves the head to point to the zenith.
<b>?</b>	Provides a list of the routines used in BlickO.

### *3.5.1 Alignment Visualization*

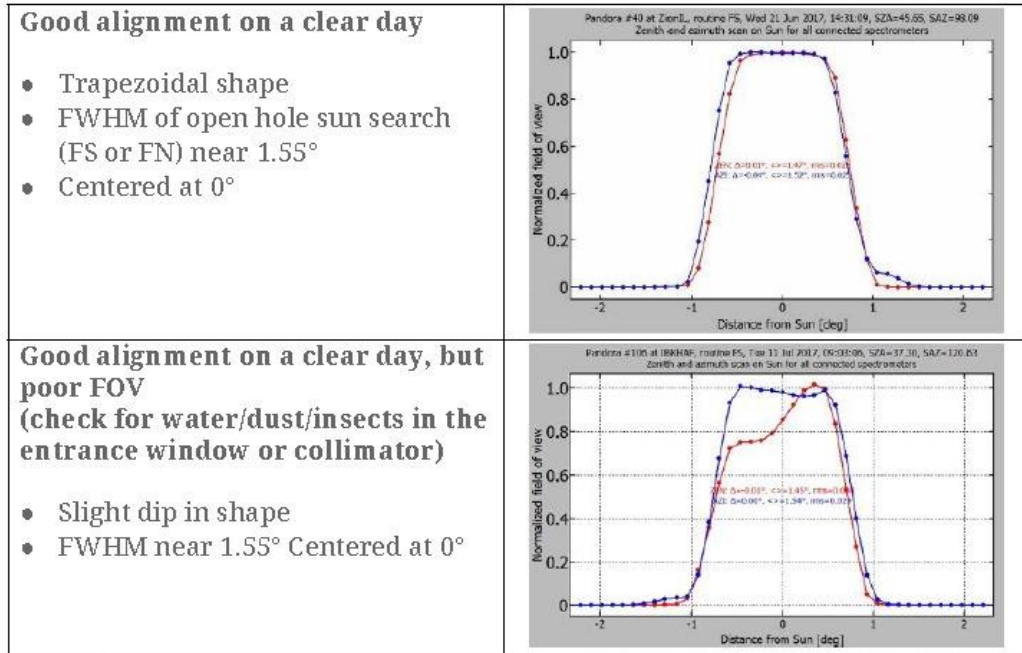


**Figure 19: Good Alignment of NASA Spectrometer**

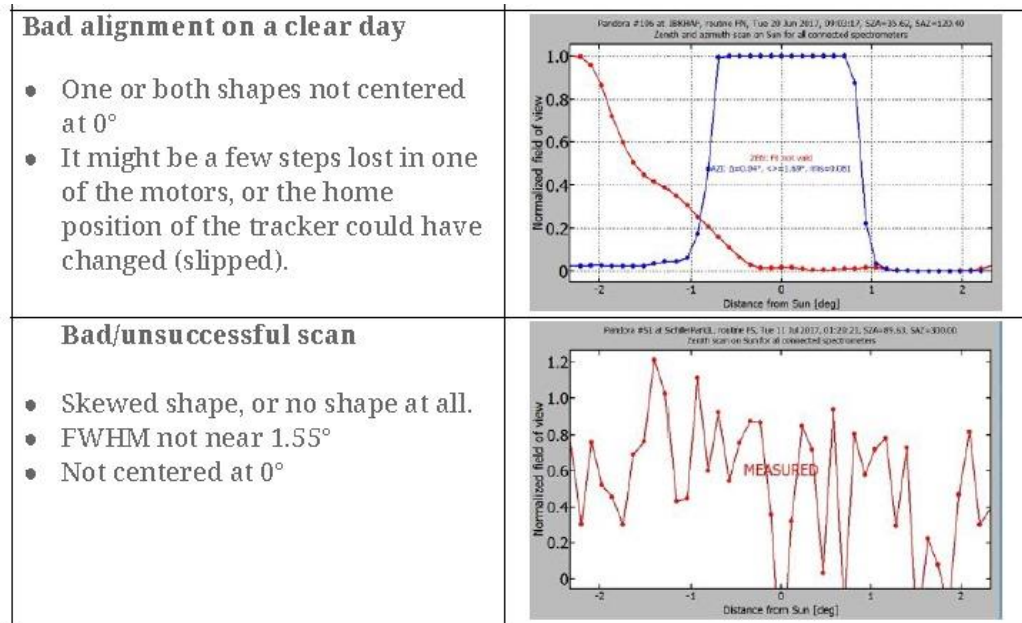


**Figure 20: Bad Alignment of NASA Pandora Spectrometer**

### 3.5.2 Maintenance Check

There is a need to regularly do the maintenance checks that Blick O, Blick F, and Blick P are working properly and there is no such abnormality in the slog, diagnostic, and figures of the operative Blick schedules. Checking the insights of the main control box unit, pandora spectrometer head sensor, and pandora sun tracker. If the data files are pushing through Blick F or not. There is a must once weekly cleansing of the collimator to remove the dust of the collimator using a chem wipe and a 90% distilled water and 10% isopropyl alcohol solution. The desiccant in the spectrometer box needs to be regularly checked whether it is good or needs to be replaced with new ones to manage the humidity in the spectrometer box (once a month).

## 3.6 Data Products of NASA Pandora Spectrometer

### 3.6.1 Formaldehyde (*fuh5*):

HCHO Tropospheric Column, Surface Concentrations and Tropospheric Profiles & **Formaldehyde (fus5)** HCHO Total Column.

### 3.6.2 Nitrogen Dioxide (*nvh3*):

NO<sub>2</sub> Tropospheric Column, Surface Concentration and Tropospheric Profile & **Nitrogen Dioxide (nvs3)** for Total Column

### 3.6.3 Ozone (*ous1*):

O<sub>3</sub> Total Column (Field Calibration Required) **Ozone (out2)** (Weak Absorber)

### 3.6.4 Sulphur Dioxide (*sus1*)

SO<sub>2</sub> Total Column & Cross sections used for Spectral Fittings

### 3.7 OMI & TROPOMI

**OMI:** Timeseries area averaged OMI (30 per cent cloud screened) data for Tropospheric NO<sub>2</sub> Vertical Column was extracted out from Earth Data Giovanni website by entering start, end date, Longitude & Latitude (72.98,33.62). By plotting data, there are various output formats available on Giovanni's website (Netcdf, CSV, PNG) and also give the visual representation.

**TROPOMI:** A JavaScript-based code for the L3 NO<sub>2</sub> offline product was made to obtain TROPOMI data via Google Earth Engine. There is a need for careful understanding of the code as there are multiple factors needed to take account of cloud cleaning, data quality filters, longitude & latitude and type of geometry involved for the area or point averaged values. The data downloading limit is only 1 year in one go. Data was acquired from 24<sup>th</sup> October 2022 to 31<sup>st</sup> March 2024. Results were downloaded in a CSV format by clicking on the right-corner option of opening in the next window that will open up the graph of the required timespan in CSV, SVG & PNG formats.

The downloaded CSV data file of TROPOMI was analyzed through Microsoft Excel & Python data visualization codes. Initially data analysis was performed using Microsoft Excel but later Pandonia Global Network recommended to use of Python for data analysis and visualization purposes. The specific script was made to extract the data from specific output files of the NASA Pandora Spectrometer. The time series alignment, scatter plots, and weather patterns visualization will be discussed in the upcoming results and discussion section.



## CHAPTER 4: RESULTS & DISCUSSION

### 4.1 NO<sub>2</sub> Ground Based Measurements

#### *4.1.2 NASA Pandora Spectrometer Tropospheric NO<sub>2</sub> Column Densities*

The timeseries analysis of tropospheric NO<sub>2</sub> retrieved from Pandora Spectrometer showed concentration of NO<sub>2</sub> columns increases in winter, while lower NO<sub>2</sub> columns are detected during the monsoon season. NO<sub>2</sub>'s lifetime ranges from a few hours to a day, depending on a variety of parameters such as the amount of OH present, photolysis rate, and weather. The largest known NO<sub>x</sub> sink is the interaction of NO<sub>2</sub> with the hydroxyl (OH) radical. Winter's low temperatures and limited light exposure result in decreased NO<sub>2</sub> loss due to interactions with OH radicals, extending NO<sub>2</sub> lifespan and increasing column density. Lower precipitation rates also play a role in reducing the frequency of OH generation by diminishing the available water vapor supply. As a result, certain NO<sub>2</sub> molecules are destroyed. As a result, just a little amount of NO<sub>2</sub> molecules are removed. Moreover, during the winter, more coal, wood, and cow dung are used for space heating and cooking, which increases NO<sub>2</sub> levels. Because of the longer NO<sub>2</sub> lifespan and higher NO<sub>2</sub> emissions throughout the winter, NO<sub>2</sub> levels are at their maximum.

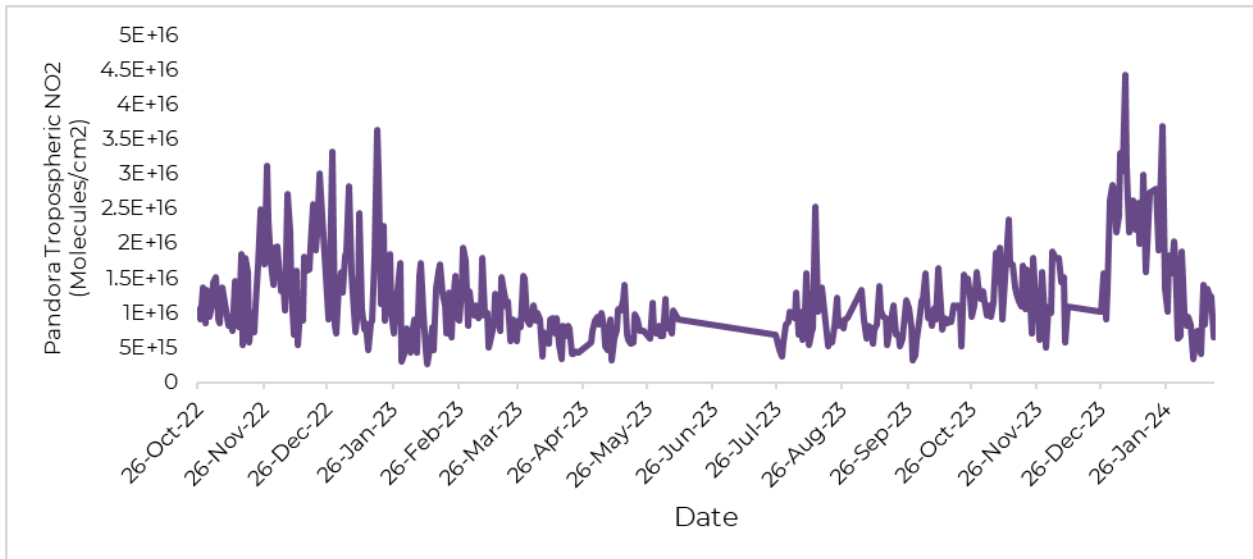


**Figure 21: Timeseries analysis of Pandora Tropospheric NO<sub>2</sub> columns**

The Diurnal cycle of NO<sub>2</sub> over Islamabad for the time span of almost 2 years (October 2022 – April 2024). The graph shows that the NO<sub>2</sub> concentration is initially low when the sun rises, but gradually increases until 12 p.m., when it begins to decline again. The highest NO<sub>2</sub> concentrations early in the day are most likely caused by traffic emissions from cars during office and school hours, as well as other combustion activities at night, and a lack of photolysis to convert nitrogen dioxides to nitrogen oxides. The oxidation of NO<sub>2</sub> in the presence of the OH radical begins as soon as the sun rises, and the amount of NO<sub>2</sub> in the atmosphere gradually decreases until it reaches a peak at noon.

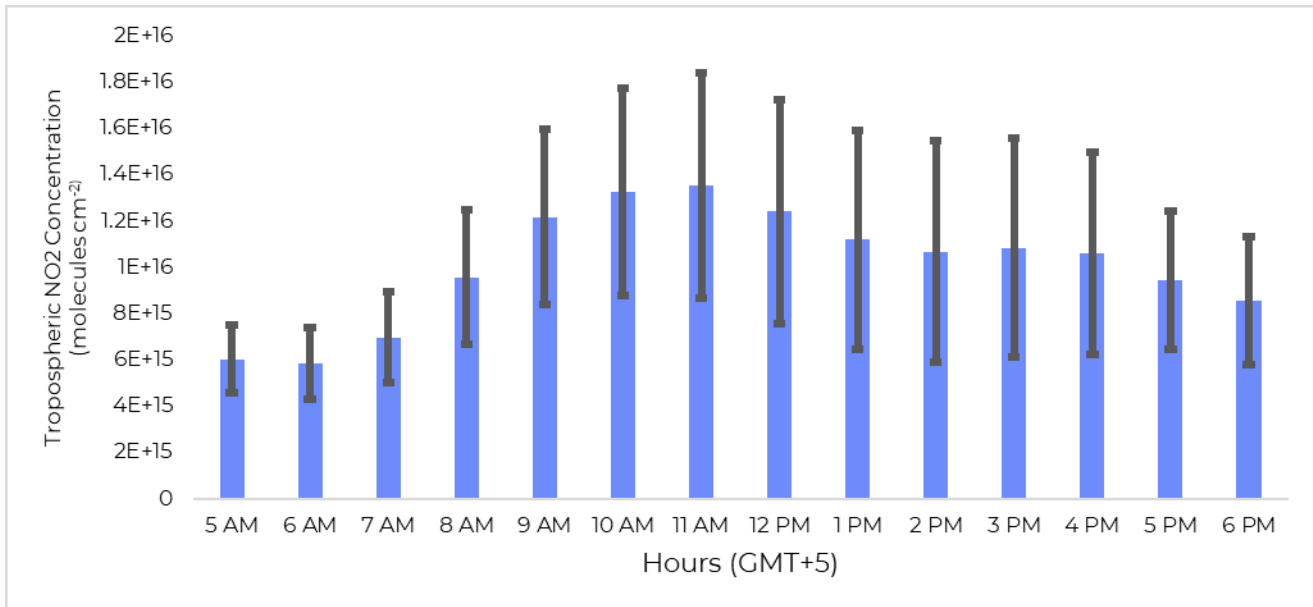


**Figure 22: Diurnal Cycle of Pandora Tropospheric NO<sub>2</sub>**

The weekly cycle for NO<sub>2</sub> shows almost similar trend along the week except Saturday and Sunday are relatively low concentrations, due to business and general holiday. A rapid increase in the concentration of NO<sub>2</sub> on Thursday may be due to transportation and resumption of businesses activities, the peak may also appear due to the movement of diesel engine trucks on Sri Nagar Highway for supplying goods to northern areas. It is also observed that people from different cities move to Islamabad on weekend for the recreational purposes, resulting in large traffic movement, which may lead towards the increase in the NO<sub>2</sub> peak. The human activities and movement are the main cause to increase tropospheric NO<sub>2</sub>, the weekly trend is totally influenced by the traffic movements in Islamabad.

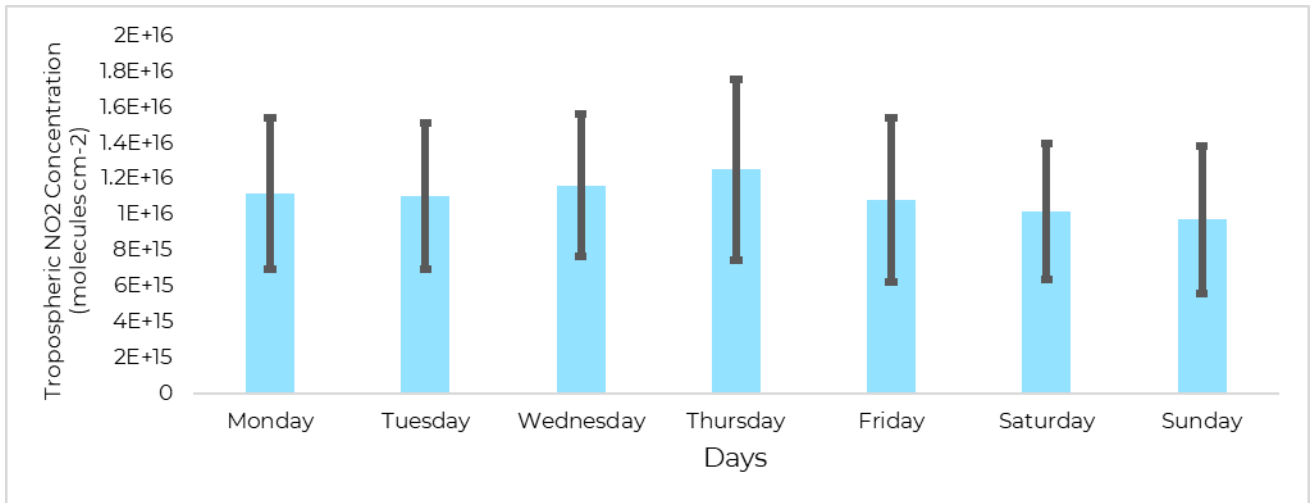


**Figure 23: Weekly Cycle of Pandora Tropospheric NO<sub>2</sub>**

The average annual trend for NO<sub>2</sub> indicates a decrease in the summer and an increase in the winter. Because NO<sub>2</sub> is broken down more quickly in the summer due to the photolysis effect, summertime NO<sub>2</sub> concentrations are lower than wintertime ones. There is a minor increase, though, in July and August. This might have to do with the monsoon season, when clouds block out the sun for most of the day and lessen the amount of light that reaches the atmosphere. This lowers the photolysis activity, raising the NO<sub>2</sub> content at that particular moment.

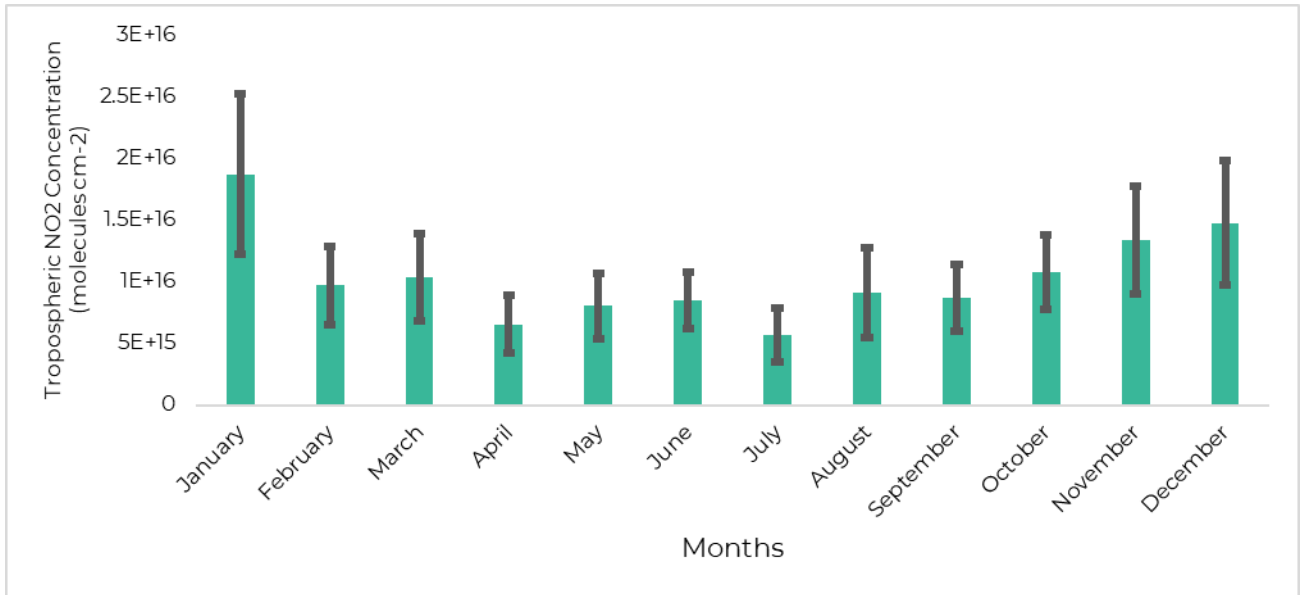


**Figure 24: Monthly Cycle of Pandora Tropospheric NO<sub>2</sub>**

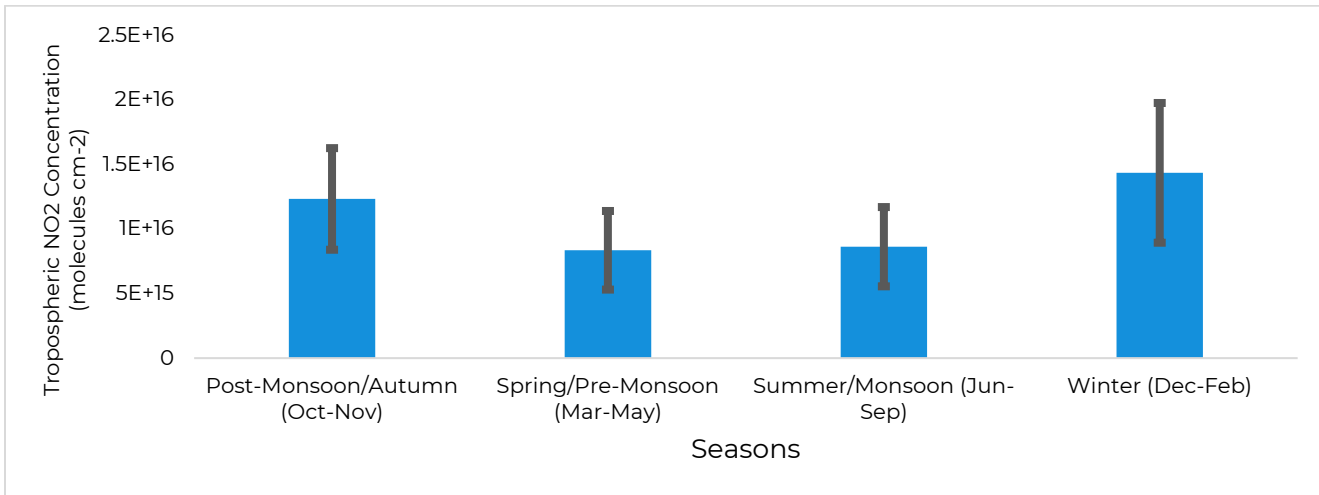


**Figure 25: Seasonal Cycle of Pandora Tropospheric NO<sub>2</sub>**

#### 4.2 NO<sub>2</sub> Satellite Based Measurements

#### 4.2.1 AURA Ozone Monitoring Instrument (OMI)

OMI Satellite (0.25x 0.25km) peaks for nitrogen dioxide were observed in the months of November, December and January. The concentration is decreased in subsequent months gradually. OMI satellite values for NO<sub>2</sub> were underestimated as they were much lesser than the Pandora values may be due to aerosol shielding effect, clouds cover and the less sensitivity of satellite observations towards surface layers. However, the trends of both OMI and Pandora concentrations were much more the same. Daily average of NO<sub>2</sub> concentrations of Pandora & OMI satellite showed 71% correlation. Monthly average of NO<sub>2</sub> concentrations of Pandora and OMI satellite were compared. OMI Satellite data, for the daily validation of NO<sub>2</sub> Pandora observations over Islamabad, was obtained from GIOVANNI website. Daily correlation for the Months of October 2022 to April 2024 was significant as the Pearson value (r) is 0.93.

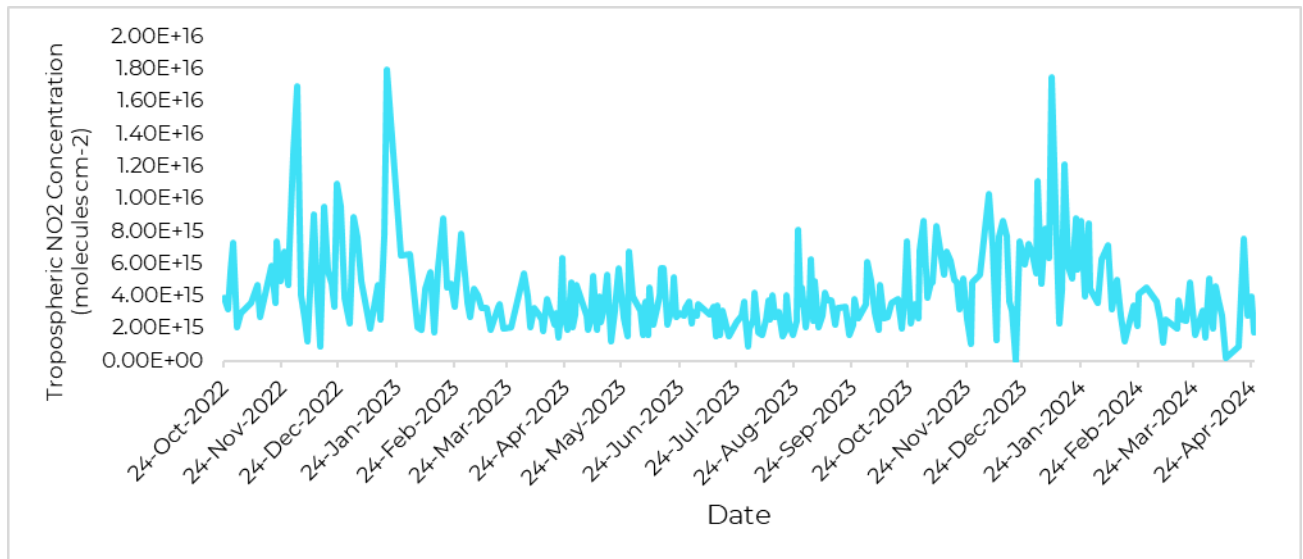


**Figure 26: Timeseries of OMI Tropospheric NO<sub>2</sub>**

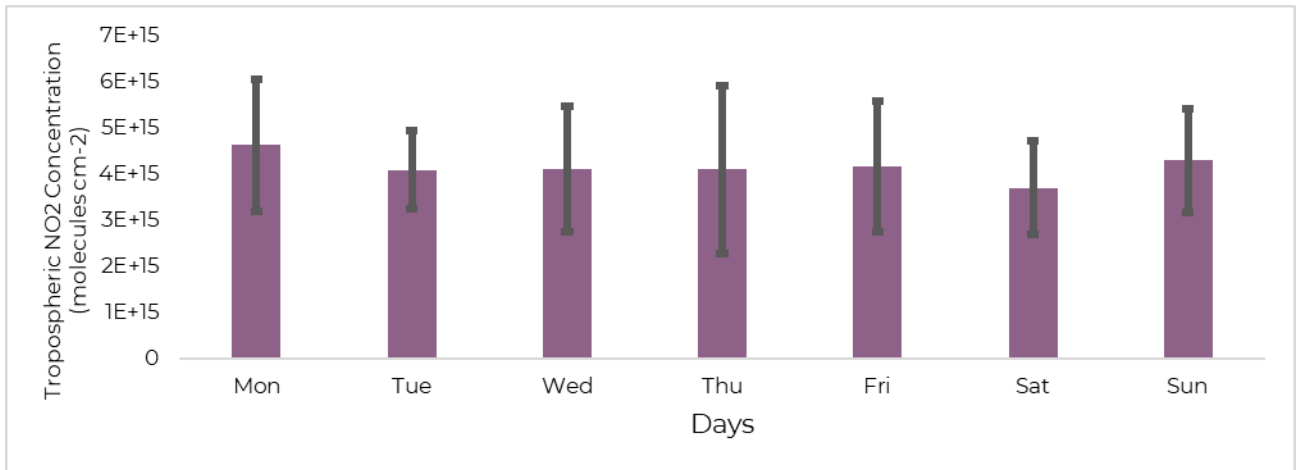


**Figure 27: Weekly Cycle of OMI Tropospheric NO<sub>2</sub>**

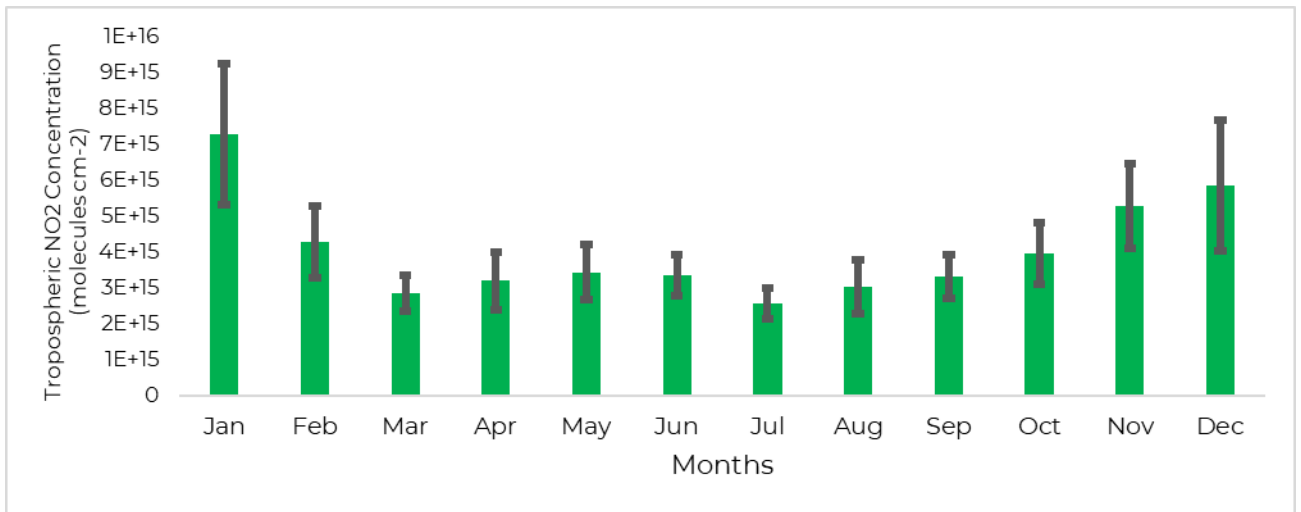


**Figure 28: Monthly Cycle of OMI Tropospheric NO<sub>2</sub>**

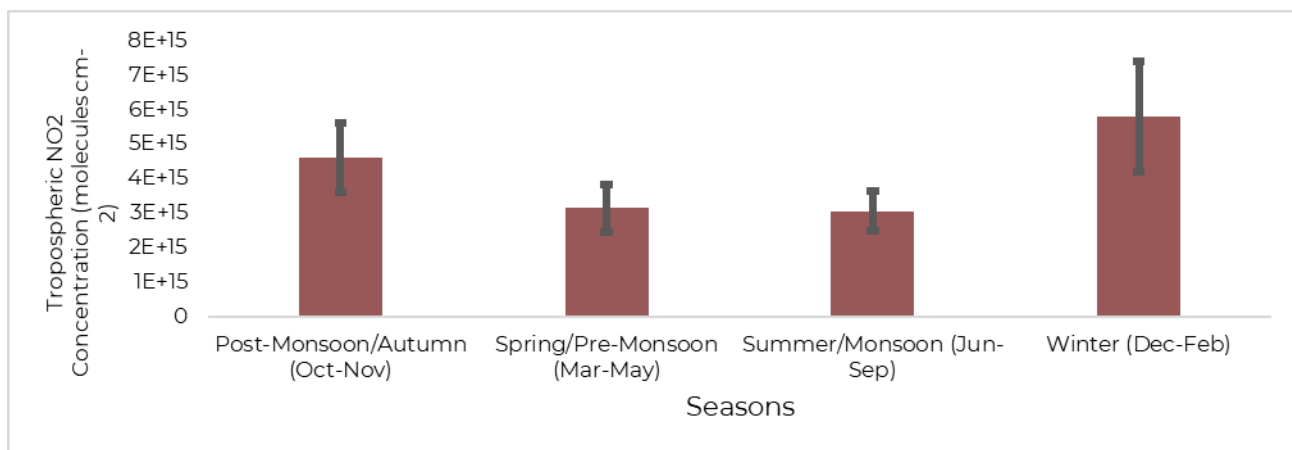


**Figure 29: Seasonal Cycle of OMI Tropospheric NO<sub>2</sub>**

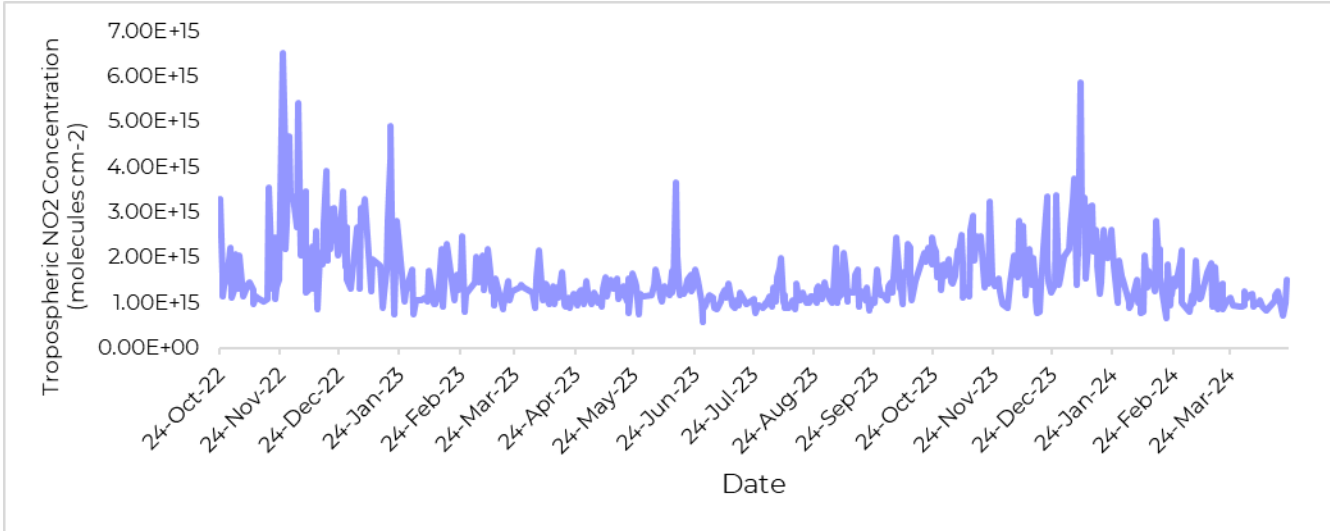
#### 4.2.2 Sentinel 5P TROPospheric Ozone Monitoring Instrument (TROPOMI)

The observation of boundary layer pollution from satellite instruments is a great challenge. The main reason could be the increasing air density and aerosol concentration towards the surface, a significant amount of atmospheric scattering usually occurs within or above the trace gas layer. Thus, the sensitivity of satellite observation decreases towards the surface. Another reason could be that many satellite observations are influenced by the presence of clouds (shielding effect) which further decreases the satellite's sensitivity for trace gases close to the surface. Both effects can be corrected, but this correction requires precise information on the vertical distributions of the trace gases, aerosols and clouds, which is usually not available for same ground scene. Therefore, validation of satellite observations with in-situ and ground-based observations is highly needed. In this section, tropospheric NO<sub>2</sub> VCDs derived from Pandora measurements are compared with Tropomi observations for respective days over Islamabad.

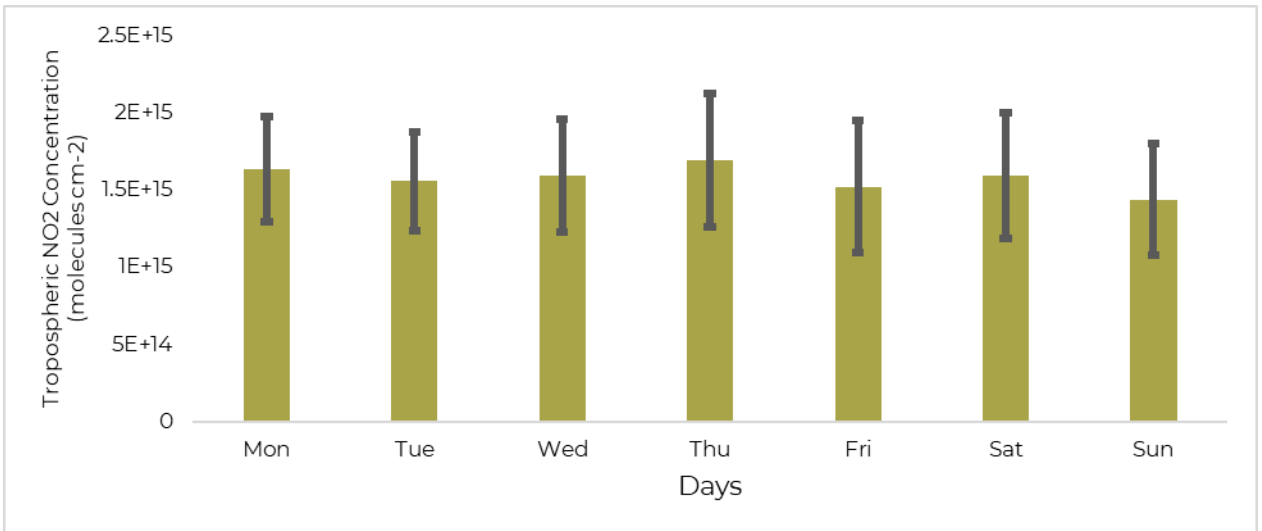
Daily average of NO<sub>2</sub> concentrations of Pandora & TROPOMI satellite showed 81% correlation. Monthly average of NO<sub>2</sub> concentrations of Pandora and TROPOMI satellite



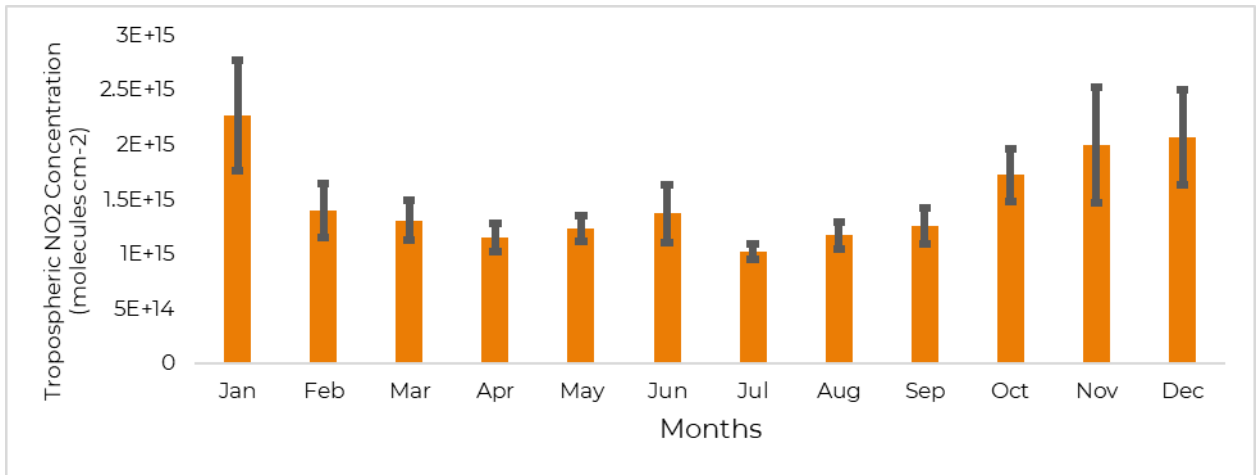
were compared. TROPOMI Satellite data, for the daily validation of NO<sub>2</sub> Pandora observations over Islamabad, was obtained through Google Earth script. Daily correlation for the Months of October 2022 to April 2024 was significant as the Pearson value (r) is 0.97.



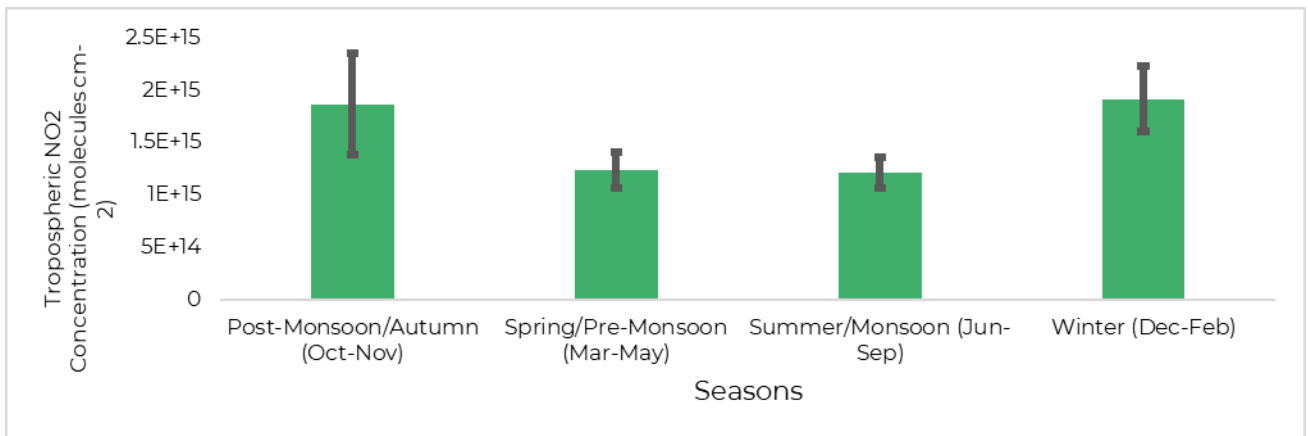
**Figure 30: Timeseries Analysis of TROPOMI Tropospheric NO<sub>2</sub>**



**Figure 31: Weekly Cycle of Pandora Tropospheric NO<sub>2</sub>**



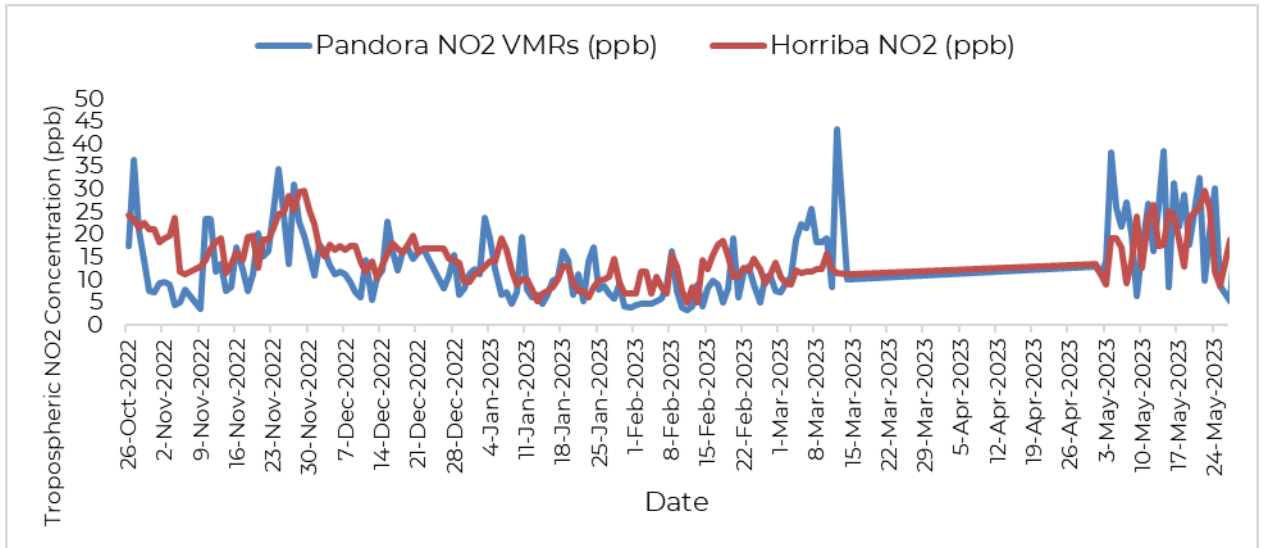
**Figure 32: Monthly Cycle of Pandora Tropospheric NO<sub>2</sub>**



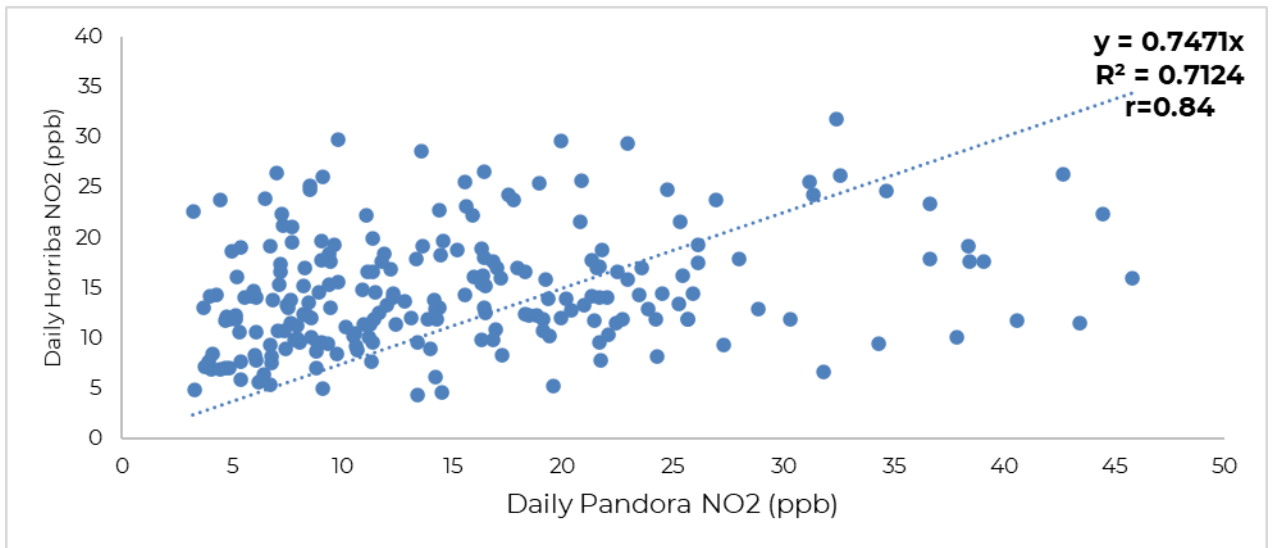
**Figure 33: Seasonal Cycle of Pandora Tropospheric NO<sub>2</sub>**

### 4.3 Ground based Instrument Intra Monitoring Validation

#### 4.3.1 NASA Pandora vs HORRIBA NO<sub>2</sub> Surface Concentration



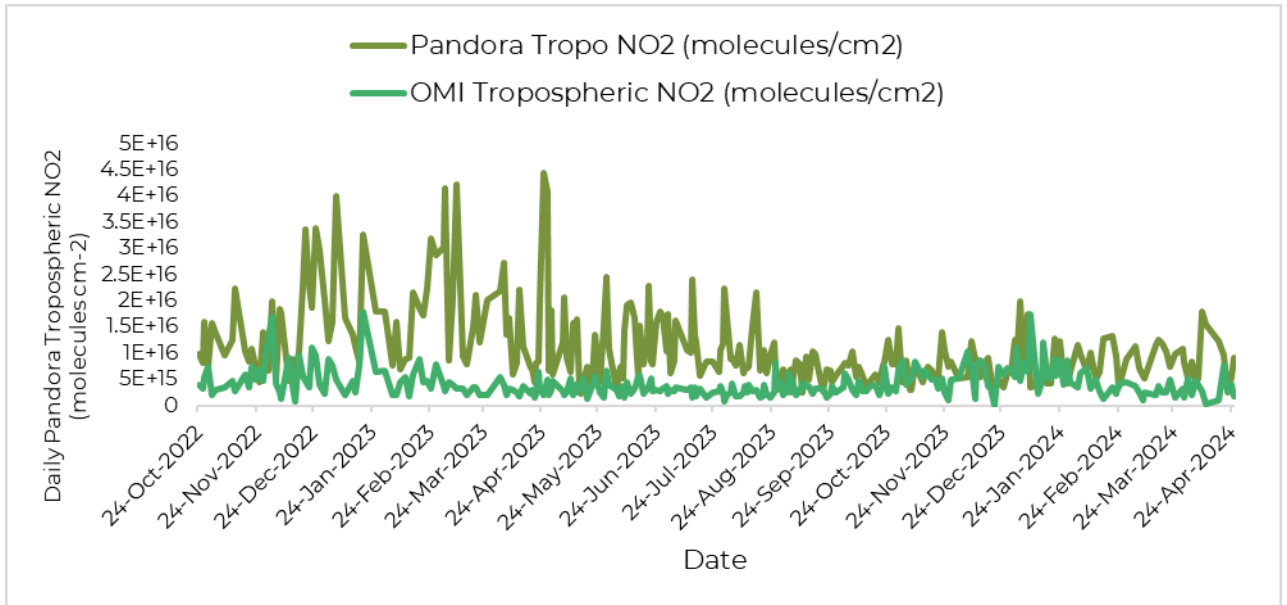
**Figure 34: Timeseries Analysis of Pandora compared to Horriba Surface Concentration (ppb)**



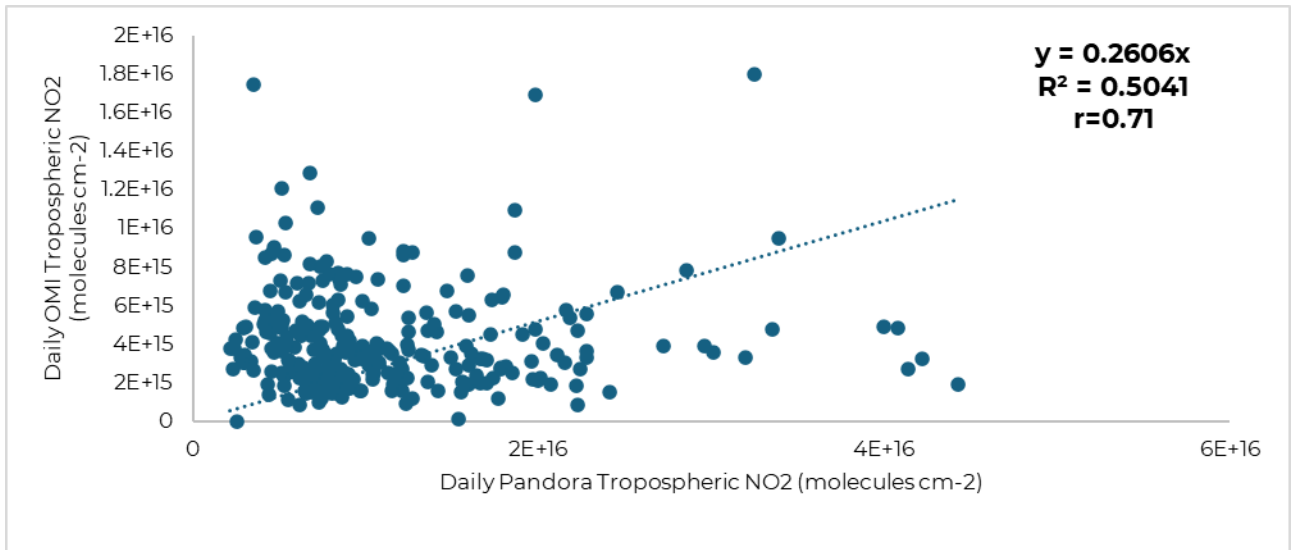
**Figure 35: Validation of Daily Tropospheric NO<sub>2</sub> Pandora and Horriba Surface Concentration**

**4.4 Ground vs Satellite Based NO<sub>2</sub> Measurements Validation**

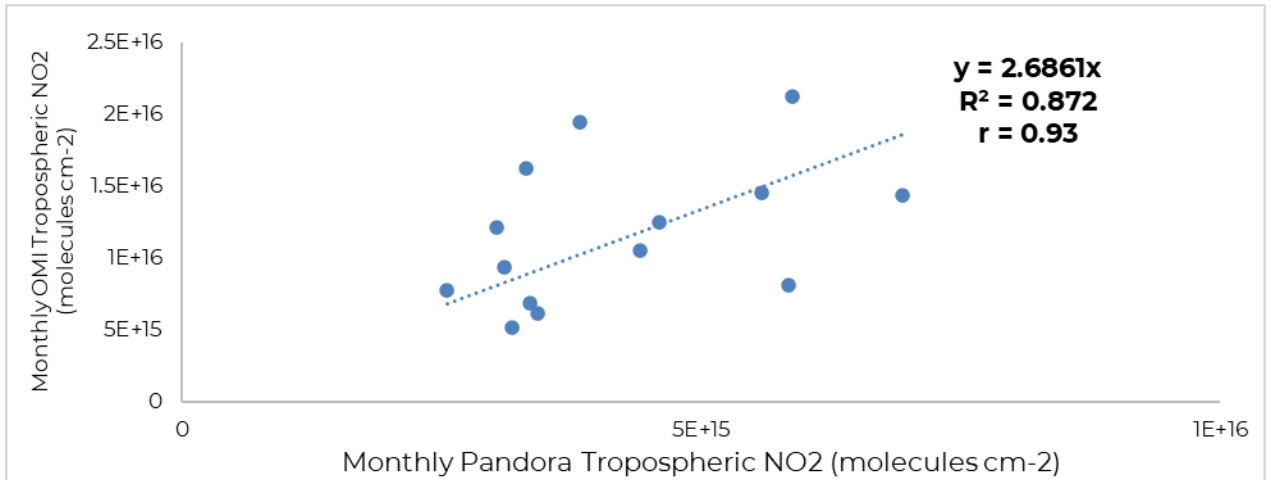
#### 4.4.1 NASA Pandora vs OMI Satellite Based Validation



**Figure 36: Timeseries Analysis of Pandora with OMI Tropospheric NO<sub>2</sub>**

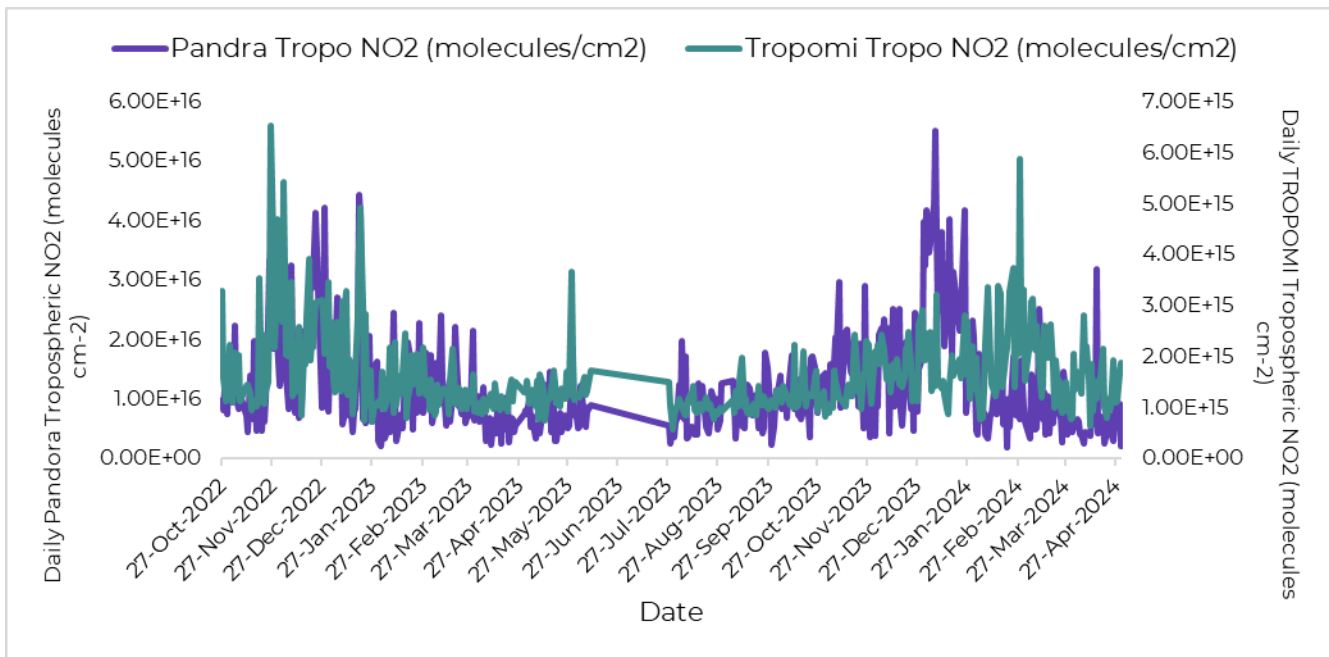


**Figure 37: Validation of Pandora Daily Tropospheric NO<sub>2</sub> with OMI**

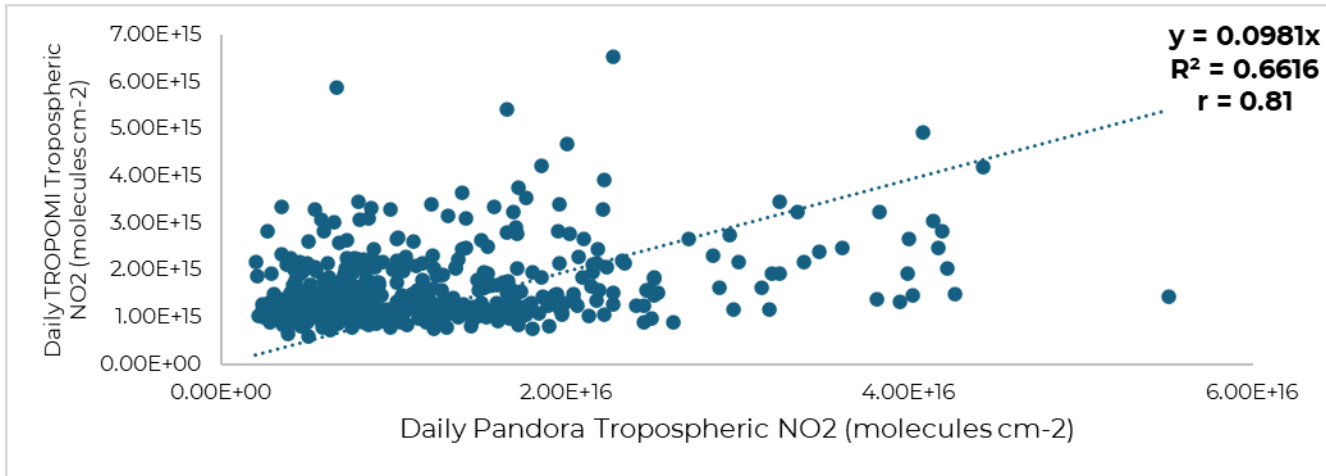


**Figure 38: Validation of Pandora Monthly Tropospheric NO<sub>2</sub> with OMI**

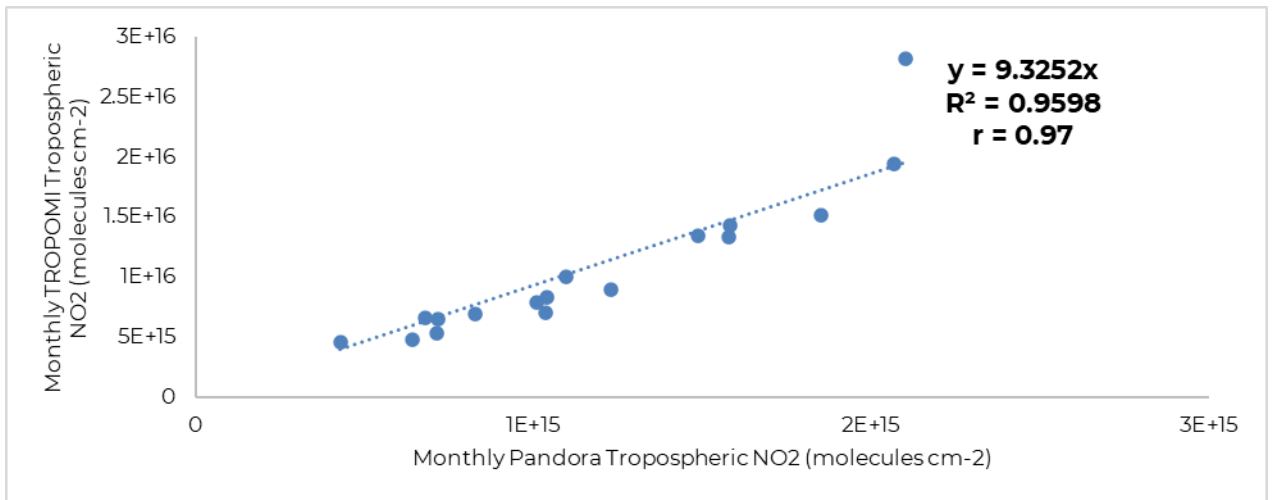
4.4.2 NASA Pandora vs TROPOMI NO<sub>2</sub> Measurements Validation



**Figure 39: Timeseries Analysis of Daily Pandora Tropospheric NO<sub>2</sub> with TROPOMI**



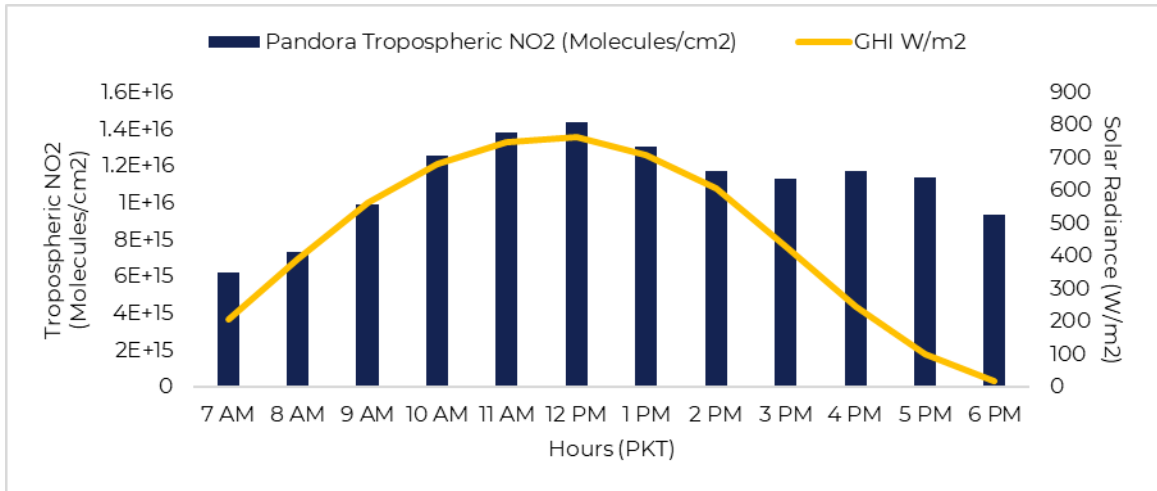
**Figure 40: Validation of Pandora Daily Tropospheric NO<sub>2</sub> with TROPOMI**



**Figure 41: Validation of Pandora Monthly Tropospheric NO<sub>2</sub> with TROPOMI**

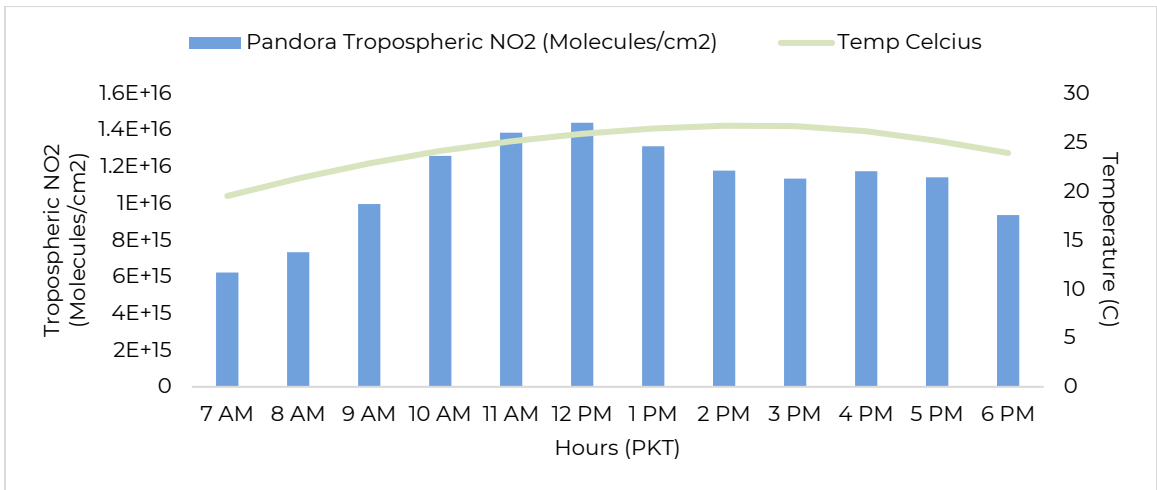
## 4.5 Meteorological Effects on NO<sub>2</sub> Measurements

### 4.5.1 Impact of Solar Radiance on NASA Pandora NO<sub>2</sub> Measurement



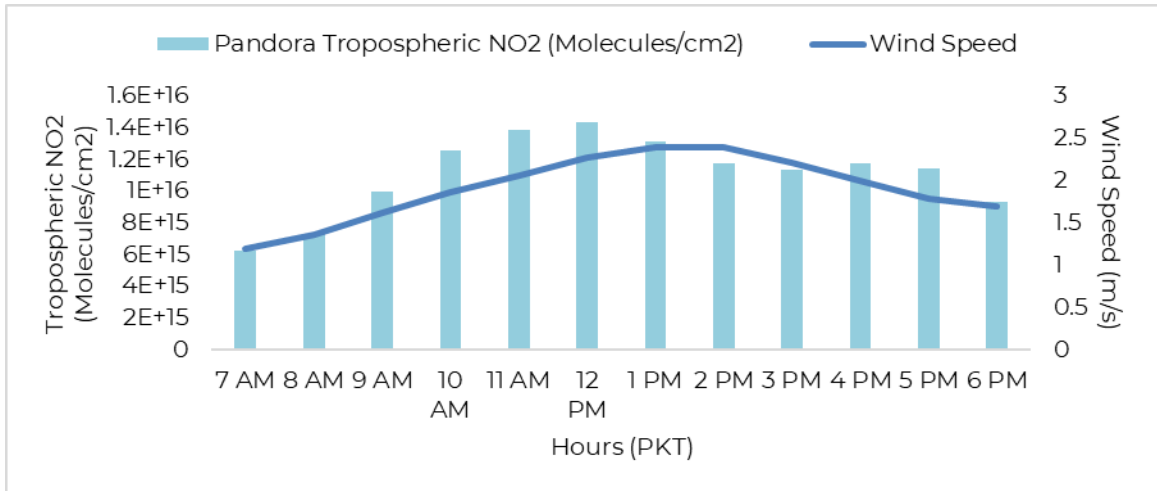
**Figure 42: Comparison of Pandora Tropospheric NO<sub>2</sub> with Solar Radiation (W/m<sup>2</sup>)**

*4.5.2 Temperature effects on NASA Pandora Spectrometer NO<sub>2</sub> Measurements*



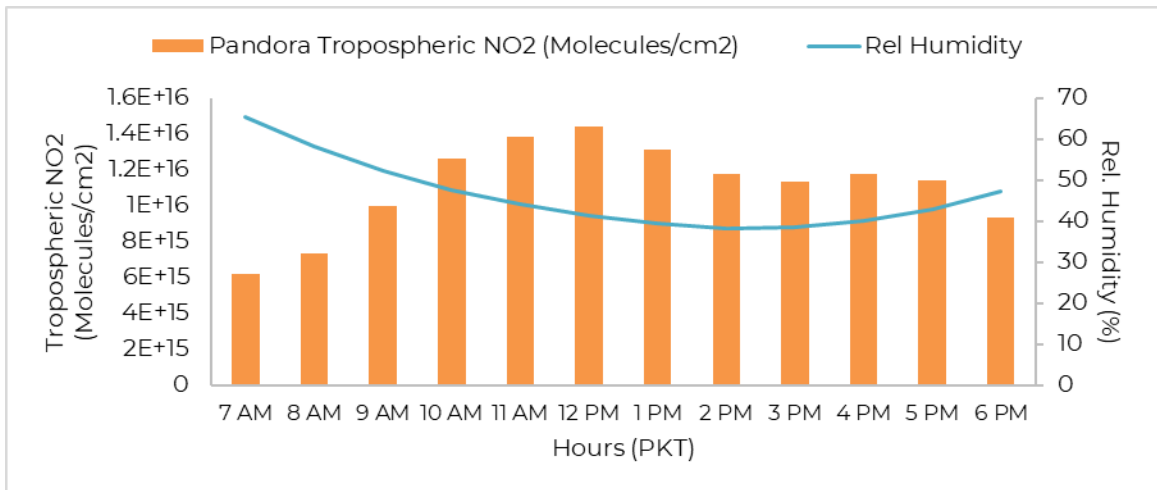
**Figure 43: Comparison of Pandora Tropospheric NO<sub>2</sub> with Temperature (C)**

*4.5.3 Wind Speed effects on NASA Pandora Spectrometer NO<sub>2</sub> Measurements*



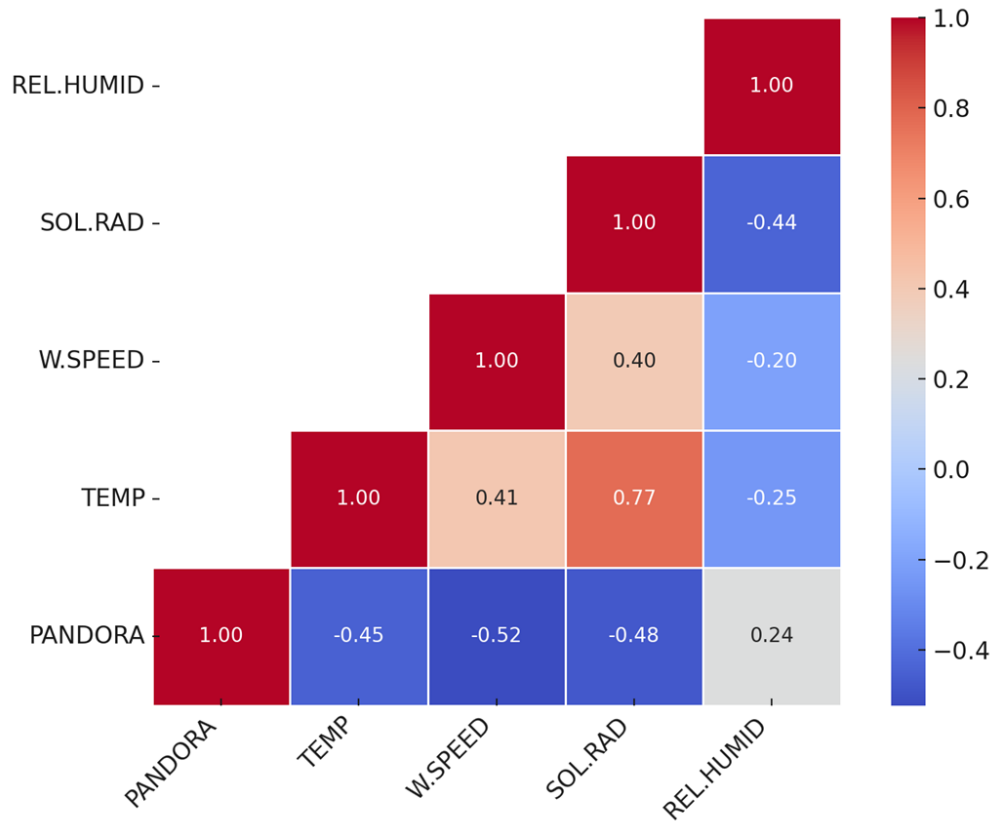
**Figure 44: Comparison of Pandora Tropospheric NO<sub>2</sub> with Wind Speed (m/s)**

*4.5.4 Impact of Relative Humidity on NASA Pandora Spectrometer NO<sub>2</sub> Measurements*



**Figure 45: Comparison of Pandora Tropospheric NO<sub>2</sub> with Relative Humidity (%)**





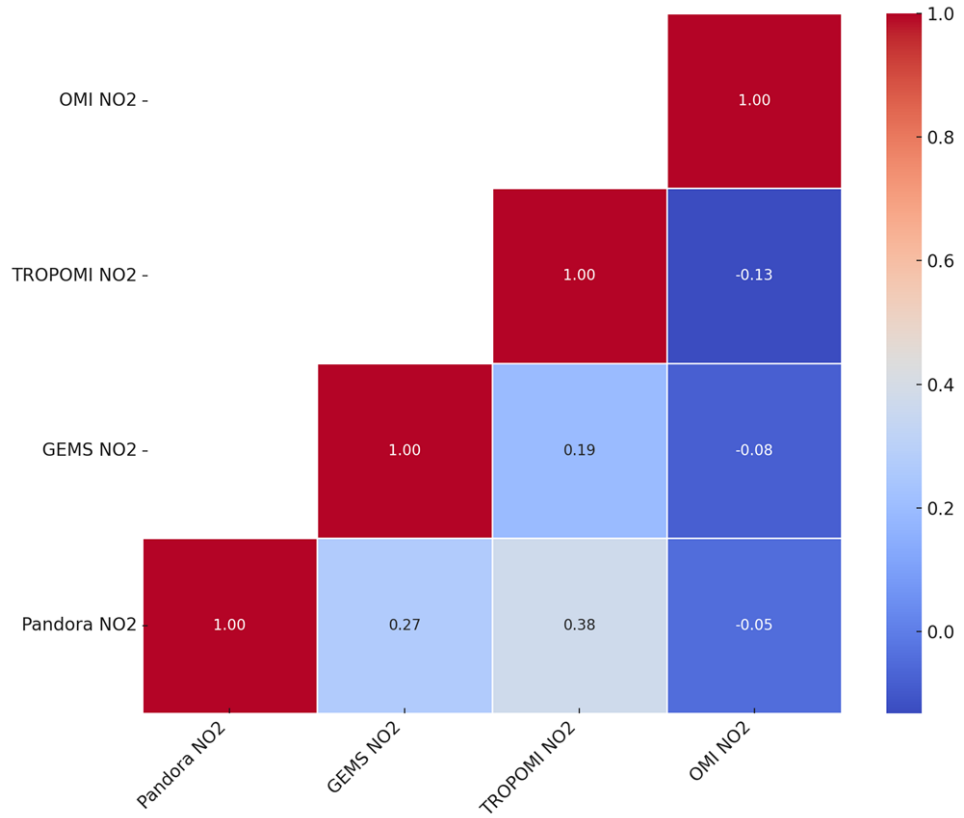


**Figure 46: Correlation Matrix of Pandora, OMI, TROPOMI, GEMS, Relative Humidity, Temperature, Solar Radiation and Wind Speed**

## 4.6 Pandora Data Validation with GEMS Satellite

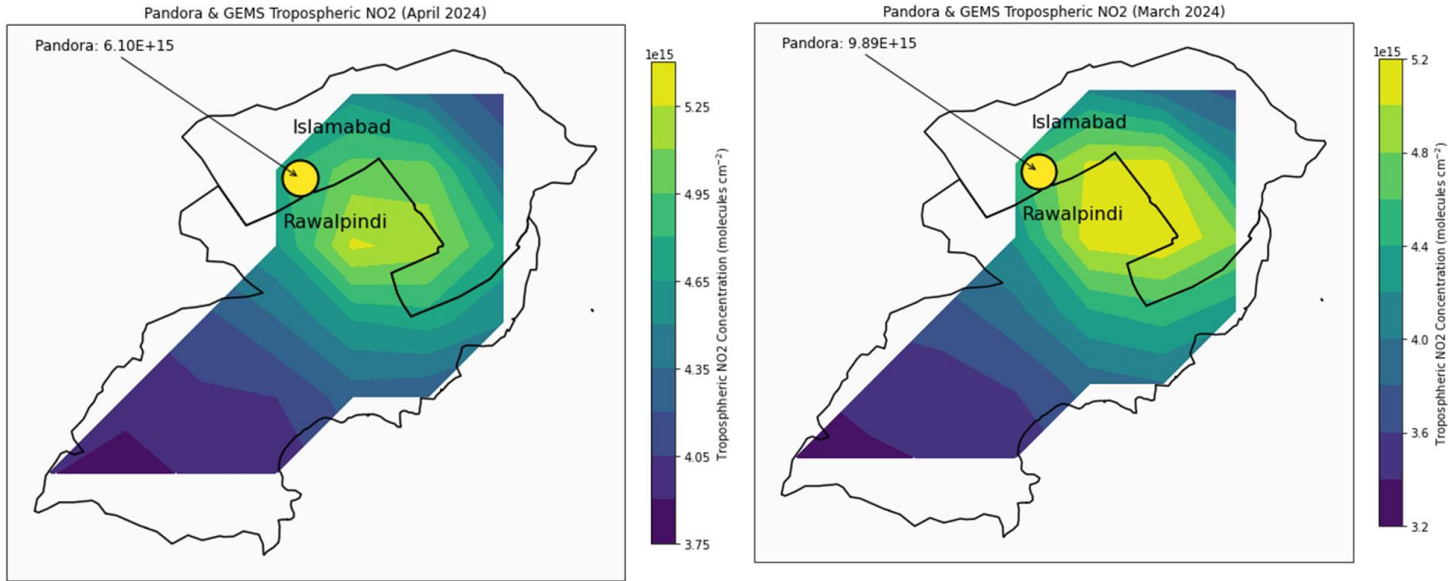


**Figure 47: Pandora & GEMS Monthly Tropospheric NO<sub>2</sub> Map for the month of May 2024 and April 2024.**

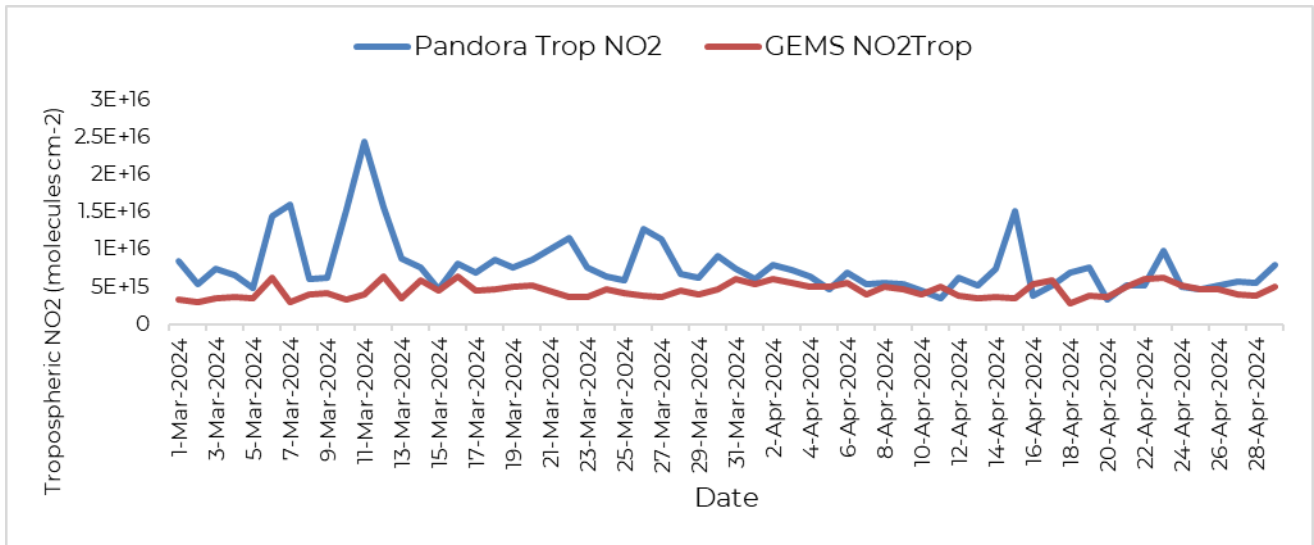


**Figure 48: Timeseries Analysis of Pandora Tropospheric NO<sub>2</sub> with GEMS Satellite \**

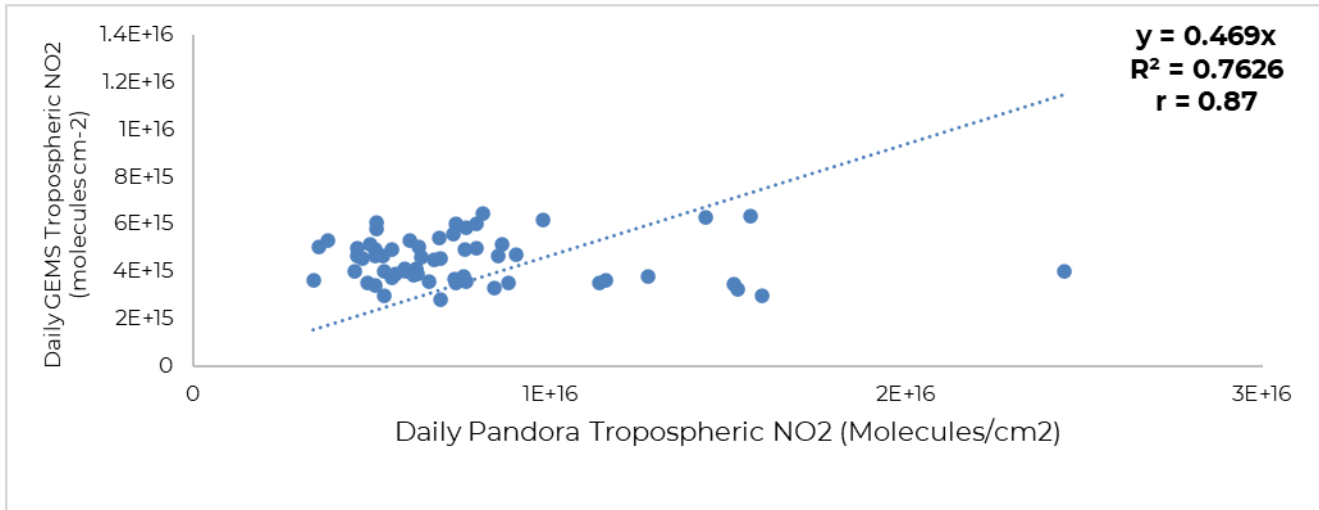


**Figure 49: Validation of Daily Pandora Tropospheric NO<sub>2</sub> with GEMS Satellite**

## CHAPTER 5: CONCLUSION & RECOMMENDATIONS

Overall, the tropospheric NO<sub>2</sub> data retrieved from the observations of research objectives were to installation, validation, seasonal and temporal analysis of South Asia' first NASA Pandora spectrometer. The research concluded following results:

The two-years (2022-2024) analysis revealed that NO<sub>2</sub> concentrations in Islamabad have consistently increased. This observed increase is attributed to a variety of factors, including increased traffic, local businesses purchasing vehicles, and individual automotive purchases. The primary driver of rising NO<sub>2</sub> concentrations is the increased use of fossil fuels in industry and transportation.

NO<sub>2</sub> emissions are especially high during office hours (9-12 pm) and departure hours (4-5 pm) due to increased traffic. At night, diminished sunshine causes less photolysis of NO<sub>2</sub>, thereby enhanced levels of NO<sub>2</sub> retrieved in daylight from satellite data, the first NASA Pandora Spectrometer in South Asia.

Seasonal fluctuations were noted, with higher NO<sub>2</sub> concentrations in the winter due to cooler temperatures and more frequent fog, as opposed to the summer and monsoon seasons, which are distinguished by higher temperatures and bright sunlight. Photolysis at the IESE monitoring station lowers NO<sub>2</sub> emissions, and there is a strong link between temperature and NO<sub>2</sub> concentrations. A significant concordance was also found between NO<sub>2</sub> levels measured by ground-based equipment and satellite data.

The results of the investigation showed that, with an 87% correlation for NO<sub>2</sub> data collected in April and March 2024, the South Korean Geostationary Environmental Monitoring Spectrometer (GEMS) and the Pandora spectrometer had the strongest correlation. This strong correlation shows how trustworthy satellite data is for tracking air quality. Additionally, the daily data validation of the Ozone Monitoring Instrument (OMI) and

TROPOspheric Monitoring Instrument (TROPOMI) with the Pandora spectrometer increased in comparison to the previous study, yielding correlations of roughly 71% and 81%, respectively. With correlations of 87 and 93% for OMI and TROPOMI, respectively, monthly data validation rose, suggesting a high degree of confidence in these findings. Since the Pandora spectrometer can record data continuously in both lunar and daylight settings, it can be used to collect data even in low light situations, an area where nighttime NO<sub>2</sub> levels are typically missed by traditional ground-based monitors.

Potential solutions include switching to renewable energy, adding catalytic converters in automobiles, and improving combustion technology. Developing large possible transport networks is critical to alleviating traffic congestion in both urban and rural locations. Improvements to existing mass transit systems can considerably reduce emissions from unneeded trips. Regular vehicle maintenance and tuning are also beneficial in reducing car emissions. Governments at all levels must recognize the need to establish and enforce air pollution control measures.

Regular air quality monitoring is required, with benchmarks set for major cities. Monthly and annual public data releases will raise awareness and provide policymakers with useful information. To raise public knowledge about the causes and consequences of air pollution, media campaigns and educational efforts targeting community organizations and educational institutions must be implemented.

To ensure the accuracy and dependability of NO<sub>2</sub> data, extensive long-term intercomparison studies of datasets from Horiba, Pandora, and satellites are required. More research is needed to understand the link between NO<sub>2</sub> and other meteorological parameters. Air quality modelling tools are critical for estimating and simulating NO<sub>2</sub> concentrations under a variety of scenarios, particularly those including climate change.

Establishing long-term monitoring networks throughout Pakistan is critical for routinely detecting NO<sub>2</sub> levels, following changes, and understanding aerosol impacts. Public education about the dangers of excessive NO<sub>2</sub> levels is critical for reducing potential health risks caused by smog and other difficulties. Rapid development of effective NO<sub>2</sub> emission reduction solutions is required to improve air quality while also protecting public health and the ecosystem.

Finally, the study indicates that NO<sub>2</sub> concentrations in Islamabad have been steadily increasing due to a variety of reasons. Implementing the proposed procedures can improve air quality monitoring practices while mitigating the negative effects of NO<sub>2</sub> emissions. These initiatives are critical to protecting both human health and the environment.

Moreover, GEMS has broad temporal coverage, making it possible to track daily variations in NO<sub>2</sub> and identify peak pollution times with greater accuracy. It offers constant data for seven to eight hours every day. When satellite data is integrated with on-the-ground measurements, air quality forecast models become more accurate. This makes it possible to project future NO<sub>2</sub> concentrations under different conditions and motivates the adoption of proactive pollution control strategies. With satellite-based monitoring providing significantly wider spatial coverage than ground-based systems, it becomes possible to identify regional pollution hotspots and trends. Large, often expensive to set up and maintain ground-based monitoring networks are no longer necessary due to improved data accuracy and extensive coverage.

In order to ensure compliance with air quality requirements, regulatory authorities can use trustworthy satellite data to enforce regulations and take corrective action against violators. Additionally, accurate and continuous monitoring of NO<sub>2</sub> levels aids in understanding the effects of air pollution on the environment and public health, which guides the development of mitigation and ecosystem preservation strategies. With the advancement of satellite-

based data collection, a full framework for NO<sub>2</sub> monitoring, better public health outcomes, regulatory compliance, and air quality management is now available.



## REFERENCES

- Blechschmidt, A. M., Arteta, J., Coman, A., Curier, L., Eskes, H., Foret, G., Gielen, C., Hendrick, F., Marécal, V., Meleux, F., Parmentier, J., Peters, E., Pinardi, G., J M Piters, A., Plu, M., Richter, A., Segers, A., Sofiev, M., Valdebenito, A. M., ... P. Burrows, J. (2020). Comparison of tropospheric NO<sub>2</sub> columns from MAX-DOAS retrievals and regional air quality model simulations. *Atmospheric Chemistry and Physics*, 20(5), 2795–2823. <https://doi.org/10.5194/ACP-20-2795-2020>
- Choi, S., Lamsal, L. N., Follette-Cook, M., Joiner, J., Krotkov, N. A., Swartz, W. H., Pickering, K. E., Loughner, C. P., Appel, W., Pfister, G., Saide, P. E., Cohen, R. C., Weinheimer, A. J., & Herman, J. R. (2020). Assessment of NO<sub>2</sub> observations during DISCOVER-AQ and KORUS-AQ field campaigns. *Atmospheric Measurement Techniques*, 13(5), 2523–2546. <https://doi.org/10.5194/AMT-13-2523-2020>
- di Bernardino, A., Mevi, G., Iannarelli, A. M., Falasca, S., Cede, A., Tiefengraber, M., & Casadio, S. (2023). Temporal Variation of NO<sub>2</sub> and O<sub>3</sub> in Rome (Italy) from Pandora and In Situ Measurements. *Atmosphere*, 14(3), 594. <https://doi.org/10.3390/ATMOS14030594/S1>
- Diémoz, H., Siani, A. M., Casadio, S., Iannarelli, A. M., Casale, G. R., Savastiouk, V., Cede, A., Tiefengraber, M., & Müller, M. (2021). Advanced NO<sub>2</sub> retrieval technique for the Brewer spectrophotometer applied to the 20-year record in Rome, Italy. *Earth System Science Data*, 13(10), 4929–4950. <https://doi.org/10.5194/ESSD-13-4929-2021>
- Farman, J. C., Murgatroyd, R. J., Survey, B. A., Silnickas, A. M., & Thrush, B. A. (1985). Ozone photochemistry in the Antarctic stratosphere in summer. *Wiley Online Library*, 111(470), 1013–1028. <https://doi.org/10.1002/qj.49711147006>
- Fleming, J. R. (1998). Arrhenius and current climate concerns: Continuity or a 100-year gap? *Eos, Transactions American Geophysical Union*, 79(34), 405–410. <https://doi.org/10.1029/98EO00310>
- Go, S., Kim, J., Mok, J., Irie, H., Yoon, J., Torres, O., Krotkov, N. A., Labow, G., Kim, M., Koo, J. H., Choi, M., & Lim, H. (2020). Ground-based retrievals of aerosol column absorption in the UV spectral region and their implications for GEMS measurements. *Remote Sensing of Environment*, 245, 111759. <https://doi.org/10.1016/J.RSE.2020.111759>

- Griffin, D., Zhao, X., McLinden, C. A., Boersma, F., Bourassa, A., Damers, E., Degenstein, D., Eskes, H., Fehr, L., Fioletov, V., Hayden, K., Kharol, S. K., Li, S. M., Makar, P., Martin, R. v., Mihele, C., Mittermeier, R. L., Krotkov, N., Snee, M., ... Wolde, M. (2019). High-Resolution Mapping of Nitrogen Dioxide With TROPOMI: First Results and Validation Over the Canadian Oil Sands. *Geophysical Research Letters*, *46*(2), 1049–1060. <https://doi.org/10.1029/2018GL081095>
- Haider Naqvi, S. L., Ayub, F., Yasar, A., Tabinda, A. B., Nawaz, H., & Tanveer, R. (2023). Pollution status monitoring and indices development for evaluating sustainable environmental management practices (SEMP) in Quaid-e-Azam Industrial Estate, Pakistan. *Journal of Cleaner Production*, *405*, 136944. <https://doi.org/10.1016/J.JCLEPRO.2023.136944>
- Herman, J., Abuhassan, N., Kim, J., Kim, J., Dubey, M., Raponi, M., & Tzortziou, M. (2019). Underestimation of column NO<sub>2</sub> amounts from the OMI satellite compared to diurnally varying ground-based retrievals from multiple PANDORA spectrometer instruments. *Atmospheric Measurement Techniques*, *12*(10), 5593–5612. <https://doi.org/10.5194/AMT-12-5593-2019>
- Herman, J., Cede, A., Spinei, E., Mount, G., Tzortziou, M., & Abuhassan, N. (2009). NO<sub>2</sub> column amounts from ground-based Pandora and MFDOAS spectrometers using the direct-sun DOAS technique: Intercomparisons and application to OMI validation. *Journal of Geophysical Research: Atmospheres*, *114*(D13), 13307. <https://doi.org/10.1029/2009JD011848>
- Ialongo, I., Virta, H., Eskes, H., Hovila, J., & Douros, J. (2020). Comparison of TROPOMI/Sentinel-5 Precursor NO<sub>2</sub> observations with ground-based measurements in Helsinki. *Atmospheric Measurement Techniques*, *13*(1), 205–218. <https://doi.org/10.5194/AMT-13-205-2020>
- Iqbal, A., Ahmad, N., Din, H. M. U., Roozendaal, M. van, Anjum, M. S., Khan, M. Z. A., & Khokhar, M. F. (2022). Retrieval of NO<sub>2</sub> Columns by Exploiting MAX-DOAS Observations and Comparison with OMI and TROPOMI Data during the Time Period of 2015–2019. *Aerosol and Air Quality Research*, *22*(6), 210398. <https://doi.org/10.4209/AAQR.210398>
- Isaksen, I. S. A., Granier, C., Myhre, G., Berntsen, T., Dalsøren, S. B., Gauss, M., Klimont, Z., Benestad, R., Bousquet, P., Collins, W., Cox, T., Eyring, V., Fowler, D., Fuzzi, S., Jöckel, P., Laj, P., Lohmann, U., Maione, M., Monks, P., ... Wuebbles, D. J. (2012). Atmospheric Composition Change: Climate–Chemistry Interactions. *The*

*Future of the World's Climate*, 309–365. <https://doi.org/10.1016/B978-0-12-386917-3.00012-9>

- Judd, L. M., Al-Saadi, J. A., Janz, S. J., Kowalewski, M. J. G., Bradley Pierce, R., Szykman, J. J., Valin, L. C., Swap, R., Cede, A., Mueller, M., Tiefengraber, M., Abuhassan, N., & Williams, D. (2019). Evaluating the impact of spatial resolution on tropospheric NO<sub>2</sub> column comparisons within urban areas using high-resolution airborne data. *Atmospheric Measurement Techniques*, *12*(11), 6091–6111. <https://doi.org/10.5194/AMT-12-6091-2019>
- Judd, L. M., Al-Saadi, J. A., Szykman, J. J., Valin, L. C., Janz, S. J., Kowalewski, M. G., Eskes, H. J., Pepijn Veefkind, J., Cede, A., Mueller, M., Gebetsberger, M., Swap, R., Bradley Pierce, R., Nowlan, C. R., González Abad, G., Nehrir, A., & Williams, D. (2020). Evaluating Sentinel-5P TROPOMI tropospheric NO<sub>2</sub> column densities with airborne and Pandora spectrometers near New York City and Long Island Sound. *Atmospheric Measurement Techniques*, *13*(11), 6113–6140. <https://doi.org/10.5194/AMT-13-6113-2020>
- Judd, L. M., Al-Saadi, J. A., Valin, L. C., Bradley Pierce, R., Yang, K., Janz, S. J., Kowalewski, M. G., Szykman, J. J., Tiefengraber, M., & Mueller, M. (2018). The dawn of geostationary air quality monitoring: Case studies from Seoul and Los Angeles. *Frontiers in Environmental Science*, *6*(AUG), 380677. <https://doi.org/10.3389/FENVS.2018.00085/BIBTEX>
- Karagkiozidis, D., Friedrich, M. M., Beirle, S., Bais, A., Hendrick, F., Voudouri, K. A., Fountoulakis, I., Karanikolas, A., Tzoumaka, P., van Roozendaal, M., Balis, D., & Wagner, T. (2022). Retrieval of tropospheric aerosol, NO<sub>2</sub>, and HCHO vertical profiles from MAX-DOAS observations over Thessaloniki, Greece: intercomparison and validation of two inversion algorithms. *Atmospheric Measurement Techniques*, *15*(5), 1269–1301. <https://doi.org/10.5194/AMT-15-1269-2022>
- Karl, T., Lamprecht, C., Graus, M., Cede, A., Tiefengraber, M., de Arellano, J. V. G., Gurarie, D., & Lenschow, D. (2023). High urban NO<sub>x</sub> triggers a substantial chemical downward flux of ozone. *Science Advances*, *9*(3). [https://doi.org/10.1126/SCIADV.ADD2365/SUPPL\\_FILE/SCIADV.ADD2365\\_S M.PDF](https://doi.org/10.1126/SCIADV.ADD2365/SUPPL_FILE/SCIADV.ADD2365_S M.PDF)
- Kern, C., Arellano, S., Campion, R., Hidalgo, S., & Kazahaya, R. (2023). Editorial: Remote sensing of volcanic gas emissions from the ground, air, and space. *Frontiers in*

- Kern, C., & Kelly, P. J. (2023). Weak degassing from remote Alaska volcanoes characterized with a new airborne imaging DOAS instrument and a suite of in situ sensors. *Frontiers in Earth Science*, 11, 1088056. <https://doi.org/10.3389/FEART.2023.1088056/BIBTEX>
- Kern, C., Lerner, A. H., Elias, T., Nadeau, P. A., Holland, L., Kelly, P. J., Werner, C. A., Clor, L. E., & Cappos, M. (2020). Quantifying gas emissions associated with the 2018 rift eruption of Kīlauea Volcano using ground-based DOAS measurements. *Bulletin of Volcanology* 2020 82:7, 82(7), 1–24. <https://doi.org/10.1007/S00445-020-01390-8>
- Khan, W. A., Khokhar, M. F., Shoaib, A., & Nawaz, R. (2018). Monitoring and analysis of formaldehyde columns over Rawalpindi-Islamabad, Pakistan using MAX-DOAS and satellite observation. *Atmospheric Pollution Research*, 9(5), 840–848. <https://doi.org/10.1016/J.APR.2017.12.008>
- Khokhar, M. F., Nisar, M., Noreen, A., Khan, W. R., & Hakeem, K. R. (2017a). Investigating the nitrogen dioxide concentrations in the boundary layer by using multi-axis spectroscopic measurements and comparison with satellite observations. *Environmental Science and Pollution Research*, 24(3), 2827–2839. <https://doi.org/10.1007/S11356-016-7907-3/FIGURES/9>
- Khokhar, M. F., Nisar, M., Noreen, A., Khan, W. R., & Hakeem, K. R. (2017b). Investigating the nitrogen dioxide concentrations in the boundary layer by using multi-axis spectroscopic measurements and comparison with satellite observations. *Environmental Science and Pollution Research*, 24(3), 2827–2839. <https://doi.org/10.1007/S11356-016-7907-3>
- Khokhar, M. F., Yasmin, N., Fatima, N., Beirle, S., & Wagner, T. (2015). Detection of Trends and Seasonal Variation in Tropospheric Nitrogen Dioxide over Pakistan. *Aerosol and Air Quality Research*, 15(7), 2508–2524. <https://doi.org/10.4209/AAQR.2015.03.0157>
- Khokhar, M., Mehdi, H., Abbas, Z., Quality, Z. J.-A. and A., & 2016, undefined. (2016). Temporal assessment of NO<sub>2</sub> pollution levels in urban centers of Pakistan by employing ground-based and satellite observations. *Aaqr.Org*, 16, 1854–1867. <https://doi.org/10.4209/aaqr.2015.08.0518>

- Khokhar, M., Yasmin, N., Fatima, N., ... S. B.-A. and A. Q., & 2015, undefined. (2015). Detection of trends and seasonal variation in tropospheric nitrogen dioxide over Pakistan. *Aaqr.Org*, 15, 2508–2524. <https://doi.org/10.4209/aaqr.2015.03.0157>
- Kirk-Davidoff, D. (2018). The Greenhouse Effect, Aerosols, and Climate Change. *Green Chemistry: An Inclusive Approach*, 211–234. <https://doi.org/10.1016/B978-0-12-809270-5.00009-1>
- Kotsakis, A., Sullivan, J. T., Hanisco, T. F., Swap, R. J., Caicedo, V., Berkoff, T. A., Gronoff, G., Loughner, C. P., Ren, X., Luke, W. T., Kelley, P., Stratton, P. R., Delgado, R., Abuhassan, N., Shalaby, L., Santos, F. C., & Dreessen, J. (2022). Sensitivity of total column NO<sub>2</sub> at a marine site within the Chesapeake Bay during OWLETS-2. *Atmospheric Environment*, 277, 119063. <https://doi.org/10.1016/J.ATMOSENV.2022.119063>
- Kreher, K., van Roozendaal, M., Hendrick, F., Apituley, A., Dimitropoulou, E., Frieß, U., Richter, A., Wagner, T., Lampel, J., Abuhassan, N., Ang, L., Anguas, M., Bais, A., Benavent, N., Bösch, T., Bognar, K., Borovski, A., Bruchkouski, I., Cede, A., ... Zhao, X. (2020). Intercomparison of NO<sub>2</sub>, O<sub>4</sub>, O<sub>3</sub> and HCHO slant column measurements by MAX-DOAS and zenith-sky UV–visible spectrometers during CINDI-2. *Atmospheric Measurement Techniques*, 13(5), 2169–2208. <https://doi.org/10.5194/AMT-13-2169-2020>
- Kulshrestha, U., & Mishra, M. (2021). Atmospheric chemistry in Asia: Need of integrated approach. *Asian Atmospheric Pollution: Sources, Characteristics and Impacts*, 55–74. <https://doi.org/10.1016/B978-0-12-816693-2.00002-0>
- Ma, J., Dörner, S., Donner, S., Jin, J., Cheng, S., Guo, J., Zhang, Z., Wang, J., Liu, P., Zhang, G., Pukite, J., Lampel, J., Lampel, J., & Wagner, T. (2020). MAX-DOAS measurements of NO<sub>2</sub>, SO<sub>2</sub>, HCHO, and BrO at the Mt. Waliguan WMO GAW global baseline station in the Tibetan Plateau. *Atmospheric Chemistry and Physics*, 20(11), 6973–6990. <https://doi.org/10.5194/ACP-20-6973-2020>
- Marais, E. A., Roberts, J. F., Ryan, R. G., Eskes, H., Folkert Boersma, K., Choi, S., Joiner, J., Abuhassan, N., Redondas, A., Grutter, M., Cede, A., Gomez, L., & Navarro-Comas, M. (2021). New observations of NO<sub>2</sub> in the upper troposphere from TROPOMI. *Atmospheric Measurement Techniques*, 14(3), 2389–2408. <https://doi.org/10.5194/AMT-14-2389-2021>
- Murtaza, R., Khokhar, M. F., Noreen, A., Atif, S., & Hakeem, K. R. (2018a). Multi-sensor temporal assessment of tropospheric nitrogen dioxide column densities over

- Pakistan. *Environmental Science and Pollution Research*, 25(10), 9647–9660. <https://doi.org/10.1007/S11356-017-1176-7/FIGURES/9>
- Murtaza, R., Khokhar, M. F., Noreen, A., Atif, S., & Hakeem, K. R. (2018b). Multi-sensor temporal assessment of tropospheric nitrogen dioxide column densities over Pakistan. *Environmental Science and Pollution Research*, 25(10), 9647–9660. <https://doi.org/10.1007/S11356-017-1176-7>
- Oppenheimer, C., Kyle, P., Eisele, F., Crawford, J., Huey, G., Tanner, D., Kim, S., Mauldin, L., Blake, D., Beyersdorf, A., Buhr, M., & Davis, D. (2010). Atmospheric chemistry of an Antarctic volcanic plume. *Journal of Geophysical Research: Atmospheres*, 115(D4), 4303. <https://doi.org/10.1029/2009JD011910>
- Oppenheimer, C., Kyle, P. R., Tsanev, V. I., McGonigle, A. J. S., Mather, T. A., & Sweeney, D. (2005). Mt. Erebus, the largest point source of NO<sub>2</sub> in Antarctica. *Atmospheric Environment*, 39(32), 6000–6006. <https://doi.org/10.1016/J.ATMOSENV.2005.06.036>
- Oppenheimer, C., Tsanev, V. I., Allen, A. G., McGonigle, A. J. S., Cardoso, A. A., Wiatr, A., Paterlini, W., & de Mello Dias, C. (2004). NO<sub>2</sub> emissions from agricultural burning in São Paulo, Brazil. *Environmental Science and Technology*, 38(17), 4557–4561. <https://doi.org/10.1021/ES0496219/ASSET/IMAGES/MEDIUM/ES0496219E00005.GIF>
- Park, J. U., Park, J. S., Diaz, D. S., Gebetsberger, M., Müller, M., Shalaby, L., Tiefengraber, M., Kim, H. J., Park, S. S., Song, C. K., & Kim, S. W. (2022). Spatiotemporal inhomogeneity of total column NO<sub>2</sub> in a polluted urban area inferred from TROPOMI and Pandora intercomparisons. *GIScience & Remote Sensing*, 59(1), 354–373. <https://doi.org/10.1080/15481603.2022.2026640>
- Pinardi, G., van Roozendaal, M., Hendrick, F., Theys, N., Abuhassan, N., Bais, A., Boersma, F., Cede, A., Chong, J., Donner, S., Drosoglou, T., Dzhola, A., Eskes, H., Frieß, U., Granville, J., Herman, J. R., Holla, R., Hovila, J., Irie, H., ... Wittrock, F. (2020). Validation of tropospheric NO<sub>2</sub> column measurements of GOME-2A and OMI using MAX-DOAS and direct sun network observations. *Atmospheric Measurement Techniques*, 13(11), 6141–6174. <https://doi.org/10.5194/AMT-13-6141-2020>
- Pinti, D. L. (2020). Composition of the Earth's Atmosphere. *Encyclopedia of Geology: Volume 1-6, Second Edition*, 5, 187–197. <https://doi.org/10.1016/B978-0-08-102908-4.00054-0>

- Platt, U. (1999). Modern methods of the measurement of atmospheric trace gases Invited Lecture. *Physical Chemistry Chemical Physics*, 1(24), 5409–5415. <https://doi.org/10.1039/A906810D>
- Platt, U. (2008). Air pollution monitoring systems-past-present-future. *Advanced Environmental Monitoring*, 3–20. [https://doi.org/10.1007/978-1-4020-6364-0\\_1/COVER](https://doi.org/10.1007/978-1-4020-6364-0_1/COVER)
- Platt, U., Heue, K. P., & Pöhler, D. (2009). Two- and three dimensional observation of trace gas and aerosol distributions by DOAS techniques. *Atmospheric and Biological Environmental Monitoring*, 3–11. [https://doi.org/10.1007/978-1-4020-9674-7\\_1/COVER](https://doi.org/10.1007/978-1-4020-9674-7_1/COVER)
- Platt, U., & Stutz, J. (2008). Atmospheric Chemistry. *Differential Optical Absorption Spectroscopy*, 5–75. [https://doi.org/10.1007/978-3-540-75776-4\\_2](https://doi.org/10.1007/978-3-540-75776-4_2)
- Polivka, B. J. (2018). The Great London Smog of 1952. *American Journal of Nursing*, 118(4), 57–61. <https://doi.org/10.1097/01.NAJ.0000532078.72372.C3>
- Qayyum, F., Tariq, S., Nawaz, H., ul-Haq, Z., Mehmood, U., & Babar, Z. bin. (2023). Variation of air pollutants during COVID-19 lockdown phases in the mega-city of Lahore (Pakistan); Insights into meteorological parameters and atmospheric chemistry. *Acta Geophysica*, 1, 1–14. <https://doi.org/10.1007/S11600-023-01208-Z/FIGURES/5>
- Reed, A. J., Thompson, A. M., Kollonige, D. E., Martins, D. K., Tzortziou, M. A., Herman, J. R., Berkoff, T. A., Abuhassan, N. K., & Cede, A. (2015). Effects of local meteorology and aerosols on ozone and nitrogen dioxide retrievals from OMI and pandora spectrometers in Maryland, USA during DISCOVER-AQ 2011. *Journal of Atmospheric Chemistry*, 72(3–4), 455–482. <https://doi.org/10.1007/S10874-013-9254-9/FIGURES/10>
- Restrepo, C. E. (2021). Nitrogen Dioxide, Greenhouse Gas Emissions and Transportation in Urban Areas: Lessons From the Covid-19 Pandemic. *Frontiers in Environmental Science*, 9, 689985. <https://doi.org/10.3389/FENVS.2021.689985/BIBTEX>
- Roscoe, H. K., van Roozendaal, M., Fayt, C., du Piesanie, A., Abuhassan, N., Adams, C., Akrami, M., Cede, A., Chong, J., Clémer, K., Friess, U., Gil Ojeda, M., Goutail, F., Graves, R., Griesfeller, A., Grossmann, K., Hemerijckx, G., Hendrick, F., Herman, J., ... Kim, Y. J. (2010). Intercomparison of slant column measurements of NO<sub>2</sub> and O<sub>4</sub> by MAX-DOAS and zenith-sky UV and visible spectrometers. *Atmospheric*

*Measurement Techniques*, 3(6), 1629–1646. <https://doi.org/10.5194/AMT-3-1629-2010>

- Rounce, D. R., Hock, R., Maussion, F., Hugonnet, R., Kochtitzky, W., Huss, M., Berthier, E., Brinkerhoff, D., Compagno, L., Copland, L., Farinotti, D., Menounos, B., & McNabb, R. W. (2023). Global glacier change in the 21st century: Every increase in temperature matters. *Science*, 379(6627), 78–83. [https://doi.org/10.1126/SCIENCE.ABO1324/SUPPL\\_FILE/SCIENCE.ABO1324\\_SM.PDF](https://doi.org/10.1126/SCIENCE.ABO1324/SUPPL_FILE/SCIENCE.ABO1324_SM.PDF)
- Schaller, N., Griesser, T., Fischer, A., ... A. S.-Vjschr. Natf. G., & 2009, undefined. (2009). Climate effects of the 1883 Krakatoa eruption: Historical and present perspectives. *Researchgate.Net*. [https://www.researchgate.net/profile/Nathalie-Schaller/publication/255700466\\_Climate\\_effects\\_of\\_the\\_1883\\_Krakatoa\\_eruption\\_Historical\\_and\\_present\\_perspectives/links/0f31752f4ab5f1da2c000000/Climate-effects-of-the-1883-Krakatoa-eruption-Historical-and-present-perspectives.pdf](https://www.researchgate.net/profile/Nathalie-Schaller/publication/255700466_Climate_effects_of_the_1883_Krakatoa_eruption_Historical_and_present_perspectives/links/0f31752f4ab5f1da2c000000/Climate-effects-of-the-1883-Krakatoa-eruption-Historical-and-present-perspectives.pdf)
- Seagren, E. A. (2005). DDT, Human Health, and the Environment. *Journal of Environmental Engineering*, 131(12), 1617–1619. [https://doi.org/10.1061/\(ASCE\)0733-9372\(2005\)131:12\(1617\)](https://doi.org/10.1061/(ASCE)0733-9372(2005)131:12(1617))
- Shoaib, A., Khokhar, M. F., & Sandhu, O. (2020). Investigating the temporal variation of formaldehyde using MAX-DOAS and satellite observations over Islamabad, Pakistan. *Atmospheric Pollution Research*, 11(1), 193–204. <https://doi.org/10.1016/J.APR.2019.10.008>
- Steinbrecht, W., Hegglin, M. I., Harris, N., & Weber, M. (2018). Is global ozone recovering? *Comptes Rendus Geoscience*, 350(7), 368–375. <https://doi.org/10.1016/J.CRTE.2018.07.012>
- Tariq, S., Nawaz, H., Ul-Haq, Z., & Mehmood, U. (2023). Remote Sensing of Greenhouse Gases and Aerosols from Agricultural Residue Burning Over Pakistan. *Vegetation Fires and Pollution in Asia*, 299–315. [https://doi.org/10.1007/978-3-031-29916-2\\_18/COVER](https://doi.org/10.1007/978-3-031-29916-2_18/COVER)
- Tzortziou, M., Herman, J. R., Cede, A., Loughner, C. P., Abuhassan, N., & Naik, S. (2015). Spatial and temporal variability of ozone and nitrogen dioxide over a major urban estuarine ecosystem. *Journal of Atmospheric Chemistry*, 72(3–4), 287–309. <https://doi.org/10.1007/S10874-013-9255-8/FIGURES/11>
- Tzortziou, M., Kwong, C. F., Goldberg, D., Schiferl, L., Commane, R., Abuhassan, N., Szykman, J. J., & Valin, L. C. (2022). Declines and peaks in NO<sub>2</sub> pollution during



the multiple waves of the COVID-19 pandemic in the New York metropolitan area. *Atmospheric Chemistry and Physics*, 22(4), 2399–2417. <https://doi.org/10.5194/ACP-22-2399-2022>

Tzortziou, M., Loughner, C. P., Goldberg, D. L., Judd, L., Nauth, D., Kwong, C. F., Lin, T., Cede, A., & Abuhassan, N. (2023). Intimately tracking NO<sub>2</sub> pollution over the New York City - Long Island Sound land-water continuum: An integration of shipboard, airborne, satellite observations, and models. *Science of The Total Environment*, 897, 165144. <https://doi.org/10.1016/J.SCITOTENV.2023.165144>

Uglietti, C., Gabrielli, P., Cooke, C. A., Vallelonga, P., & Thompson, L. G. (2015). Widespread pollution of the south american atmosphere predates the industrial revolution by 240 y. *Proceedings of the National Academy of Sciences of the United States of America*, 112(8), 2349–2354. [https://doi.org/10.1073/PNAS.1421119112/SUPPL\\_FILE/PNAS.1421119112.SD03.XLSX](https://doi.org/10.1073/PNAS.1421119112/SUPPL_FILE/PNAS.1421119112.SD03.XLSX)

ul-Haq, Z., Rana, A. D., Tariq, S., Mahmood, K., Ali, M., & Bashir, I. (2018). Modeling of tropospheric NO<sub>2</sub> column over different climatic zones and land use/land cover types in South Asia. *Journal of Atmospheric and Solar-Terrestrial Physics*, 168, 80–99. <https://doi.org/10.1016/J.JASTP.2018.01.022>

Ul-Haq, Z., Tariq, S., & Ali, M. (2015). Tropospheric NO<sub>2</sub> trends over south Asia during the last decade (2004–2014) using OMI Data. *Advances in Meteorology*, 2015. <https://doi.org/10.1155/2015/959284>

ul-Haq, Z., Tariq, S., Ali, M., Daud Rana, A., & Mahmood, K. (2017). Satellite-sensed tropospheric NO<sub>2</sub> patterns and anomalies over Indus, Ganges, Brahmaputra, and Meghna river basins. *International Journal of Remote Sensing*, 38(5), 1423–1450. <https://doi.org/10.1080/01431161.2017.1283071>

ul-Haq, Z., Tariq, S., Ali, M., Mahmood, K., Batool, S. A., & Rana, A. D. (2014). A study of tropospheric NO<sub>2</sub> variability over Pakistan using OMI data. *Atmospheric Pollution Research*, 5(4), 709–720. <https://doi.org/10.5094/APR.2014.080>

Verhoelst, T., Compornolle, S., Pinardi, G., Lambert, J. C., Eskes, H. J., Eichmann, K. U., Fjæraa, A. M., Granville, J., Niemeijer, S., Cede, A., Tiefengraber, M., Hendrick, F., Pazmiño, A., Bais, A., Bazureau, A., Folkert Boersma, K., Bognar, K., Dehn, A., Donner, S., ... Zehner, C. (2021). Ground-based validation of the Copernicus Sentinel-5P TROPOMI NO<sub>2</sub> measurements with the NDACC ZSL-DOAS, MAX-DOAS and Pandonia global networks. *Atmospheric Measurement Techniques*, 14(1), 481–510. <https://doi.org/10.5194/AMT-14-481-2021>

- Wang, S., Pongetti, T. J., Sander, S. P., Spinei, E., Mount, G. H., Cede, A., & Herman, J. (2010). Direct Sun measurements of NO<sub>2</sub> column abundances from Table Mountain, California: Intercomparison of low- and high-resolution spectrometers. *Journal of Geophysical Research: Atmospheres*, *115*(D13), 13305. <https://doi.org/10.1029/2009JD013503>
- Wang, Y., Lampel, J., Xie, P., Beirle, S., Li, A., Wu, D., & Wagner, T. (2017). Ground-based MAX-DOAS observations of tropospheric aerosols, NO<sub>2</sub>, SO<sub>2</sub> and HCHO in Wuxi, China, from 2011 to 2014. *Atmospheric Chemistry and Physics*, *17*(3), 2189–2215. <https://doi.org/10.5194/ACP-17-2189-2017>
- Xue, J., Zhao, T., Luo, Y., Miao, C., Su, P., Liu, F., Zhang, G., Qin, S., Song, Y., Bu, N., & Xing, C. (2022). Identification of ozone sensitivity for NO<sub>2</sub> and secondary HCHO based on MAX-DOAS measurements in northeast China. *Environment International*, *160*, 107048. <https://doi.org/10.1016/J.ENVINT.2021.107048>
- Zeb, N., Khokhar, M. F., Pozzer, A., & Khan, S. A. (2019). Exploring the temporal trends and seasonal behaviour of tropospheric trace gases over Pakistan by exploiting satellite observations. *Atmospheric Environment*, *198*, 279–290. <https://doi.org/10.1016/J.ATMOSENV.2018.10.053>
- Zhao, X., Fioletov, V., Alwarda, R., Su, Y., Griffin, D., Weaver, D., Strong, K., Cede, A., Hanisco, T., Tiefengraber, M., McLinden, C., Eskes, H., Davies, J., Ogyu, A., Sit, R., Abboud, I., & Lee, S. C. (2022). Tropospheric and Surface Nitrogen Dioxide Changes in the Greater Toronto Area during the First Two Years of the COVID-19 Pandemic. *Remote Sensing 2022, Vol. 14, Page 1625, 14*(7), 1625. <https://doi.org/10.3390/RS14071625>
- Zhao, X., Griffin, D., Fioletov, V., McLinden, C., Cede, A., Tiefengraber, M., Müller, M., Bognar, K., Strong, K., Boersma, F., Eskes, H., Davies, J., Ogyu, A., & Chi Lee, S. (2020). Assessment of the quality of tropomi high-spatial-resolution NO<sub>2</sub> data products in the greater toronto area. *Atmospheric Measurement Techniques*, *13*(4), 2131–2159. <https://doi.org/10.5194/AMT-13-2131-2020>
- Zhao, X., Griffin, D., Fioletov, V., McLinden, C., Davies, J., Ogyu, A., Lee, S. C., Lupu, A., Moran, M. D., Cede, A., Tiefengraber, M., & Müller, M. (2019). Retrieval of total column and surface NO<sub>2</sub> from Pandora zenith-sky measurements. *Atmospheric Chemistry and Physics*, *19*(16), 10619–10642. <https://doi.org/10.5194/ACP-19-10619-2019>

## **PLAGIARISM REPORT**

# Talha Saeed Thesis Plagiarism Check File.docx

## ORIGINALITY REPORT

7%

SIMILARITY INDEX

4%

INTERNET SOURCES

5%

PUBLICATIONS

0%

STUDENT PAPERS

## PRIMARY SOURCES

1	"Differential Optical Absorption Spectroscopy", Springer Nature, 2008 Publication	1%
2	nbn-resolving.de Internet Source	<1%
3	acp.copernicus.org Internet Source	<1%
4	www.science.gov Internet Source	<1%
5	www.pandonia-global-network.org Internet Source	<1%
6	amt.copernicus.org Internet Source	<1%
7	archiv.ub.uni-heidelberg.de Internet Source	<1%
8	Physics of Earth and Space Environments, 2011. Publication	<1%
9	disc.gsfc.nasa.gov	

Internet Source

<1 %

10

[www.grin.com](http://www.grin.com)

Internet Source

<1 %

11

[link.springer.com](http://link.springer.com)

Internet Source

<1 %

12

[www.researchgate.net](http://www.researchgate.net)

Internet Source

<1 %

13

Jieshu Zou, Fei Wang. "Simultaneous measurement of SO<sub>2</sub> and NO<sub>2</sub> concentration using an optical fiber-based LP-DOAS system", Chinese Optics Letters, 2020

Publication

<1 %

14

Ocean-Atmosphere Interactions of Gases and Particles, 2014.

Publication

<1 %

15

Theano Drosoglou, Maria-Elissavet Koukouli, Ioannis-Panagiotis Raptis, Stelios Kazadzis et al. "Nitrogen dioxide spatiotemporal variations in the complex urban environment of Athens, Greece", Atmospheric Environment, 2023

Publication

<1 %

16

F. Xu. "Concentration evaluation method using broadband absorption spectroscopy for

<1 %

# sulfur dioxide monitoring", Applied Physics Letters, 2006

Publication

17

[aaqr.org](http://aaqr.org)

Internet Source

<1 %

18

S.F. Schreier, E. Peters, A. Richter, J. Lampel, F. Wittrock, J.P. Burrows. "Ship-based MAX-DOAS measurements of tropospheric NO<sub>2</sub> and SO<sub>2</sub> in the South China and Sulu Sea", Atmospheric Environment, 2015

Publication

<1 %

19

Submitted to VHS Virtual High School

Student Paper

<1 %

20

[hal.archives-ouvertes.fr](http://hal.archives-ouvertes.fr)

Internet Source

<1 %

21

Jiyoung Kim, Jhoon Kim, Hi-Ku Cho, Jay Herman, Sang Seo Park, HyunKwang Lim, Jae-hwan Kim, Koji Miyagawa. "Intercomparison of total column ozone data from the Pandora spectrophotometer with Dobson, Brewer, and OMI measurements over Seoul, Korea", Copernicus GmbH, 2016

Publication

<1 %

22

Submitted to National University of Singapore

Student Paper

<1 %

23

Salman Tariq, Muhammad Khan. "Assessment of nighttime air quality over an urban location

<1 %

in Indo-Gangetic plain using remote sensing observations", Atmospheric Pollution Research, 2023

Publication

24

Submitted to University of Leeds

Student Paper

<1 %

25

Yongjoo Choi, Yugo Kanaya, Hisahiro Takashima, Kihong Park, Haebum Lee, Jihyo Chong, Jae Hwan Kim, Jin-Soo Park. "Changes in Tropospheric Nitrogen Dioxide Vertical Column Densities over Japan and Korea during the COVID-19 Using Pandora and MAX-DOAS", Aerosol and Air Quality Research, 2023

Publication

<1 %

26

[www.atmos-meas-tech.net](http://www.atmos-meas-tech.net)

Internet Source

<1 %

27

[tudr.thapar.edu:8080](http://tudr.thapar.edu:8080)

Internet Source

<1 %

28

[agupubs.onlinelibrary.wiley.com](http://agupubs.onlinelibrary.wiley.com)

Internet Source

<1 %

29

[doaj.org](http://doaj.org)

Internet Source

<1 %

30

John T. Sullivan, Ryan M. Stauffer, Anne M. Thompson, Maria A. Tzortziou et al. "Surf, Turf, and Above the Earth: Unmet Needs for

<1 %

## Coastal Air Quality Science in the Planetary Boundary Layer (PBL)", Earth's Future, 2023

Publication

---

31

Ortega, I., T. Koenig, R. Sinreich, D. Thomson, and R. Volkamer. "The CU 2-D-MAX-DOAS instrument – Part 1: Retrieval of 3-D distributions of NO<sub>2</sub> and azimuth-dependent OVOC ratios", Atmospheric Measurement Techniques, 2015.

Publication

---

<1 %

32

Schreier, Stefan F., Andreas Richter, Folkard Wittrock, and John P. Burrows. "Estimates of free-tropospheric NO<sub>2</sub> and HCHO mixing ratios derived from high-altitude mountain MAX-DOAS observations at midlatitudes and in the tropics", Atmospheric Chemistry and Physics, 2016.

Publication

---

<1 %

33

Syeda Laiba Haider Naqvi, Fizzah Ayub, Abdullah Yasar, Amtul Bari Tabinda, Hassan Nawaz, Rameesha Tanveer. "Pollution status monitoring and indices development for evaluating sustainable environmental management practices (SEMP) in Quaid-e-Azam Industrial Estate, Pakistan", Journal of Cleaner Production, 2023

Publication

---

<1 %



34

Ulrich Pöschl. "Atmospheric Aerosols: Composition, Transformation, Climate and Health Effects", *Angewandte Chemie International Edition*, 2005

Publication

<1 %

35

W. Berry Lyons, Carmen A. Nezat, Kathleen A. Welch, Steven T. Kottmeier, Peter T. Doran. "Fossil Fuel Burning in Taylor Valley, Southern Victoria Land, Antarctica: Estimating the Role of Scientific Activities on Carbon and Nitrogen Reservoirs and Fluxes", *Environmental Science & Technology*, 2000

Publication

<1 %

36

Xiao-Yi Zhang, Jing-Min Sun, Wei-Li Lin, Wan-Yun Xu, Gen Zhang, Yan-Ling Wu, Xin Dai, Jin-Rong Zhao, Da-Jiang Yu, Xiao-Bin Xu. "Long-term variations in surface ozone at the Longfengshan Regional Atmosphere Background Station in Northeast China and related influencing factors", *Environmental Pollution*, 2024

Publication

<1 %

37

[docplayer.net](https://www.docplayer.net)

Internet Source

<1 %

38

[esdd.copernicus.org](https://esdd.copernicus.org)

Internet Source

<1 %

39

[openscience.ub.uni-mainz.de](https://openscience.ub.uni-mainz.de)

Internet Source

<1 %

40

[pure.iiasa.ac.at](https://pure.iiasa.ac.at)

Internet Source

<1 %

41

Chemistry and Radiation Changes in the Ozone Layer, 2000.

Publication

<1 %

42

Chengzhi Xing, Cheng Liu, Hongyu Wu, Jinan Lin, Fan Wang, Shuntian Wang, Meng Gao. "Ground-based vertical profile observations of atmospheric composition on the Tibetan Plateau(2017–2019)", Earth System Science Data, 2021

Publication

<1 %

43

Fayma Mushtaq, Mili Ghosh Nee Lala, Abhishek Anand. "Spatio-temporal variability of lightning activity over J&K region and its relationship with topography, vegetation cover, and absorbing aerosol index (AAI)", Journal of Atmospheric and Solar-Terrestrial Physics, 2018

Publication

<1 %

44

Maria Tzortziou, Jay R. Herman, Alexander Cede, Christopher P. Loughner, Nader Abuhassan, Sheenali Naik. "Spatial and temporal variability of ozone and nitrogen dioxide over a major urban estuarine

<1 %

ecosystem", Journal of Atmospheric  
Chemistry, 2013

Publication

---

45

Masoud Ghahremanloo, Yunsoo Choi,  
Deveshwar Singh. "Deep learning bias  
correction of GEMS tropospheric NO<sub>2</sub>: A  
comparative validation of NO<sub>2</sub> from GEMS  
and TROPOMI using Pandora observations",  
Environment International, 2024

Publication

---

<1 %

46

Muhammad Khan, Salman Tariq, Zia Ul Haq.  
"Variations in the aerosol index and its  
relationship with meteorological parameters  
over Pakistan using remote sensing",  
Environmental Science and Pollution  
Research, 2023

Publication

---

<1 %

47

N. Theys, R. Campion, L. Clarisse, H. Brenot et  
al. "Volcanic SO<sub>2</sub> fluxes derived  
from satellite data: a survey using OMI,  
GOME-2, IASI and MODIS", Atmospheric  
Chemistry and Physics Discussions, 2012

Publication

---

<1 %

48

Siyang Cheng, Jianzhong Ma, Weiping Cheng,  
Peng Yan, Huaigang Zhou, Liyan Zhou, Peng  
Yang. "Tropospheric NO<sub>2</sub> vertical column  
densities retrieved from ground-based MAX-  
DOAS measurements at Shangdianzi regional

<1 %

atmospheric background station in China",  
Journal of Environmental Sciences, 2019

Publication

---

49 Sourangsu Chowdhury, Risto Hänninen,  
Mikhail Sofiev, Kristin Aunan. "Fires as a  
source of annual ambient PM2.5 exposure  
and chronic health impacts in Europe",  
Science of The Total Environment, 2024  
Publication

---

50 Ulrich Platt. "Air Pollution Monitoring Systems  
—Past—Present—Future", Advanced  
Environmental Monitoring, 2007  
Publication

---

51 [directory.eoportal.org](http://directory.eoportal.org)  
Internet Source

---

52 [insight.cumbria.ac.uk](http://insight.cumbria.ac.uk)  
Internet Source

---

53 [journals.ametsoc.org](http://journals.ametsoc.org)  
Internet Source

---

54 [mafiadoc.com](http://mafiadoc.com)  
Internet Source

---

55 [satellite.mpic.de](http://satellite.mpic.de)  
Internet Source

---

56 [v-des-dev-lnx1.nwu.ac.za](http://v-des-dev-lnx1.nwu.ac.za)  
Internet Source

---

[web.archive.org](http://web.archive.org)

57

Internet Source

<1 %

---

58

[www.mdpi.com](http://www.mdpi.com)

Internet Source

<1 %

---

59

[www.russellville.kyschools.us](http://www.russellville.kyschools.us)

Internet Source

<1 %

---

60

Hongmei Ren, Ang Li, Pinhua Xie, Zhaokun Hu et al. "Investigation of the Influence of Water Vapor on Heavy Pollution and Its Relationship With AOD Using MAX-DOAS on the Coast of the Yellow Sea", *Journal of Geophysical Research: Atmospheres*, 2021

Publication

<1 %

---

61

*UV Radiation in Global Climate Change, 2010.*

Publication

<1 %

---

62

Yoojin Kang, Jungho Im. "Mitigating underestimation of fire emissions from the Advanced Himawari Imager: A machine learning and multi-satellite ensemble approach", *International Journal of Applied Earth Observation and Geoinformation*, 2024

Publication

<1 %

---

63

Christoph Kern, Peter J. Kelly. "Weak degassing from remote Alaska volcanoes characterized with a new airborne imaging DOAS instrument and a suite of in situ sensors", *Frontiers in Earth Science*, 2023

<1 %

64

H. R. Dieterich, G. E. Grant, B. Fasth, J. J. Major, K. V. Cashman. "Can Lava Flow Like Water? Assessing Applications of Critical Flow Theory to Channelized Basaltic Lava Flows", *Journal of Geophysical Research: Earth Surface*, 2022

Publication

---

<1 %

65

Isabella M. Dressel, Mary Angelique G. Demetillo, Laura M. Judd, Scott J. Janz et al. "Daily Satellite Observations of Nitrogen Dioxide Air Pollution Inequality in New York City, New York and Newark, New Jersey: Evaluation and Application", *Environmental Science & Technology*, 2022

Publication

---

<1 %

66

Ujjal Deka Baruah, Scott M. Robeson, Anup Saikia, Nitashree Mili, Kang Sung, Pritam Chand. "Spatio-temporal characterization of tropospheric ozone and its precursor pollutants NO<sub>2</sub> and HCHO over South Asia", *Science of The Total Environment*, 2021

Publication

---

<1 %

67

[elib.dlr.de](http://elib.dlr.de)  
Internet Source

---

<1 %

---